Cortical alterations of peptidergic secretion in Alzheimer's disease

Alteraciones corticales de la secreción peptidérgica en la enfermedad de Alzheimer

Virginia Teresa Plá Requena

CORTICAL ALTERATIONS OF PEPTIDERGIC SECRETION IN ALZHEIMER'S DISEASE

Virginia Teresa Plá Requena

Barcelona, 2017

UNIVERSITAT DE BARCELONA

Departamento de Biología Celular, Fisiología e Inmunología
Facultad de Biología

Programa de Doctorado en Biomedicina

Cortical alterations of peptidergic secretion in Alzheimer's disease

Alteraciones Corticales de la Secreción Peptidérgica en la Enfermedad de Alzheimer

Memoria presentada por

Virginia Teresa Plá Requena

para optar al grado de

DOCTORA

por la Universitat de Barcelona

Director de Tesis:
Dr. Fernando Aguado Tomás

Visto bueno del director y tutor,

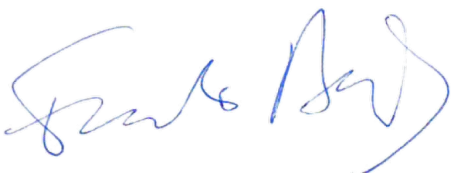

Dr. Fernando Aguado Tomás

El doctorando,

Virginia Teresa Plá Requena

Barcelona
Junio 2017

AGRADECIMIENTOS

Realizar esta tesis doctoral ha sido el reto más difícil al que he debido de enfrentarme hasta ahora. Ha requerido cada minuto que he podido dedicarle y me ha hecho hacer frente a mil problemas que han necesitado de todo mi ingenio y paciencia para solventarlos. Pero también ha sido una experiencia increíble de aprendizaje, científico y personal, acerca de técnicas y problemas biológicos, pero también de límites, esfuerzo y superación. La he peleado con uñas y dientes y puedo decir que no será la mejor, pero he puesto mi alma y una gran cantidad de trabajo en ella. Espero que con los años pueda demostrar todo lo que he aprendido y lo que me he formado como persona en este primer contacto con el mundo de la ciencia.

He tenido la suerte de no estar sola en este viaje. Y de tener mucha gente a la que agradecer el apoyo, las risas y la compañía. Estoy segura de que esta experiencia me ha marcado de por vida y que su recuerdo me acompañará siempre y me salpicará aleatoriamente con recuerdos y anécdotas que me arrancarán una sonrisa, esté donde esté. Sea como sea, este será mi principio, donde me formé como investigadora y aprendí a ser algo así como un adulto.

En primer lugar, me gustaría agradecer la suerte de haber caído en el departamento de Biología Celular, en el que me sentí como en casa desde el primer día. Cuando estás fuera se agradece mucho el poder contar con un lugar en el que sentirte a gusto y donde siempre hay alguien con quien charlar cuando tienes un mal día o prevés que la jornada va a ser eterna. Siempre recordaré con cariño los pica-picas de Navidad con sus divertidos discursos, las comidas, las cenas y las celebraciones de cumpleaños improvisadas que siempre reunían a gente suficiente para ser un éxito. Gracias por arroparme y alegraros conmigo cuando había algo que celebrar.

Gracias especialmente a las secres: Isabel, Yolanda, Mariajosé y Susana, quienes han demostrado una gran paciencia y sentido del humor para solucionar todos los problemas que iban surgiendo. ¡Teneros ha hecho mi vida más fácil! Mariajosé, siempre recordaré que me hiciste mi primer contrato de investigadora (¡con lo grande que me quedaba esa palabra por aquel entonces!) … y tus sabios consejos, que siempre tuve en cuenta.

Gracias también a Mercè por cuidar nuestros niveles de omega-3 con su aporte de nueces diario (¡ya no puedo comerlas sin acordarme del departamento!) y por cuidarnos, manteniendo un departamento agradable y acogedor. En los últimos días de diciembre, habitualmente cargados de trabajo, siempre consiguió arrancarme una sonrisa algún espumillón en un rincón inesperado -como una ducha de seguridad-. Gracias también a la gente del comedor (Mónica, Carme, Félix, Xavi, Maria, Jordi, Ester, …), que ha ayudado a que la rutina del tupper sepa más a casa y especialmente a Isabel y Yolanda, siempre pendientes de que no nos faltara de nada.

Gracias a la gente de citometría: Sonia, Chari, Ricard y Jaume, quienes me ofrecieron la oportunidad de poder seguir con mi tesis cuando hizo falta. Gracias por la comprensión de mis horarios locos y la paciencia en escuchar todas las historias del lab y, sobretodo, gracias por el aprendizaje, por los cafés y por las risas. Me considero afortunada de haber tenido la oportunidad de formar parte de vuestro equipo, aunque fuese temporalmente. Y por

extensión, gracias a Ramón, quién siempre ha estado dispuesto a echar una mano en todo, incluso cuando la genómica nos sonaba a chino... siempre te agradeceré los consejos y la paciencia infinita.

I would like to thank Reiner, who opened his lab to me for my first scientific adventure abroad, which help me a lot to develop myself as a researcher. Thanks for your patience (and Helene's!) and your closeness. Also, I would like to thank Luis for kindly allowing me to visit his lab where I learned a lot, specially from Hiroshi, who was a great teacher! And I am grateful to Ayesha, who made my stay infinitely more fun and who took care of whatever I needed.

He de agradecer también el apoyo a mi piso-patera, ¡por supuesto! Marta, Pablo y Bárbara, qué bien lo hemos pasado juntos, con nuestros horarios locos, la casa siempre llena y aprovechando cada hueco para montar algún plan divertido para aliviar el estrés de las tesis. Me gustó mucho compartir estos años con vosotros, ojalá sigamos coincidiendo para rememorar anécdotas… ¡y montar trivials en el baño!

Y entrando ya en el día a día... Gracias a mis compañeros de laboratorio, quienes me han ayudado a aprender y a abrirme paso entre cultivos, westerns, slices y excels. Ha sido genial poder contar con vosotros para superar los retos y avanzar en todas las cuestiones que han ido surgiendo. Sin ellos no hubiese podido aguantar el ritmo exigido por este trabajo... y todo hubiese sido mucho más aburrido, ¡seguro! Greg, Adriana, Enrique, Meritxell, Miguel, Vanessa, Paula, Carla… habéis sido muchos los que habéis pasado por el laboratorio y todos habéis dejado vuestra huella. Me llevo las mil batallitas que hemos vivido juntos... y las cenas, las celebraciones y las aventuras. Greg, no olvidaré tu sentido del humor, tus piques con Jordi y que fuiste el primero que pasaste por aquí. Vanessa, gracias por tu amistad sincera, tu buen corazón y tus enormes ganas de ayudar siempre, fue una suerte poder contar contigo.

Sonia, gracias especialmente por tu paciencia al enseñarme las primeras recetas… y por tu profesionalidad. Recuerdo (¡y uso!) todos tus trucos y sigo transmitiéndolos a los estudiantes que pasan por el laboratorio. Tu organización y perfeccionismo marcó mi forma de trabajar y te lo agradezco. Y gracias también por haberte convertido en una verdadera amiga, siempre ahí para dar ánimos, consejos y montar algún plan bueno, bonito y barato para desconectar. Fue una suerte tenerte de compañera y poderte contar ahora entre mis amigos.

Neus e Irene, gracias por hacer crecer este grupo. Ha sido muy positivo el poder contar con vosotras y me alegro mucho de que vayáis a continuar con el proyecto. Gracias por vuestra disposición y el apoyo, tanto dentro como fuera del laboratorio. ¡Y los donuts cuando eran necesarios! Habéis hecho que el trabajo sea mucho más agradable y divertido. Hemos tenido mucha suerte de que llegarais al laboratorio. Cuidad lo que tenéis, porque es muy difícil conseguir un grupo de trabajo con tan buen ambiente. Y si hace falta recuperarlo, ¡estoy disponible para ir a Copenhague cuando queráis!

Jordi, gracias por estar siempre dispuesto a ayudar y a escuchar mis penas. Menos mal que has estado ahí, me has salvado de un montón de problemas y he agradecido mucho que siempre me animases a luchar por mí. Ha sido genial saber que podía contar contigo.

Ester, gracias por todo amiga. Has sido un apoyo increíble. Siempre hemos estado conectadas y ha bastado una mirada para saber lo que la otra está pensando. Has sido un gran faro estos años, quien me ayudaba encajar las piezas y a no perder el norte. Tus consejos me han ayudado mucho y tu voluntad y esfuerzo siempre han sido un ejemplo.

Gracias Fernando, por creer en mi valía desde el principio y darme la oportunidad de entrar a tu laboratorio. Tenerte como director de tesis ha sido un orgullo, ya que no conozco a nadie más apasionado por su trabajo y tu entusiasmo ha sido contagioso. Gracias por implicarte en este proyecto y luchar por que pudiese hacer esta tesis doctoral. No ha sido fácil, pero siempre hemos encontrado una ventana. ¡Y es que hacemos un muy buen equipo! Gracias por no perder nunca esa curiosidad que hace la ciencia interesante y por querer saber siempre más. Gracias también por tu paciencia y por ser estar siempre abierto a nuevas ideas y proyectos, en los que siempre he contado con tu apoyo. Durante estos años me has enseñado muchísimo como investigadora, pero también como persona. Ética, respeto, profesionalidad, tesón: son lecciones que he aprendido de ti. Estoy segura de que estos principios son los que guiarán mi carrera investigadora y espero que a la larga puedas estar orgulloso.

Gracias también a mi familia, quienes han aceptado la distancia sin que ésta nos separase. Gracias porque cada vez que nos vemos es como si nos hubiésemos visto ayer y por creer que esto merecía la pena. Siempre recordaré a mi abuelo, confiando en que sacásemos alguna *cosica* para el Alzheimer antes de que le pudiese tocar a ellos. Qué increíble apoyo habéis sido. Gracias a mi hermano Rubén, quien siempre ha estado al otro lado del teléfono para que le confiara mis dilemas vitales, que fuesen los que fuesen siempre acababan en risas.

Gracias también a Alberto, quien siempre ha creído más en mí que yo misma. Es quién mejor conoce lo difícil que ha sido este camino en ocasiones, quien más ha sufrido las consecuencias de mis horarios y mis errores de planificación y, a pesar de ello, siempre me ha animado a seguir. Se ha implicado en mil locuras por ayudarme y ha sufrido cada paso deseando que saliese bien. No sé qué haría sin ti. Gracias por tu paciencia, por tu apoyo, por ser como eres. Suerte que somos dos contra el mundo.

Y por supuesto, gracias especialmente a mis padres. Han hecho lo indecible por apoyarme, incluso cuando no entendían la importancia de que estuviese en el laboratorio a las 2 de la mañana de un sábado… Han aprendido de becas, cultivos, animales de laboratorio, normativas, horarios de metros y trenes y se han convertido en unos expertos en Skype por mi culpa… y nunca han dejado de creer en mí. Gracias por ser siempre la red que me recoge cuando algo sale mal y estar siempre ahí para hacerme sentir lo mucho que me queréis. Tengo una suerte infinita de que siempre me hayáis animado para perseguir mis sueños, por muy lejos que me llevaran, y de que me alentaseis a correr aventuras. Sois los mejores padres que podría soñar. Si he conseguido esto es por vosotros.

INDEX

LIST OF ABBREVIATIONS

A	ACh	Acetylcholine
	AD	Alzheimer Disease
	APOE	Apoprotein E
	APP	Amyloid Precursor Protein
	ATP	Adenosine Triphosphate
	Aβ	Amyloid-B
B	BBB	Brain Blood Barrier
	BDNF	Brain-Derived Neurotrophic Factor
	BPSD	Behavioral and Psychiatric Signs and Symptoms of Dementia
C	CAA	Cerebral Amyloid Angiopathy
	CgA	Chromogranin A
	CNS	Central Nervous System
	CPE	Carboxypeptidase E
	CSF	Cerebrospinal Fluid
D	DCV	Dense Core Vesicle
E	ER	Endoplasmic Reticulum
G	GABA	γ-Aminobutyric Acid
	GFAP	Glial Fibrillar Acidic Protein
L	LTD	Long Term Depression
M	MRI	Magnetic Resonance Imaging
	MCI	Mild Cognitive Impairment
	mRNA	Messenger RNA
N	NFT	Neurofibrillary Tangles
	NMDAR	N-Methyl-D-Aspartate Receptor
	NPY	Neuropeptide Y
	NT	Neurotrophin
P	p75NTR	75 kDa Neurotrophin Receptor
	PC	Proprotein Convertase
	PET	Positron Emission Tomography
	P-Tau	Phosphorylated Tau
R	ROS	Reactive Oxygen Species
	RSP	Regulated Secretory Pathway
S	SgII	Secretogranin II
	SgIII	Secretogranin III
T	TGN	Trans-Golgi Network
	T-Tau	Total Tau

1 INTRODUCTION

The Alzheimer's Disease (AD) is a neurodegenerative disease characterized by neurological alterations that lead to a severe cognitive decline and dementia. Nowadays has become the main cause of dementia, accounting for 50–70% of cases (Winblad *et al.*, 2016). Commonly, the first symptom of the dementia is the difficulty in the recall of recent events, which can progress rapidly into different personality and behavioral changes and a more severe impairment of the memory. Progressive advance of cognitive impairment interferes in the development of daily activities, causing a high grade of dependence, mainly in the final phases of the disease. (Winblad *et al.*, 2016). As the prevalence of overall dementia rises steeply with age, being this factor the strongest risk factor for AD (American Psychiatric Association, 2013), the progressive aging of the population is increasing the incidence of the disease, which has become a global health problem. In fact, an estimated 40 million people, mostly older than 60 years, have dementia worldwide, and this number is estimated to double every 20 years, until at least 2050 (Qiu *et al.*, 2009). This insidious onset and the gradual progression of impairment of AD -the average duration of illness is 8–10 years (Masters *et al.*, 2015)- makes this pathology specially harmful compared to other diseases with a more clear clinical onset, and often abrupt resolution (Jack, 2012). Because of that, the disease has become an important economic charge for the health systems, which have to take care of a rising number of highly dependent people.

Global cost estimations of the disease in 2009 were $604 billion per year, 1% of the world's gross domestic product (Jack, 2012). In fact, in December, 2013, the G8 stated that dementia should be made a global priority that a cure or a disease-modifying therapy could be available by 2025 (Scheltens *et al.*, 2016). Also in 2011, President Obama initiated the National Alzheimer's Project with the aim to coordinate the global research, accelerate the development of treatments and improve diagnosis of the disease. However, notwithstanding the invested resources, no cure or substantial symptom-relieving treatment is available for AD or other dementias (Winblad *et al.*, 2016). That is why it is still necessary a leap in research to give an answer to all the suffering patients and families of this terrible disease.

And we must accept the challenge.

1.1 ALZHEIMER'S DISEASE

The AD is a progressive neurodegenerative disorder characterized by the appearance of two neuropathological hallmarks, the senile plaques formed from the accumulation of amyloid-β (Aβ) insoluble species and the neurofibrillary tangles (NFT) caused by the aggregation of the microtubule-associated protein tau (Masters *et al.*, 2015). Also, other abnormalities are usually found in the brain of AD patients, being the most affected areas the frontal and temporal lobes where they mainly consisted in a progressive thinning and atrophy of the cortical areas (Serrano-Pozo *et al.*, 2011). The first subjective complain is amnesia caused by an impairment on episodic memory, followed by a broad grade of daily living activities breakage based on difficulties on language and executive function, psychiatric symptoms and behavioural disturbances (Cummings & Cole, 2002; Burns & Iliffe, 2009).

Aging is the main risk factor for AD (Plassman *et al.*, 2007), reason why some researchers claim that the development of this pathology is an inevitable consequence of increasing life expectance, where the healthy elderly is the beginning point of the same progressive process (Herrup, 2015). The extraordinarily complex network of neurons and glial cells which conforms the cerebral cortex undergoes age-related modifications that implicates memory decline (age-associated memory impairment, AAMI), reduction in executive function (Clarys *et al.*, 2009; Turner & Spreng, 2012) and, in some cases, the presence of area-restricted senile plaques and NFT, but in an extend far less severe than in AD (Green *et al.*, 2000). However, some evidences showed that the pattern of latent changes in normal elderly do not resemble the pathological early alterations of the amyloid disease (Fjell *et al.*, 2014). During aging, a mild brain atrophy affecting principally fronto-striatal network supporting executive function; in turn, degeneration of the medial temporo-parietal memory network has been described that the characteristics signature for AD (Buckner, 2004; Head *et al.*, 2005). Those results show that the process of aging and AD have both differential and partially overlapping effects (Bakkour *et al.*, 2013). where the synaptic plasticity has been suggested to be the main player on the brain insult compensatory capacity which draw the line between healthy ageing and AD early events (Fjell *et al.*, 2014).

In conjunction with brain atrophy, has been described an important loss of presynaptic cholinergic markers in the central nervous system (CNS) of AD patients, suggesting a hypofunction of those pathways that could be related with cognitive symptoms and memory impairment (Bartus, 2000; Schliebs & Arendt, 2006). Also, the dramatic loss of synaptic proteins in AD brains as postsynaptic density-95 (PSD-95), dynamin-1 and synaptophysin, suggest a specific Aβ-targeting of synapses that could induce neuronal death (Sze *et al.*, 1997; Sivanesan *et al.*, 2013). This effect has been demonstrated by ultrastructural studies that showed a decrease in the synaptic density in the neocortical association areas and hippocampus of AD patients (DeKosky & Scheff, 1990). Furthermore, the existing general decrease in neuropeptides levels such Neuropeptide Y (NPY) or somatostatin either if cerebrospinal fluid (CSF) or brain tissue might be also affecting neurotransmission (Van Dam *et al.*, 2013).

1.1.1 Clinical signs and symptoms: Classification

Based on consensual clinical criteria, AD diagnosis is established (McKhann et al., 1984) and its severity is classified accordingly to clinical scores of cognitive function (Table 1). In short, three stages have been defined in a clinical continuum: preclinical, mild cognitive impairment (MCI) and dementia, as establish the National Institute on Aging–Alzheimer's Association (NIA-AA) sponsored consensus reports. Postmortem brain analysis by immunohistochemistry allows a further case classification regarding the neuropathological changes found in the tissue (Table 2). However, there is consensus to disentangle the clinicopathologic term "Alzheimer's disease" from AD histopathologic change (Hyman *et al.*, 2012). The first is settled based on cognitive symptoms and behavioural changes, while the second refers to the presence and extent of AD neuropathological changes observed at autopsy, regardless of the clinical setting.

Stages of Alzheimer's Disease					
Stage	**Memory**	**Language**	**Visuospatial Skills**	**Executive Function**	**Daily Living Activities**
Mild Cognitive Impairment	Ammnesia	Normal	Normal	Minimally affected	No impairment
Mild AD	Ammnesia	Decreased verbal fluency	Mildy abnormal	Mildy abnormal	Instrumental Daily Living Activities Affected
Moderate AD	Ammnesia plus remote memory impairment	Anomia; decreased comprehension	Moderately abnormal	Moderately abnormal	Daily Living Activities
Severe AD	Absent	Aphasia	Severely abnormal	Untestable	Totally dependent

Table 1: AD classification (Cummings, 2008)

AD neuropathologic change should be ranked along three parameters (Amyloid, Braak, CERAD) to obtain an "ABC score":	
A. Aβ plaque score:	A0 no Aβ or amyloid plaques A1 Thal phases 1 or 2 A2 Thal phase 3 A3 Thal phases 4 or 5
B. NFT stage (modified from Braak for silver-based histochemistry or phospho-tau immunohistochemistry)	B0 no NFTs B1 Braak stage I or II B2 Braak stage III or IV B3 Braak stage V or VI
C. Neuritic plaque score	C0 no neuritic plaques C1 CERAD score sparse C2 CERAD score moderate C3 CERAD score frequent

Table 2: Classification of AD neuropathologic change (Hyman *et al.*, 2012)

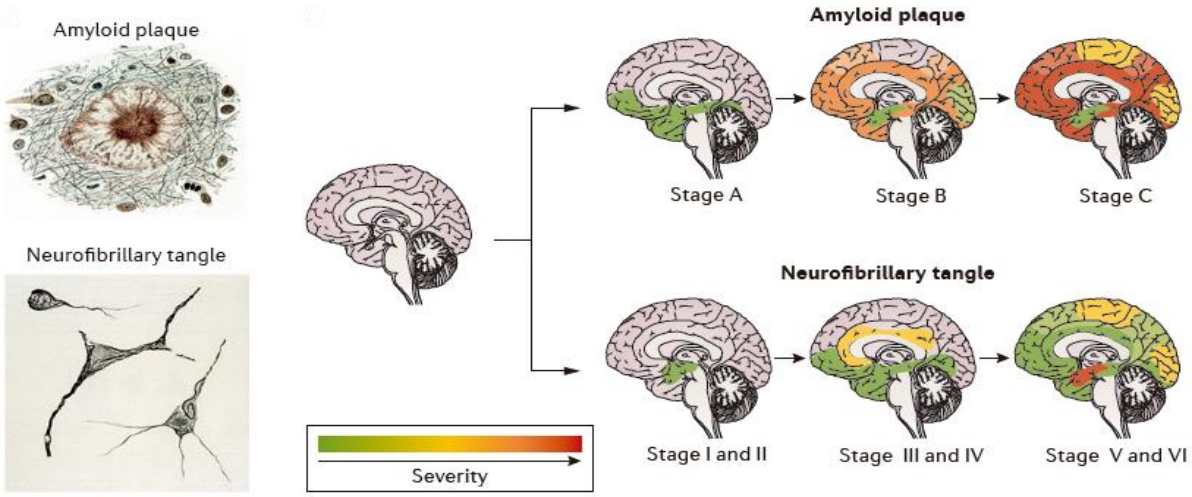

Figure 1. Amyloid plaques and NFT allow the classification of the pathological states based on the neuropathological hallmarks found in post-mortem analysis (Masters *et al.*, 2015)

Even when the sensitivity and specificity of this method is adequate, mild dementia is rarely diagnosed and even moderately severe dementia is underrecognized in clinical practice (Callahan et al., 1995). Also, the necessity of an earlier and more accurate diagnosis that integrate clinical and neuropathological standards requires an update of the current criteria, that did not change since their establishment in 1984. This would lead to a better patient disease-stage classification that would help to the treatment and in the development of new ones. To do so, it is essential a better understanding of the physiopathology of the AD, that might allow the establishment of new biomarkers to follow up the undergoing disease progress.

1.1.2 Etiology: familiar and spontaneous AD

The causes of AD remain obscure. AD is commonly classified as early or late onset based on the occurrence of the disease before or after age 65 years, being the late onset sporadic disease accounting for over 95% of cases (Jack, 2012). Early onset seems to be related with mutations in one of three genes: the amyloid precursor protein gene on chromosome 21, the presenilin-1 gene on chromosome 14, or the presenilin-2 gene on chromosome 1 (Bird, 1993; Tang & Gershon, 2003), although dominantly inherited forms accounts for less than 1% of the total AD cases (Goedert & Spillantini, 2006). However, the general phenotype for familiar and spontaneous AD strongly suggests that the mechanism that could be identified in the autosomal dominant forms could be applicable to the apparently nonfamilial forms of the disease (Selkoe, 2001).

Even when deterministic genetic mutations for late onset AD have not been found, the ε4 allele of the lipid metabolism protein apoprotein E (APOE) gene is the most prevalent genetic risk factor (Michaelson, 2014), being associated with impaired synaptic plasticity (Teter, 2004), an increased hippocampal atrophy and loss of dendritic spines (Ji *et al.*, 2003). Also, other risk factors have been determined, with a variable range of potential modification, as diabetes mellitus, mid-life hypertension,

mid-life obesity, physical inactivity, depression, smoking and low educational attainment (Norton *et al.*, 2014).

1.1.3 AD Onset

The fact that the four genetic factors (APP, Apoε4, PS1 and PS2; Table 3) unequivocally increasing AD risk are linked with the production and/or the cerebral deposition of Amyloid-β (Aβ) (Selkoe, 1997), confer to this protein a central role in the progress of the pathology. Also, less strongly associated genetic risk factors have been identified for phosphatidylinositol-binding clathrin assembly protein (PICALM), CD33, triggering receptor expressed on myeloid cells 2 (TREM2), the ATP-binding cassette transporter ABCA7, clusterin (CLU) and complement receptor type 1 (CR1), which, in addition to APOE, might intervene in the Aβ clearance pathways (Masters *et al.*, 2015). In fact, have been stated that cerebral accumulation of Aβ is and early, invariant and necessary event in the initiation of AD (Selkoe, 2001).

Chromosome	Gene Defect	Phenotype
21	β-APP mutations	↑ Production of all Aβ peptides or $A\beta_{40}$ peptides
19	ApoE4 polymorphism	↑ Density of Aβ plaques and vascular deposits
14	Presenilin 1 mutations	↑ Production of $A\beta_{42}$ peptides
1	Presenilin 2 mutation	↑ Production of $A\beta_{42}$ peptides

Table 3: Confirmed genetic factors predisposing to Alzheime's disease: relationships to the Aβ phenotype (Selkoe, 2001)

Aβ peptides are natural products of metabolism consisting of 36 to 43 amino acids, which overproduction can lead to accumulation and self-aggregation into non-soluble deposits (Querfurth & LaFerla, 2010). However, its occurrence in AD brains only correlates partially with cognitive decline (Hardy & Selkoe, 2002), fact that have been argued to defense the Tau hyperphosphorylation as a more important event in the physiopathology, since predicts better the cognitive status. Although NFT are not specific for AD but -at least under some conditions- a secondary response to injury, the fact that Tau gene mutations can produce clinical dementia with NFTs may link directly this alteration with primary neurodegenerative changes (Nelson *et al.*, 2012). However, transgenic mouse models expressing Tau, did not develop neuritic plaques (Götz *et al.*, 2007). This has led to open the question about the sequence of apparitions of disturbances for Tau or Aβ in the pathology.

Recent findings stood on transgenic mice models had shed light on the matter by demonstrating that both molecules have a functional link, showing definitively that Aβ-driven toxicity is Tau-dependent (Bloom, 2014). Briefly, the presence of Aβ forms in Tau-mutant mice, either by direct stereotaxic delivery or by crossing mice with APP-mutated strain, markedly accelerated tangle formation without effects on the occurrence or conformation of amyloid plaques produced by the enhanced Tau pathology. Those results demonstrate that Aβ has a function upstream of Tau, which

mechanisms remains to be elucidated. Then, to evaluate the requirement of tau for Aβ toxicity in vivo, Tau knockout mice was crossed with mutant APP mice, finding that loss or decrease of Tau expression, even not affecting the plaque accumulation, did effect a protective role against learning, memory deficits and excitotoxicity on hybrids comparing with the former APP strain (Roberson *et al.*, 2007). The implied influence of Tau on Aβ effects, raises the possibility that Aβ initiates a pathological feedback loop with tau (Bloom, 2014).

Study	System	Summary of Main Results
Götz et al, 2001	Mouse	Tangle formation accelerated by injection of Aβ fibrils into the brain
Lewis et al, 2001 and Hurtado et al, 2010	Mouse	Mutant APP expression accelerates tangle formation by mutant tau
Roberson et al, 2007	Mouse	Tau required for learning and memory deficits when plaques are present
Leroy et al, 2012	Mouse	A feedback loop connects Aβ and tau pathologies
Ittner et al, 2010	Mouse	Aβ causes tau-dependent excitotoxicity at N-methyl-D-aspartate receptors
Rapoport et al, 2002	Primary Neurons	Aβ fibrils are cytotoxic
King et al, 2006	Primary Neurons	AβOs cause tau-dependent MT loss
Nussbaum et al, 2012	Primary Neurons	Pyroglutamylated AβOs cause tau-dependent cytotoxicity
Seward et al, 2013	Primary Neurons	AβOs cause tau-dependent, ectopic cell cycle reentry
Shipton et al, 2011	Brain Slices	AβOs cause tau-dependent impairment of long-term potentiation
Vossel et al, 2010	Primary Neurons	AβOs cause tau-dependent inhibition of mitochondrial transport on MTs
Zempel et al, 2013	Primary Neurons	AβOs cause tau-dependent MT severing and synaptic damage in dendrites

Table 4: Tau-Dependent Effects of Aβ (Bloom, 2014)

1.1.4 Hypothesis of AD Pathogenesis

A growing body of recent evidence points to a key role of Aβ in the AD pathogenesis that led to the statement of the amyloid cascade hypothesis, which postulates that the neurodegeneration in AD is caused by abnormal accumulation of Aβ plaques in various areas of the brain. Accordingly to assumption, Aβ deposition in senile plaques acts as a trigger for the pathology, that includes neuritic injury, formation of NFT and inflammation that leads to synaptic dysfunction, neuronal death and dementia (Hardy & Higgins, 1992; Hardy & Selkoe, 2002).

The complexity of the undergoing process makes difficult to define the sequence of events that participate on the disease mechanism, that could be concurrent and be interrelated. However, since senile plaques are composed of Aβ peptides (Masters et al., 1985) an imbalance on the production and clearance of Aβ has been suggested. Aβ is produced by the cleavage of amyloid precursor protein (APP) by sequential action of the β-secretase β-site amyloid precursor protein-cleaving enzyme 1 (BACE-1)

at the citosol and a membrane-associated γ-secretase, a protein complex with presenilin 1 at its catalytic core (Haass & Selkoe, 2007). From the variably sized resulting peptides, Aβ40 and Aβ42 have been found to be the predominant forms, being the last more prone to aggregation, and, consequently, more neurotoxic than and other Aβ variants (Sheng et al., 2012).

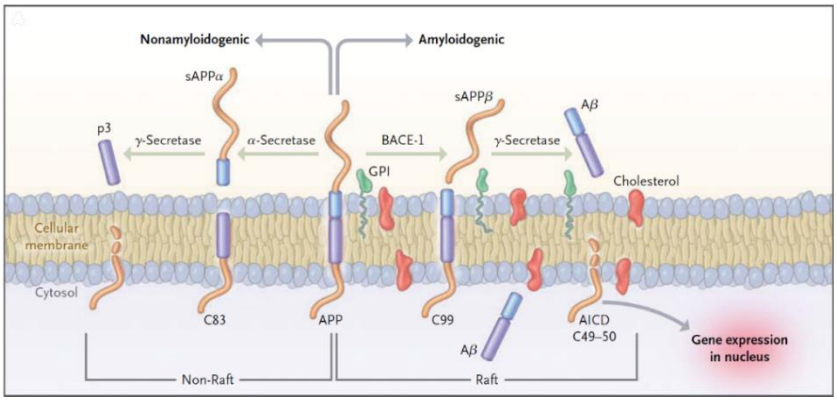

Figure 2: Alternative APP processing pathways present in the brain. Dysregulation of both products is thought to be a possible trigger of the Aβ-cascade. (Querfurth & LaFerla, 2010)

Produced Aβ spontaneously self-aggregates into several interconvertible forms, ranging from oligomers (2 to 6 peptides) to β-sheet arranged insoluble fibrils, including various intermediate assemblies (Querfurth & LaFerla, 2010). Soluble oligomers and intermediate amyloid are the most neurotoxic species (Walsh & Selkoe, 2007), as long as they had shown to be toxic for synapses. Normal neuronal function of APP is still unknown but it is thought that could be implicated in synaptic plasticity (Sheng et al., 2012), having and homeostatic role in the modulation of neuronal activity(Turner et al., 2003).

The rising accumulation of Aβ triggers a cascade of consequences that could be classified into three stages: the biochemical, the cellular and the clinical phase.

1.1.4.1 Biochemical Phase

The biochemical phase of AD is characterized by the initiation of the aberrant Aβ aggregation and formation of hyperphosphorylated Tau tangles. Afterwards, a prion-like mechanism is suggested to be implied on the spreading of the pathological changes, where the protein deposits serve as a template for the misfolding of other molecules (Walker & Jucker, 2015). Initially, the effects of this proteopathy are attenuated by brain compensatory mechanisms that imply biochemical and functional changes to maintain the homeostasis where synaptic plasticity and inflammatory responses play a central role (De Strooper & Karran, 2016). Nevertheless, the overtake of the compensating mechanism by the progressive accumulation of toxic species leads to chronic, irreversible and pathological processes that make the disease advance inexorable.

The early events elicited by Aβ are the impairment of the synaptic transmission (Palop & Mucke, 2010) and the increase of reactive oxygen species (ROS) generated as a consequence of mitochondrial dysfunction (Ye *et al.*, 2012), additionally to an strengthening of the inflammatory response (Raskin *et al.*, 2015). Pathological elevated Aβ may be involved in the induction of long term depression (LTD)

and synaptic loss by blocking of N-methyl-D-aspartate receptors (NMDARs) signaling by internalization or desensitization that provoke collapse of dendritic spines and synaptic failure. Also, an impairment of glutamate uptake at the synapses and abnormal patterns of neuronal activity have been described, suggesting that elevated Aβ destabilizes neural network activity (Palop & Mucke, 2010; Danysz & Parsons, 2012). Furthermore, alterations in energy metabolism and accumulation of Aβ in mitochondrial membranes suggest that its function could be disrupted (Zhao & Zhao, 2013), causing a stress response that implies an contributes to the augment of ROS production and an energy depletion (Moreira *et al.*, 2005; Ye *et al.*, 2012).

Although the physical separation of Aβ and Tau could indicate an independent progress of the abnormalities affecting this protein, recent findings show that Aβ can significantly accelerate phosphorylation of Tau (Zheng *et al.*, 2002) and NFT formation (Götz *et al.*, 2001). Abnormal hyperphosphorylation of Tau impairs its binding to tubulin, preventing it to promote microtubule assembly. In addition to this, aberrant Tau present misfolding and self-assembly into tangles of paired helical and or straight filaments (Iqbal *et al.*, 2009). As Tau is required for the normal axonal transport, the aggregation blocks this crucial process, restringing the protein supply and turnover of the distal synapses (Chevalier-Larsen & Holzbaur, 2006). Also, as mitochondrial functionality is necessary for the energetic supply of the axonal transport, the Aβ-driven energy breakage exacerbate this effect.

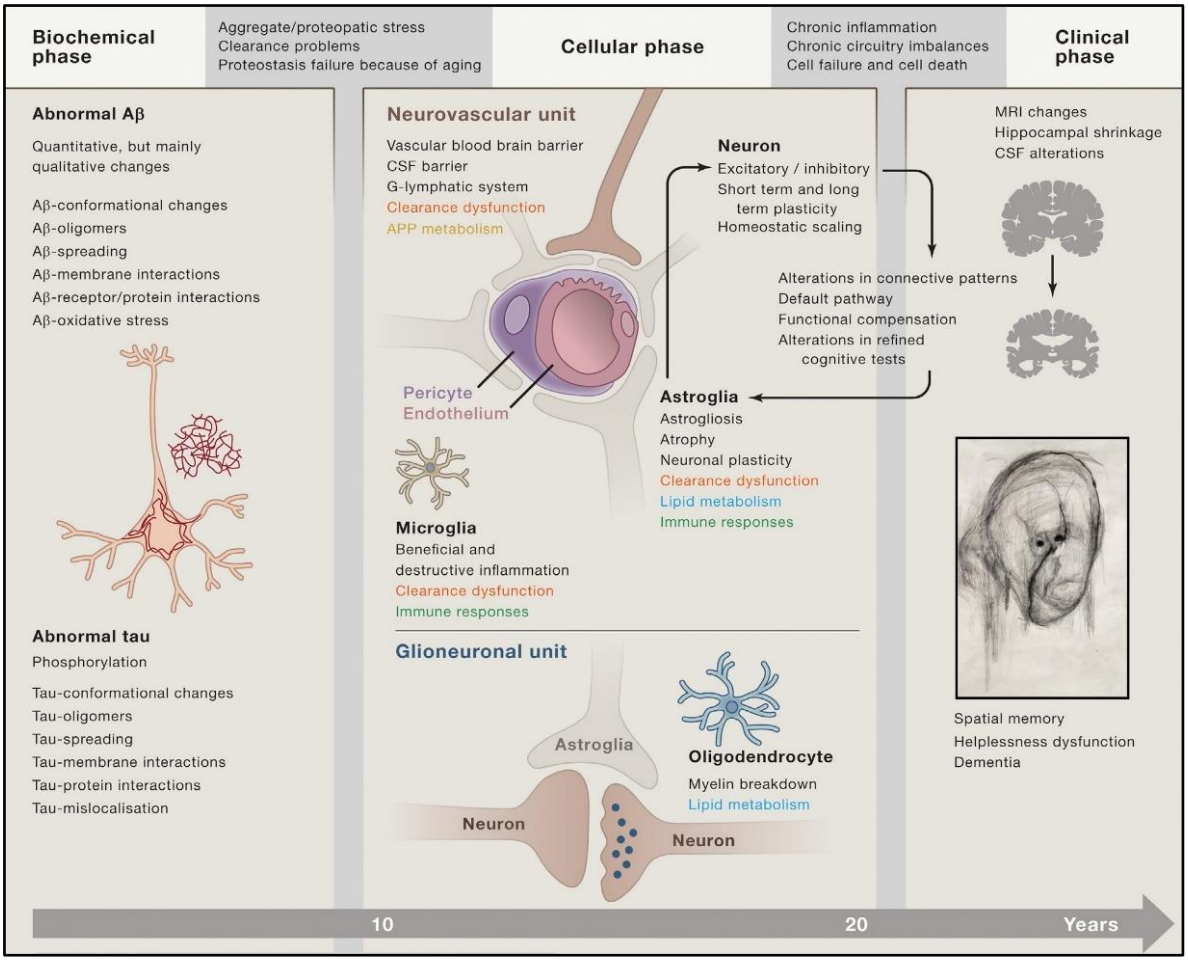

Figure 3: Stages of AD (De Strooper & Karran, 2016)

1.1.4.2 Cellular Phase

Once the compensatory processes are insufficient to maintain brain homeostasis, the cellular phase of AD is initiated. At this point, the clearance mechanisms of aberrant proteins become defective and an inflammatory response is produced. Microglia that have been phagocyting Aβ depositions and redundant neurons (Lee & Landreth, 2010), switch to the production of cytokines, becoming a new source of ROS and activating a classic complement-mediated response (Selkoe, 2001). Consequently, reactive astrogliosis is settled and astrocyte become hypertrophic, proliferate and increase their expression of intermediate filaments (glial fibrillar acidic protein (GFAP), vimentin and nestin) (De Strooper & Karran, 2016). Activated astrocytes also participate in Aβ clearance through receptor-mediated uptake (Pihlaja *et al.*, 2008) and internalized peptides undergo enzymatic degradation (Ries & Sastre, 2016).

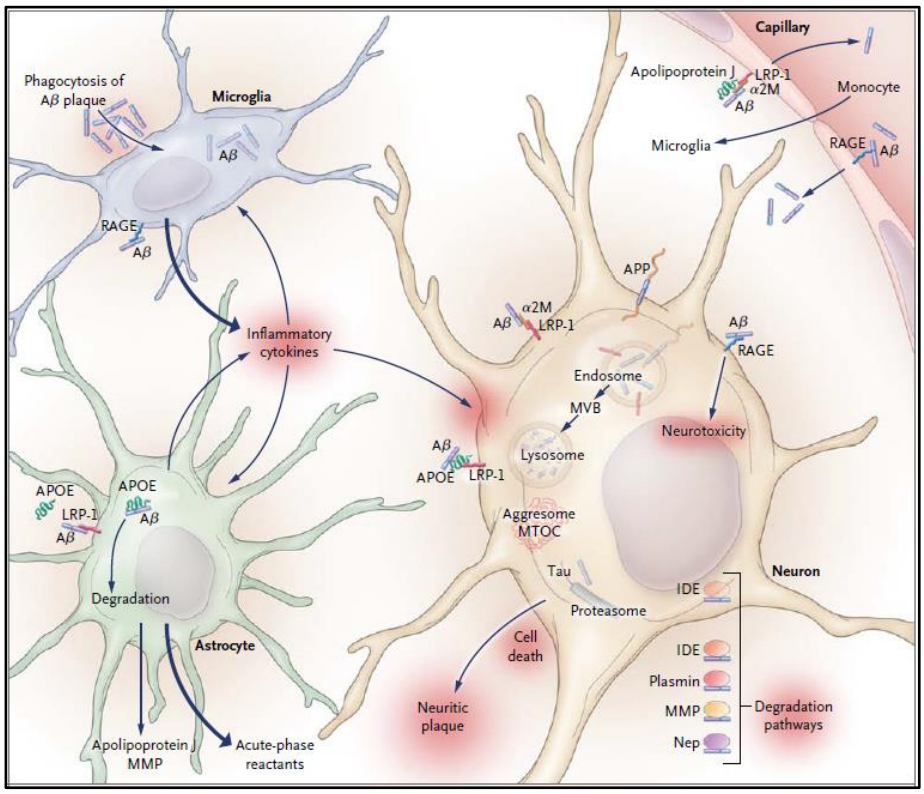

Figure 4: Inflamation and mechanism of Aβ clearance (Querfurth & LaFerla, 2010)

Besides the degradation clearance, one of the most important pathways of Aβ clearance is the efflux of intact soluble Aβ to the peripheral circulation through different routes (Lee & Landreth, 2010). Those include the outflow of amyloid peptides over the brain-blood barrier (BBB) by specialized transport receptors (low-density lipoprotein receptor-related protein 1, very low-density lipoprotein receptor, P-glycoprotein efflux pump and others) and the glymphatic system, that transport wasted protein over to the cerebrospinal fluid (CSF) through the astrocytes endfeet processes which cover

most the parenchymal vasculature (Yoon & Jo, 2012). The characteristic accumulation of Aβ found on the walls of capillaries and arteries in the cerebral amyloid angiopathy (CAA) present in approximately 90% of AD patients seems to reflect a failure in this elimination mechanism (Thal et al., 2008). Furthermore, reactive astrocytes display a downregulation of Aquaporin 4, that can interfere with normal glymphatic flow (Xiao & Hu, 2014; De Strooper & Karran, 2016).

Early astrocyte response play a neuroprotective role by extending their hypertrophic processes to physically separate the neurons from A*β* fibrils (Wegiel *et al.*, 2000). However, A*β* uptake from the extracellular space by interaction with the nicotinic acetylcholine receptor alpha7nAChR (Wang *et al.*, 2000) and A*β* generation from intern APP causes a specific accumulation of amyloid peptides inside neurons, which have been described to triggers early synaptic deficits and neuronal death (Bayer & Wirths, 2010).

A rising number of results points to the synapse lost as a key hallmark of AD (Selkoe, 2002; Mucke & Selkoe, 2012). In non-pathological situations, synaptic homeostatic turnover is controlled by astrocytes through selective trimming in which redundant synapses are eliminated to allow the strengthen of more active inputs (Chung, Allen, *et al.*, 2015). This synaptic pruning is the process underlying the neuronal plasticity and is believed to provide a crucial approach for remodeling and reorganize our nervous system during learning (Yang *et al.*, 2009; Chung, Allen, *et al.*, 2015). Studies done during development had shown that previously opsonized synapsis are recognized and engulfed by microglia (Stevens *et al.*, 2007). Recent findings indicate that the expression of the C1q messenger RNA (mRNA) which points the connections to be removed is dependent of the astroglial secreted factor transforming growth factor-β (TGF-β) (Bialas & Stevens, 2013). This glial regulation of neuronal activity demonstrates the enduring relation existing between neurons and astrocytes.

Moreover, astrocytes itself can prune synapsis by direct phagocytosis by MEGF10 and MERTK receptors by neuronal activity-dependent process promoting circuit refinement (Chung *et al.*, 2013; Chung, Allen, *et al.*, 2015). Strikingly, a recent study has indicated that the C1q/C3 complement-mediated trimming of synapses is inappropriately active and may mediate AD synaptic loss through microglia phagocytosis (Hong *et al.*, 2016). Furthermore, a relation between APOE isoform expressed by astrocytes -the major producers of this protein- and the rate of synaptic pruning by astrocytes has been suggested (Chung *et al.*, 2016).

Because astrocytes normally ensheath synapses, they are in the optimal position to sense and modulate synaptic activity (Chung, Welsh, *et al.*, 2015). In fact, astrocytes are active part of tripartite synapsis, cooperating in the intercellular communication that takes place at the synapsis and modulating neurotransmission (Araque *et al.*, 1999). In response to neural activity, astrocytes show an intracellular Ca^{2+}-elevation and activate the release of gliotransmitters as D-serine, ATP and glutamate, which elicit a neuronal response (Nedergaard & Verkhratsky, 2012; Harada *et al.*, 2016). The mechanism of release of this cells is not well understood, but it appears to be mediated by the intracellular calcium increase

caused by the inositol 1,4,5-trisphosphate release from endoplasmic reticulum (Halassa *et al.*, 2007; Khakh & McCarthy, 2015) and be SNARE-dependent (Henneberger *et al.*, 2010; Navarrete *et al.*, 2012), similarly to what happens in neurons and secretory cells. Astrocyte reactivity seems to impair gliotransmission by a chronic rise in $[Ca^{2+}]_i$ (Halassa *et al.*, 2007) and disrupt astrocytic supportive functions as potassium buffering and uptake of neurotransmitters glutamate and GABA (Tanaka *et al.*, 1997; Rangroo Thrane *et al.*, 2013), resulting in an affected synaptic function and exocytosis. The local changes in network activity patters would progressively affect connected brain structures, followed by the spread of pathology (De Strooper & Karran, 2016).

1.1.4.3 Clinical Phase

Finally, accumulation of unbalance causes the apparition of the clinical symptoms of the AD. Nonetheless, the neurodegeneration in AD is estimated to start 20 to 30 years before the appearance of the first sings of pathology (Goedert & Spillantini, 2006). Currently available evidences demonstrated that Aβ levels decrease in cerebrospinal fluid (CSF) 25 years before the expected onset of dementia, while Aβ deposition is detectable 15 years before onset (Sala Frigerio & De Strooper, 2016). Cognitive impairment, in turn, only shows a detectable deterioration 5 years the dementia outbreak (Wilson *et al.*, 2011), shortening the available time to apply therapeutic treatments. Importantly, animal models research has shown that changes in neuronal network function and cerebral metabolism precede behavioral abnormalities (Ashe & Zahs, 2010; Palop & Mucke, 2010).

Neurotrophic factors are secreted protein that display a main role in synaptic plasticity by regulating the synaptic and neuronal growth, pruning, myelination, differentiation, and survival of neurons (Querfurth & LaFerla, 2010; Budni *et al.*, 2015). Several lines of evidence indicate that levels of these neurotrophins are also severely affected in AD, which can correlate with cognitive decline and lie behind the network dysfunction described in the pathology.

1.1.4.4 MCI: Window of opportunity for treatment

With the aim to classify the patients at the early stages of cognitive deficit that could lead to the development of AD, mild cognitive impairment (MCI) was defined as an intermediate prodromal stage of memory impairment that often, but not invariably, precedes dementia (Petersen et al., 2014). The objective of this classification was to define a temporal window when the treatments could be applied in order to modify the progression of the disease, ideally avoiding -or delaying- the dementia apparition with a retrieval of the cognitive abilities of the subject. The term MCI was introduced in the late 1980s by Reisberg (Reisberg et al., 1988) and its definition has changed since it first statement following changes in diagnostic criteria, being stated at this moment as the absence of dementia, no or minimal functional impairment, subjective cognitive complaints, and objective cognitive impairment (Hampel & Lista, 2016).

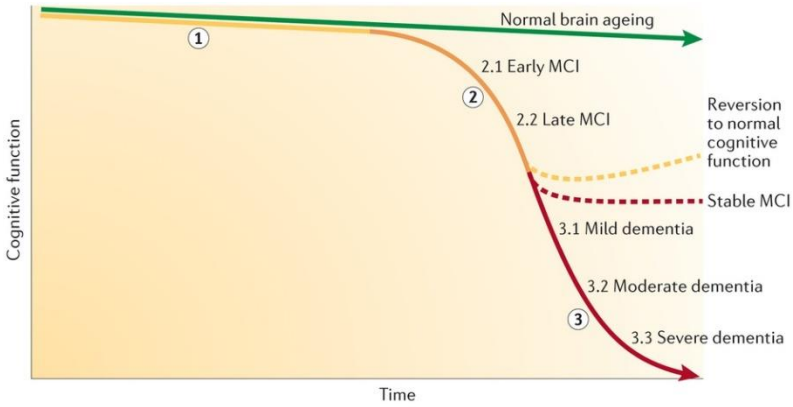

Figure 5: MCI could be a crucial timepoint to apply disease modifying therapy in order to rescue the individual from the AD progression (Hampel & Lista, 2016)

However, the lack of certainty of identification of individuals destined to develop dementia makes imperative to improve the MCI diagnosis by using biomarkers as objective indicators of the underlying AD aetiology in course. Only in this case we will be able to establish a clinico-biological definition for the condition that allow us to differentiate individuals with prospective cognitive decline from those with age-related late-onset memory impairment as well as from those who will not develop progressive cognitive decline (stable MCI). For that is necessary to define the physiopathology of the AD with the aim to determine the early events that allow the definition of proper biomarkers.

1.2 BIOMARKERS

Nowadays, the definitive diagnosis of AD requires post-mortem analysis of the brain to ascertain whether or not the neuropathological signs support the clinical conclusion based on cognitive function tests (Williams, 2011). Besides that, the current criteria to determine the presence of the pathology do not allow to determine precisely how far the disease has progressed until this moment and which is it probable prognosis. The unknowledge of the patient stage provokes a double deadlock: firstly, it prevents the application of a modifying therapy that could change the curse of the disease and, secondly, it frustrates the efforts of the researchers to make progress on the searching of the etiology of the disease, since all the clinical studies have the handicap of not having well characterized subjects, which could be interfering with the results obtaining. To break with this harmful dynamic, biomarkers need to be defined, potentially displaying the biological aging of the brain and the pathophysiological process on going in the CNS. Additionally, this markers need to reflect the pharmacological treatments effects with a high sensitivity, specificity and reproductivity, and, ideally, they should be easy collectible and inexpensive (Blennow, 2005; Zetterberg *et al.*, 2010; Sharma & Singh, 2016), allowing the clinical cases follow up. Within those criteria two categories of biomarkers have been defined: state markers, that reflect the intensity of the disease progress and stage markers, that give a measure of how far the degenerative process has proceeded (Blennow *et al.*, 2003).

Since brain atrophy in temporal lobes and parietal cortices have been related to cognitive impairment progress in AD, structural magnetic resonance imaging (MRI) has been proposed as neuroimaging marker to evaluate the advance of the disease. Together with this exam, fluorodeoxyglucose uptake and radiotracer amyloid retention on positron emission tomography (PET) has shown its utility in the detection of decreases in the glucose metabolism indicating lower synaptic

activity related to neurodegeneration, and Aβ deposits evolution. Collectively, these indicators have provided to have potential value as biomarkers of AD pathology for the detection and prediction of AD before the onset of dementia (Ewers *et al.*, 2011), although further research need to be done to validate them.

CSF has been widely analyzed in search of new biomarkers, since this fluid constitute a window to the undergoing brain activity due to its direct contact with the brain and spinal cord. Even when the access to the sample requires a complex process with limited reproducibility (Sharma & Singh, 2016), the value of the obtained information worth it. Due to the constrain of AD pathology to the CNS, peripheral blood samples are considered poor sources of biomarkers, despite of their accessibility (Zetterberg & Blennow, 2008). CSF profile allows the identification of several biochemical and metabolic profiles reflecting pathogenic processes ongoing in the brain, among which the inflammation and oxidative stress have been related to AD (Lista *et al.*, 2015). However, the high variability associated with those processes and low specificity, as they are commonly found in other neurological diseases, have preclude the establishment of them as widely accepted state biomarkers, although they could be useful as prospective stage progression markers.

Up to now, the most consistent AD CSF signature reside in a decrease of $A\beta_{1\text{-}42}$ related to cortical deposition, and increase in total and phosphorylated Tau (T-Tau and P-Tau) due to cortical neuronal loss and tangle formation, respectively (Blennow *et al.*, 2003). Used in combination, those parameters -known as *core biomarkers*- have reach a high diagnosis accuracy, with 85-90% of sensibility and specificity (Table 4) (Olsson *et al.*, 2016), that justify the progressive incorporation of the CSF biomarkers to clinical care and trials (Alcolea *et al.*, 2014), being supported to become part of the standard clinical criteria (Albert *et al.*, 2011; McKhann *et al.*, 2011).

Biomarker	Pathogenic process	Change in biomarker level in AD and prodromal AD	Comment
Aβ1-42	Amyloidogenic pathway of APP metabolism	Reduced to around 50% of control levels	CSF Aβ1-42 is the central CSF biomarker for brain Aβ metabolism and plaque formation
P-Tau	Tau phosphorylation	Increased to around 200% of control levels	High CSF P-Tau is specific to AD
T-Tau	Neuronal degeneration	Increased to around 300% of control levels	High CSF T-Tau is found in AD but also in other brain disorders with neuronal damage such as stroke and brain trauma non-AD dementias; very high CSF T-Tau, together with normal P-Tau, is found in Creutzfeldt-Jakob Disease

Table 5: Performance of core biomarkers in AD (Blennow *et al.*, 2015)

However, is starting being evident that in the long run we might end up using a collection of biomarkers that could help us to define the pathological process stage underlying the clinical condition of each patient (Zetterberg & Blennow, 2008; Lleó *et al.*, 2015). Currently available markers aid in the final decision of a possible AD case, but it is still needed a proper assortment of markers that could act as flag for the disease events taking place in the brain. Since network dysfunction and synaptic abnormalities are a well characterized feature found in initial stages of AD, an implication of cellular communication abnormalities in early pathological changes is suggested.

1.3 NEUROTRANSMISSION

Considering the progressive loss of neuronal synapsis, a consequent disturbance in neurotransmission have been expected in AD. Because of that, several studies had been performed in the hunt of disturbances that could be present. One of the first reported changes was a significant decrease in choline acetyltransferase activity in post-mortem brain tissues of AD patients, positively correlating with cognitive impairment (Wilcock *et al.*, 1982) and degeneration of the cholinergic nucleus basalis of Meynert (Arendt *et al.*, 1983). Specific degeneration of cholinergic neurons, downregulation of acetylcholine (ACh) synthesis (Sims *et al.*, 1983) and reduced choline uptake (Rylett *et al.*, 1983) and ACh release (Nilsson *et al.*, 1986) have been also reported. Those results, showed deficits on the these neurotransmitter system function, which led to the establishment of the cholinergic hypothesis that advocates for a cholinergic dysfunction as a main AD alteration and was behind of the current available treatments for the disease (Lleó *et al.*, 2006).

Additionally to the cholinergic disturbances, changes in the levels of neurotransmitters have been also detected. Studies done from late 1960s and early 1970s reported a drop-off in monoamine metabolite concentrations, suggesting a breakdown of these neurotransmitter systems (Gottfries *et al.*, 1969). A decreased turnover of dopamine and serotonin was suggested in AD patients affected with severe forms of mental deterioration and senile dementia, since they present most prominent decrease in their metabolites homovanillic acid and 5-hydroxyindoleacetic acid CSF levels (Soininen *et al.*, 1981; Bareggi *et al.*, 1982). As reduced concentrations of neurotransmitters noradrenaline and serotonin -and its receptors- were also present (Keverne & Ray, 2008), a systemic damage of monoaminergic neurons in AD was hypothesized (Strac *et al.*, 2015). Furthermore, CSF and brain tissue alterations in the aminoacidic neurotransmitter gamma-aminobutyric acid (GABA) levels also have been related to AD (Gueli & Taibi, 2013; Strac *et al.*, 2015), adding up this effect to the role played by glutamate and its ionotropic receptor NMDARs in the synapsis loss characteristic of the disease. Hence, on the basis of the existent disturbances in several neurotransmitter systems, had been suggested that AD physiopathology may imply a general dysfunction of neuronal networks affecting globally to the brain activity causing a imbalance between excitation and inhibition (Palop *et al.*, 2007).

Transmitter	Parameter	Change
Acetylcholine	Choline acetyltransferase	↓
	Acetylcholinesterase	↓
	Butyryl cholinesterase	↑
	Acetylcholine release	↓
	Muscarinic receptors	↔ ↓
	Nicotinic receptors	↓
	High-affinity choline uptake	↓
	Nerve growth factor receptors	↓
	Number of neurons	↓
Glutamate	Glutamate	↓
	CSF	↓
Serotonin	Serotonin	↓
	5-hydroxyindoleacetic acid	↔
	Serotonin uptake site	↓ ↔
	$Serotonin_{1A/2}$ receptors	↓
	Number of neurons	↔
Noradrenaline	Noradrenaline	↓
	Dopamine β-hydroxylase	↓
	Number of neurons	↓
Dopamine	Dopamine	↔
	Number of neurons	↔
GABA	Glutamic acid decarboxylase	↓

Table 6: Summary of reported neurochemical changes in Alzheimer's disease.
↓: Decrease, ↑: Increase, ↔: No changes

Besides the effects on the classic neurotransmitters, significant research has been made to determine changes in neuropeptides in the degenerating brain. Neuropeptides, defined as neuronal signaling molecules that function as messenger hormones, neurotransmitters or neuromodulators in the CNS (Dam *et al.*, 2013), have a major effect on conduct as well as other cognitive functions such as memory and learning, so they have been associated with the behavioral and psychiatric signs and symptoms of dementia (BPSD) found in AD. Since the first report of a significant decline of somatostatin in AD patients brain (Davies *et al.*, 1980), several neuropeptides -as vasopressin, neuropeptide Y and substance P- have also been reported to be reduced in AD (Crystal & Davies, 1982; Beal *et al.*, 1986; Fujiyoshi *et al.*, 1987). The origin of those decreases is thought to be a degeneration of the neuropeptide producing neurons, that could be caused by abnormalities in neurotrophin regulation.

Neuropeptide	Cerebral Cortex	Hippocampus	Basal Ganglia	CSF	Others
Corticotrophin Release Hormone	↓ in frontal, temporal and occipital lobes	-	↓	↓	↑ in hypothalamus
Somatostatin	↓	↓	-	↓	-
Neuropeptide Y	↓ or normal	-	↑	↓ or normal	↑ in hypothalamus
Vasopressin	↑ in temporal lobe, normal or ↓ in other areas	↓	↓	↓	↓ in nucleus accumbens
Galanin	-	-	-	↑ or ↓	↓ in serum
Vasoactive Intestinal Peptide	-	-	-	Normal	-
Cholecystokinin	↓ in temporal lobe, normal in other areas	-	-	-	-
Substance P	↓	↓	↓	↓	-
β-Endorphin	-	-	-	↓	-
Dynorphin	↑ in frontal cortex	-	-	↓	-
Leuenkephalin	↑ in frontal cortex	-	-	-	-

Table 7: Concentration of neuropeptides in the brain, CSF and other tissues of AD patients. Modified from (Jiménez-Corral *et al.*, 2006)

Inside neuropeptides transmitters, the neurotrophins are small proteins vital for neuronal and glial growth, differentiation and survival, having a key role on plasticity (Schindowski et al., 2008; Querfurth & LaFerla, 2010). The neurotrophin family includes nerve growth factor (NGF), brain-derived neurotrophic factor (BDNF), neurotrophin-3 (NT-3), neurotrophin-4/5 (NT-4/5) and neurotrophin-6 (NT-6) (Lang et al., 2004), whose effects are mediated by 3 tropomyosin receptor kinase (Trk) receptors (TrkA, TrkB and TrkC) and the 75 kDa neurotrophin receptor (p75 NTR) (Patapoutian & Reichardt, 2001; Bothwell, 2016). Since the knockdown of any of these factors is deleterious or causes severe neural defects (Bartkowska et al., 2010), the neurotrophins are considered essential for the preservation of the normal brain function. An increasing body of evidence points to a lack of growth factors as a cause of neuronal death found in the disease and multiple studies have shown that neurotrophin application may prevent the cell death and support the neuronal proliferation and maturation (Connor & Dragunow, 1998). In fact, has been described that a reduction of NGF levels -as found in basal forebrain cholinergic neurons in AD- leads to cholinergic neuron shrinkage and reduction in fiber density which resulted into decreased cholinergic neurotransmission (Svendsen et al., 1991), as a result of the important role played by this growth factor in development and maintenance of sensory and sympathetic nervous system, cholinergic function of central nervous system, cognition and memory formation (Rylett & Williams, 1994).

As several studies suggest the low bioavailability of neuropeptides as a key factor implicated in the neuronal loss found in AD, to unravel the process that mediate in their release could be crucial to understand their control on the neural function.

1.4 REGULATED SECRETORY PATHWAY

Active neuropeptides are synthetized as precursors by both neuronal and non-neuronal cell types (Seidah et al., 1996). Secretory proteins contain a signal peptide (pre-protein) and the precursor protein (pro-protein), which is farther cleaved to release an N-terminal prodomain peptide and a C-terminal mature active form (Bartkowska et al., 2010; Bothwell, 2016), either within the secretory pathway or following secretion. Intracellularly, this cleavage is done by the proprotein convertases (PCs) processing enzymes furin, PC1/3, PC2, PACE4, PC5 or PC5/6-B (Seidah et al., 1996). In the case of neurotrophins, both neuropeptide forms -proprotein and mature- are released to the extracellular media, the two of them can interact with the receptor and, interestingly, their binding elicits functional opposite effects (Bartkowska et al., 2010), acting in a paracrine and/or autocrine way.

The classical theory of target-derived neurotrophic molecules suggest that neurotrophins are secreted in limited amounts by target tissue and sustain the survival and differentiation of the innervating neurons (Levi-Montalcini, 1987). This requires a fine regulation of neurotrophin signaling, which is controlled in two ways: firstly, by regulation of the expression through the neuronal activity and secondly, by regulation of the release (Lessmann et al., 2003). It have been described that neurotrophic factors are produced by classically considered constitutively secreting cells, as fibroblasts and glial cells, and cells with a proper regulated secretory pathway (RSP), as neurons (Seidah et al., 1996).

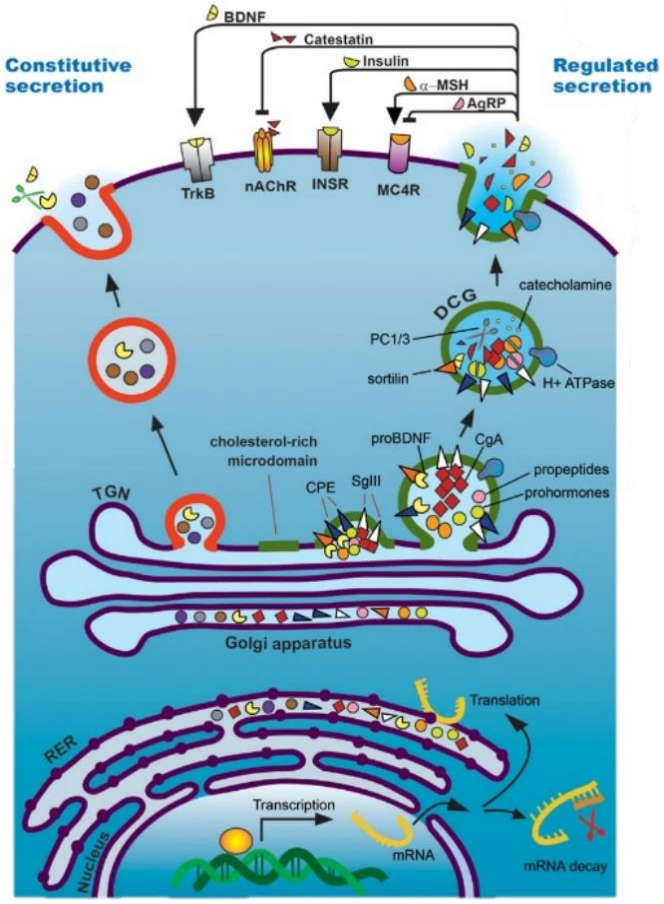

Figure 6: Regulated secretory pathway. (Lin & Salton, 2013)

That so-called signal peptide directs the synthesis of the nascent protein to the endoplasmic reticulum (ER) attached ribosomes, where they are synthesized as pre-proproteins and the signal peptide is cleaved off immediately (Lessmann et al., 2003). Afterwards, the pro-peptides transit to the Golgi apparatus, most likely via intermediate non-clatrin-coated transport vesicles and finally accumulate in the membrane stacks of the trans-Golgi network (TGN).

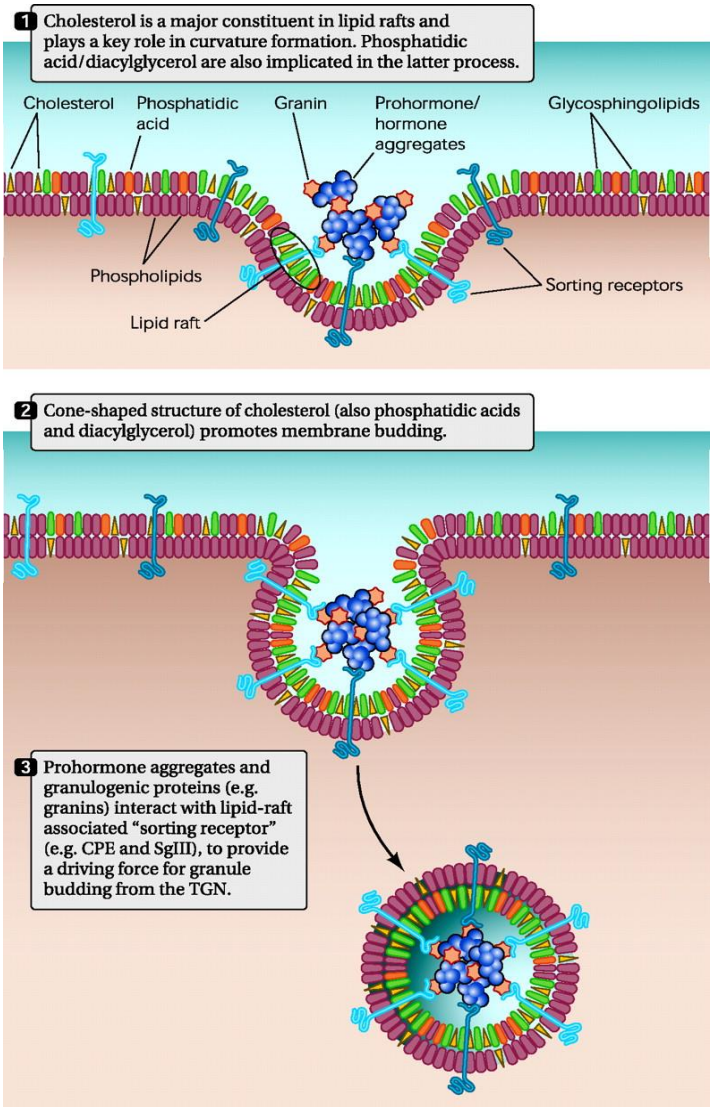

Figure 7: Cargo selection and vesicle budding. (Kim et al., 2006)

At the TGN, neurotrophins, together with neuronal and endocrine peptides and hormones, are aggregated and targeted into immature dense core vesicles (DCVs). Although the sorting of proteins into DCVs is a process not fully understood, interaction of DCV cargo proteins with molecular sorters Carboxypeptidase E (CPE), Secretogranin III (SgIII) and Sortilin is critical. Protein selectors interact with TGN lipid raft, which is essential for docking and cargo concentration of the DCVs that results in vesicle biogenesis. Once the proteins destined to the regulated secretory cargo had been selected, there is an immature secretory granule budding from the TGN, followed a process of maturing that

implies acidification, removal of constitutive secretory proteins and lysosomal enzymes inadvertently packaged, loss of the clathrin coat and other coat proteins, water loss and condensation of granule contends to originate the mature secretory granules. The DCV content includes proteins of the granin family as Chromogranin A (CgA), Chromogranin B (CgB), Secretogranin II (SgII) and SgIII that are believed to participate into the condensation process of the cargo. Also, the prohormone convertases 1/3 and 2 (PC1/3 and PC2) and the exopeptidase CPE, which are necessary for the processing of the RSP proteins, are jointly packaged into the DCVs being their function activated by the pH decrease during the maturing process.

Once the mature granules have been generated, DCV, unlike constitutive secretory vesicles, require an intracellular calcium raise to release their contend to the extracellular media. Since several results have report calcium dyshomeostasis related to AD, the calcium hypothesis was first proposed by Khachaturian which propose that the deleterious effects of Aβ could be depending on a dysregulation of Ca^{2+} signaling (Khachaturian, 1989). Considerable number of evidences support the existence of disturbances of this divalent cation as the increased resting levels found in transgenic animal models of the disease (Kuchibhotla *et al.*, 2008; Lopez *et al.*, 2008) or alteration both in sporadic and in familial cases of AD (Ito *et al.*, 1994; Etcheberrigaray *et al.*, 1998), but there is still controversy regarding if aberrant calcium levels are a cause or a consequence of the Aβ accumulation.

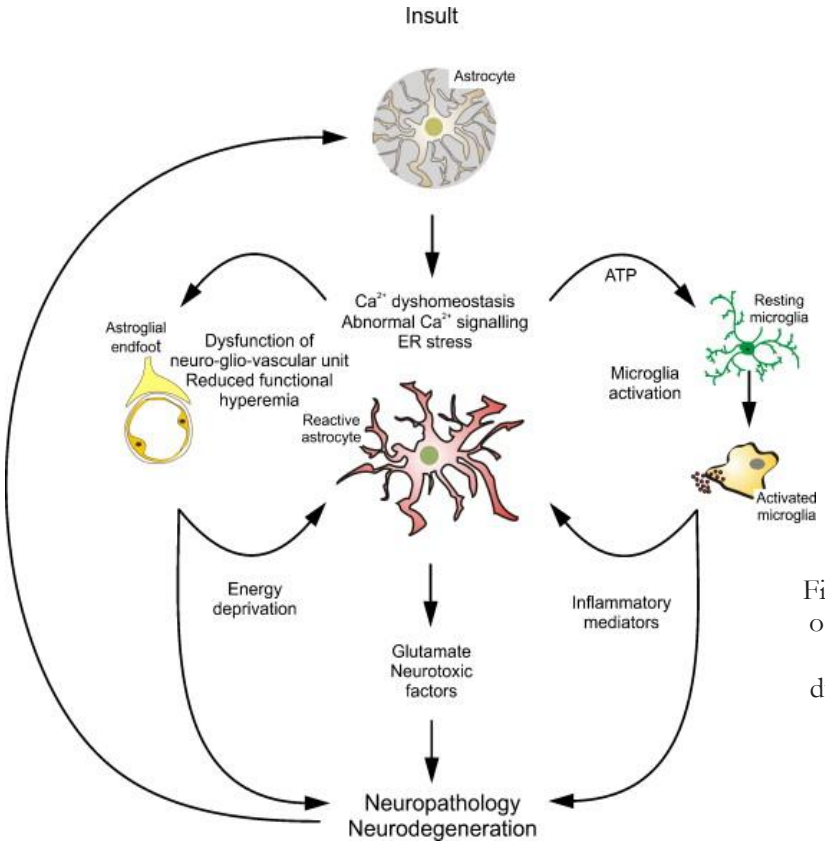

Figure 8: possible implication of Aβ activated astrocytes in calcium dysregulation(Nedergaard et al., 2010)

Due to the critical role of calcium as intracellular messenger, the balance in its concentration is critical to the cellular survival. The calcium buffering is tightly balanced within a narrow physiological range mainly by ER and partially by mitochondria, which act as an intracellular reserves of the ion (Magi *et al.*, 2016). On the event of depolarization, calcium can be released into the cytoplasm from the ER through inositol-1,4,5-triphosphate (IP3R) and ryanodine receptors (RYR). Current results suggest that prolonged intracellular calcium elevation due to the Aβ-triggered excitotoxicity may be a crucial early event in AD pathogenesis (Berridge, 2014). Also, astrocytes are also emerging as active players in the disease, since they are the intrinsic brain defense system, in charge of the maintenance of physiological conditions in the brain (Nedergaard *et al.*, 2010). In response to Aβ accumulation in the late stages of AD, astrocytes become reactive and the tripartite synapsis loss its function through an uncoupling of astroglial calcium oscillations from neuronal activity (Kuchibhotla *et al.*, 2009).

The existent disturbances in neuronal network and neurotransmitters levels, added to the imbalanced neuropeptide levels, suggest an affectation of the cellular communication in the brain. Moreover, the alterations on imbalanced calcium signaling in AD, support the existence of network dysfunction, that could be consequence of an impairment of the regulated secretory pathway, since this process mediates in peptidergic transmission.

2 OBJECTIVES

The general objective of this study is to determine the cortical alterations of peptidergic secretion in Alzheimer's disease.

It will be the object of this work to accomplish the following statements:

1. **Characterize the distribution, production and release dynamics of the cargos of the regulated secretory pathway in the cerebral cortex.**

2. **Determine the possible changes in the dense core vesicle secretion undergoing with aging.**

3. **Analyze the changes in the traffic and release of peptidergic secretory vesicles in response to amyloid neurotoxicity.**

4. **Evaluate the participation of the regulated secretory pathway in the pathophysiology of the Alzheimer's disease.**

5. **Study the existence of correlations between Alzheimer's disease progression and regulated secretory pathway disturbances, in order to evaluate the possible value of DCV proteins as stage biomarkers of the pathology.**

3 DOCTORAL THESIS INFORM

Fernando Aguado Tomás, Doctoral Thesis Director of Virginia Plá Requena, certify that the PhD student has contributed to the four scientific articles as follow:

1 SECRETORY SORTING RECEPTORS CARBOXYPEPTIDASE E AND SECRETOGRANIN III IN AMYLOID β-ASSOCIATED NEURAL DEGENERATION IN ALZHEIMER'S DISEASE

Virginia Plá[1]; Sonia Paco[1]; Gregory Ghezali[1]; Victor Ciria[1]; Esther Pozas[2,3]; Isidro Ferrer[4]; Fernando Aguado[1]

1 Department of Cell Biology, University of Barcelona, Barcelona, Spain
2 August Pi i Sunyer Biomedical Research Institute (IDIBAPS), Barcelona, Spain
3 Institute of Biomedical Research of Barcelona, CSIC, Barcelona, Spain
4 Institute of Neuropathology, IDIBELL-Bellvitge University Hospital, University of Barcelona, CIBERNED, L'Hospitalet de Llobregat, Spain

Brain Pathology 2013 May; 23(3):274-84. doi: 10.1111/j.1750-3639.2012.00644.x.
Impact Factor: 4.354 (Neurosciences, 59/252)

2 AMYLOID-β IMPAIRS VESICULAR SECRETION IN NEURONAL AND ASTROCYTE PEPTIDERGIC TRANSMISSION

Virginia Plá[1, 2], Neus Barranco[1, 2], Esther Pozas[1], Fernando Aguado[1, 2]

1 University of Barcelona, Spain,
2 Institute of Neurosciences of the University of Barcelona, Spain

Frontiers in Molecular Neuroscience 2017 Jun; 28: 10:202. doi: 10.3389/fnmol.2017.00202
Impact Factor: 5.076 (Neurosciences, 42/258)

3 DENSE CORE VESICLE MARKERS DECLINE IN CEREBROSPINAL FLUID AND ACCUMULATE IN DYSTROPHIC NEURITES AND GRANULOVACUOLAR DEGENERATION BODIES IN ALZHEIMER'S DISEASE

Virginia Plá [1,2,*], Neus Barranco [1,2,*], Daniel Alcolea[3,4], Iris Lindberg[5], Reiner Fischer-Colbrie[6], Isidro Ferrer[4,7], Alberto Lleó[3,4] and Fernando Aguado[1,2]

1 Department of Cell Biology, Physiology and Immunology, University of Barcelona, Barcelona E-08028, Spain.
2 Institute of Neurosciences, University of Barcelona.
3 Memory Unit, Department of Neurology, Sant Pau Biomedical Research Institute. Sant Pau Hospital, Autonomous University of Barcelona, Barcelona.
4 Centro de Investigaciones en Red en Enfermedades Neurodegenerativas (CIBERNED), Spain
5 Department of Anatomy and Neurobiology, University of Maryland Medical School, Baltimore, MD, 21201, USA.
6 Medical University of Innsbruck, Institute of Pharmacology, Innsbruck, Austria
7 Institute of Neuropathology, Bellvitge Biomedical Research Institute, Bellvitge University Hospital, University of Barcelona, Hospitalet de Llobregat, Spain.

In preparation

4 DENSE CORE VESICLE CARGOS IN MOUSE CEREBRAL CORTEX AND CEREBROSPINAL FLUID DURING AGING AND IN A MODEL OF ALZHEIMER'S DISEASE

Virginia Plá [1,2], Esther Aso[3], Reiner Fischer-Colbrie[3], Carla Rodríguez[1], Isidro Ferrer [2, 4, 5, 6] and Fernando Aguado[1,2]

1 Department of Cell Biology, Physiology and Immunology, University of Barcelona, Barcelona, Spain
2 Institute of Neurosciences of the University of Barcelona, Spain
3 Medical University of Innsbruck, Institute of Pharmacology, Innsbruck, Austria
4 Institute of Neuropathology, Pathologic Anatomy Service, Bellvitge University Hospital, IDIBELL, Hospitalet de Llobregat, Spain.
5 Department of Pathology and Experimental Therapeutics, University of Barcelona, Spain.
6 Biomedical Network Research Center on Neurodegenerative Diseases (CIBERNED), Institute Carlos III, Hospitalet de Llobregat, Spain.

In preparation

In the four papers included in the doctoral thesis, Virginia Plá Requena has performed most of the experimental work. The work includes experiments on cell cultures, *ex-vivo* preparation, tissues samples, animals, etc. She used an array of cellular, biochemical and molecular techniques. It should be noted that many of the techniques used were optimized by the student. Virginia Plá has also been actively involved in experiment planning, interpretation of results and writing of manuscripts. In the paper corresponding to the human CSF study, the work was equivalently performed by the two first co-authors. So far no other co-author has implicitly or explicitly used this work for another doctoral thesis.

PhD Supervisor

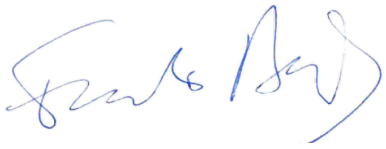

Dr. Fernando Aguado Tomás
Barcelona
Junio 2017

4 CHAPTERS

4.1 Chapter 1: Secretory Sorting Receptors Carboxypeptidase E and Secretogranin III in Amyloid β-Associated Neural Degeneration in Alzheimer's Disease

Brain Pathology ISSN 1015-6305

RESEARCH ARTICLE

Secretory Sorting Receptors Carboxypeptidase E and Secretogranin III in Amyloid β-Associated Neural Degeneration in Alzheimer's Disease

Virginia Plá[1]; Sonia Paco[1]; Gregory Ghezali[1]; Victor Ciria[1]; Esther Pozas[2,3]; Isidro Ferrer[4]; Fernando Aguado[1]

[1] Department of Cell Biology, University of Barcelona, Barcelona, Spain
[2] August Pi i Sunyer Biomedical Research Institute (IDIBAPS), Barcelona, Spain
[3] Institute of Biomedical Research of Barcelona, CSIC, Barcelona, Spain
[4] Institute of Neuropathology, IDIBELL-Bellvitge University Hospital, University of Barcelona, CIBERNED, L'Hospitalet de Llobregat, Spain

Keywords
Alzheimer's disease, astrocytes, carboxypeptidase E, dystrophic neurites, secretogranin III, transgenic.

Corresponding author:
Fernando Aguado, PhD, Department of Cell Biology, University of Barcelona, Av. Diagonal 643, Barcelona E-08028, Spain (E-mail: *faguado@ub.edu*)

Received 22 May 2012
Accepted 12 September 2012
Published Online Article Accepted 24 September 2012

doi:10.1111/j.1750-3639.2012.00644.x

Abstract

The secretory sorting receptors carboxypeptidase E (CPE) and secretogranin III (SgIII) critically activate peptidic messengers and targeting them at the regulated secretory pathway. In Alzheimer's disease (AD), the wide range of changes includes impaired function of key secretory peptidic cargos such as brain-derived neurotrophic factor (BDNF) and neuropeptides. Here, we analyzed CPE and SgIII in the cerebral cortex of AD patients and transgenic mice. In the normal human cortex, a preferential location in dendrites and perikarya was observed for CPE, whereas SgIII was mainly associated with axons and terminal-like buttons. Interestingly, SgIII and CPE were consistently detected in astroglial cell bodies and thin processes. In AD cortices, a strong wide accumulation of both sorting receptors was detected in dystrophic neurites surrounding amyloid plaques. Occasionally, increased levels of SgIII were also observed in plaque associate-reactive astrocytes. Of note, the main alterations detected for CPE and SgIII in AD patients were faithfully recapitulated by APPswe/PS1dE9 mice. These results implicate for the first time the sorting receptors for regulated secretion in amyloid β-associated neural degeneration. Because CPE and SgIII are essential in the process and targeting of neuropeptides and neurotrophins, their participation in the pathological progression of AD may be suggested.

INTRODUCTION

Alzheimer disease (AD) is the most prevalent neurodegenerative disorder, characterized by profound cognitive dysfunction and memory loss. The hallmarks of AD include occurrence of senile plaques and neurofibrillary tangles, synaptic and neural loss, and glia-mediated inflammation (13, 42). Moreover, aberrant function of classical neurotransmitters, neuropeptides and growth factors such as Ach, somatostatin and brain-derived neurotrophic factor (BDNF) is also a feature of this disorder (6, 47, 51). Although the pathogenesis of AD has not been established, identification of amyloid-β (Aβ) as the main component of senile plaques, together with subsequent genetic studies, has sustained the critical role of Aβ in the etiology of AD over the last two decades (45). In fact, considerable effort has been focused on inactivating detrimental effects of Aβ deposits through multiple anti-Aβ therapeutics (18).

Peptidic transmitters in neurons and endocrine cells are targeted, processed and stored in the so-called dense-core vesicles (DCV) and secretory granules, respectively. In response to a physiological signal, secretion of neuropeptides, peptidic hormones and specific growth factors, for example, BDNF, is triggered by regulated exocytosis (7). Aggregates of granin family members with unprocessed peptidic transmitters are critical for the biogenesis of these shuttle organelles (23). Moreover, "secretory sorting receptors" play crucial roles in connecting the core aggregates with the vesicular membrane to target them at the regulated secretory pathway (20, 24). The enzyme carboxypeptidase E (CPE, also known as carboxypeptidase H and enkephalin convertase) proteolytically actives peptidic hormone and neuropeptide precursors (9, 16). In addition to its exopeptidase activity, CPE has been revealed as a key secretory sorting receptor targeting proopiomelanocortin/adrenocorticotropic hormone and pro-BDNF at the regulated secretory pathway in pituitary cells and hippocampal neurons (11, 27). Secretogranin III (SgIII, originally identified as the 1B1075 gene product) has been identified as another secretory sorting receptor, which targets chromogranin A (CgA) at endocrine secretory granules (19). Furthermore, through a cooperative mechanism, proopiomelanocortin-derived peptides have been described as being transferred from CPE to SgIII, and subsequently to CgA for the efficient processing, storage and release of endocrine hormones (21).

Although SgIII and CPE are key components of the regulated secretory pathway, study of them in the central nervous system (CNS) have been poor. Moreover, to the best of our knowledge, analyses of these proteins in the human brain have not yet been performed. Recent reports could implicate these proteins in AD. First, SgIII and CPE are downregulated in the cerebrospinal fluid of AD patients (1, 38). Moreover, *in vivo* CPE elimination leads to neuronal degeneration and memory deficits (49, 50). Here, we analyze the expression of CPE and SgIII in the human cerebral cortex and their changes in AD subjects. Strikingly, aberrant accumulation of these sorting receptors was detected in senile plaques of AD patients. Moreover, the recapitulation of human CPE and SgIII alterations by amyloid-forming transgenic mice suggests a role for Aβ in impairing secretory sorting receptors in AD.

MATERIALS AND METHODS

Human brain tissues

Thirteen non-AD and 11 AD post-mortem human samples (aged 49–81; post-mortem delays between 2.15 and 8.5 h) were obtained from the Institute of Neuropathology Brain Bank IDIBELL-Hospital Universitari de Bellvitge (Hospitalet de Llobregat, Spain) following approval by the local ethics committee. Subjects were selected on the basis of post-mortem diagnosis of AD according to Consortium to Establish a Registry for Alzheimer's Disease (CERAD) criteria (31). AD cases corresponded to Braak stages V and VI. No neurological symptoms or signs were recorded in control cases.

Transgenic mouse

The experiments were carried out on male APPswe/PS1dE9 mice (n = 4) and wild-type littermates (n = 4) from The Jackson Laboratory (Bar Harbor, ME, USA) (22). Genotypes were identified by polymerase chain reaction (PCR) amplification of tail DNA. The animal colony was kept under controlled temperature (22 ± 2°C), humidity (40–60%) and light (12-h cycles) conditions, and treated in accordance with the European Community Council Directive (86/609/ECC). The study was approved by the local ethical committee (University of Barcelona).

Antibodies

Polyclonal antibodies against SgIII were purchased from Sigma-Aldrich (Diesenhofen, Germany) and Proteintech Group Inc. (Chicago, IL, USA). Monoclonal and polyclonal antibodies against CPE were obtained from BD Transduction Laboratories (San Jose, CA, USA) and Proteintech Group Inc., respectively. Antibodies against glial fibrillary acidic protein (GFAP), β-actin, Aβ, AT8 and voltage-dependent anion channel (VDAC) were from Millipore Iberica (Madrid, Spain), DAKO (Glostrup, Denmark), Innogenetics (Gent, Belgium) and Calbiochem (La Jolla, CA, USA).

Immunohistochemistry

Human and mouse samples were fixed in 4% paraformaldehyde in 0.1 M phosphate buffer, pH 7.4, by immersion and intracardiac perfusion, respectively. Animals were perfused under deep anesthesia (ketamine hydrochloride/xylazine hydrochloride). Brain samples were cryoprotected in a 30% sucrose solution, frozen and sectioned with a cryostat. For peroxidase immunohistochemistry, histological sections were soaked for 30 minutes in phosphate buffered saline (PBS) containing 10% methanol and 3% H_2O_2 and subsequently washed in PBS. Pretreatment with formic acid was used to enhance labeling of plaques. To suppress nonspecific binding, brain sections were incubated in 10% serum-PBS containing 0.1% Triton X-100, 0.2% glycine and 0.2% gelatin for 1 h at room temperature. Incubations with the primary antibodies were carried out overnight at 4°C in PBS containing 1% fetal calf serum, 0.1% Triton X-100 and 0.2% gelatin. SgIII and CPE detection in human and mouse brains was indistinctively performed with antibodies from different sources. Immunoglobulin binding was detected with the avidin-biotin-peroxidase method (Vectastain ABC kit, Vector Laboratories Inc., Burlingame, CA, USA). The peroxidase complex was visualized by incubating the sections with 0.05% diaminobenzidine and 0.01% H_2O_2 in PBS. Some immunoreactions were enhanced with the cobalt-nickel coprecipitation technique. Sections were mounted, dehydrated and coverslipped in Eukitt® (Sigma-Aldrich).

For double-label peroxidase immunohistochemistry, the first immunostaining was performed as above. The second immunolabeling reaction was developed in a medium containing 0.01% benzidine dihydrochloride, 0.025% sodium nitroprusside (Merck, Darmstadt, Germany) and 0.005% H_2O_2 in PBS, pH 6 (37). Double-label fluorescent immunohistochemistry was performed by incubation with different fluorochrome-conjugated secondary antibodies (Alexa Fluor 488 and Alexa Fluor 568, Molecular Probes, Eugene, OR, USA), and cell nuclei were stained with 4',6-diamidino-2-phenylindole (Molecular Probes). Endogenous autofluorescence was quenched by Sudan Black B (Sigma-Aldrich) treatment. Sections were mounted with Mowiol (Merk Chemicals Ltd., Nottingham, UK) and observed with a Leica TCS SPE scanning confocal microscope. The specificity of the immunostaining was tested by preincubating the primary antibodies with an excess of antigen (Proteintech Group Inc.), replacing the primary antibodies with an equivalent concentration of nonspecific IgG and omitting them. No immunostaining was observed in these conditions.

Electron microscopy

APPswe/PS1dE9 and wild-type mice aged 9 months were deeply anaesthetized prior to intracardiac perfusion with 4% paraformaldehyde and 0.1% glutaraldehyde. Brains were removed, dissected and then postfixed by immersion in 1% osmium tetraoxide. Tissue specimens were embedded in epon-812 (Electron Microscopy Sciences, Hatfield, PA, USA) and cut with an ultramicrotome. Semithin sections of the hippocampus, entorhinal cortex and neocortex were stained with toluidine blue, and selected ultrathin sections (70 nm) were subjected to an etching treatment in order to expose hidden antigenic sites. Ultrathin sections were incubated in a blocking and quenching free-aldehyde solution prior to incubation with the primary antibodies. After washing, the sections were incubated in a gold-conjugated secondary antibody (Agar, Monocomp, Madrid, Spain) and directly visualized with a Jeol Jem 1011 electron microscope (JEOL GmbH, München, Germany).

Western blotting

Human brain tissues were homogenized in ice-cold lysis buffer containing 50 mM Tris-HCl pH 7.4, 150 mM NaCl, 5 mM $MgCl_2$, 1 mM EGTA, 1% Triton X-100 and protease inhibitor cocktail (Roche Diagnostics GmbH, Mannheim, Germany). Samples of postnuclear lysates were electrophoresed in 12% SDS-PAGE (Bio-Rad Laboratories, Hercules, CA, USA) and then transferred to nitrocellulose membranes (Whatman® Schleicher & Schuell, Keene, NH, USA). The membranes were blocked in a solution containing 5% nonfat milk powder in Tris-buffered saline and Tween 20 (TBST; 140 mM NaCl, 10 mM Tris/HCl, pH 7.4 and 0.1% Tween 20) for 1 h at room temperature and then incubated with primary antibodies in blocking buffer for 2 h at room temperature. SgIII and CPE were detected with antibodies from Sigma-Aldrich and BD Transduction Laboratories, respectively. After several washes in blocking solution, the membranes were incubated for 1 h with horseradish peroxidase-conjugated secondary antibodies (DAKO). Bound antibodies were visualized with enhanced chemiluminescence reagents ECL™ (GE Healthcare, Buckinghamshire, UK). Blot images were captured with a scanner.

RESULTS

CPE and SgIII are distributed in specific neuronal and astroglial microdomains in the human cerebral cortex

To study CPE and SgIII in the human cerebral cortex, we performed an immunocytochemical analysis of samples from autopsies with different well-validated antibodies. We examined cortical areas typically affected in AD, such the neocortex, the entorhinal cortex, the subiculum and the hippocampal formation. In general, we found that both proteins were abundant in all analyzed cortices, although CPE immunostaining was more intense and more extended than that for SgIII. Both proteins were widely detected through the gray and white matter, associated with neuronal and non-neuronal cell bodies and processes (Figures 1–3). Similar results were consistently obtained using antibodies from different sources (data not shown).

In the neocortex, robust CPE immunolabeling was detected filling dendrites and neuronal perikarya. Dendritic staining was found mainly in apical shafts running across the entire thickness of

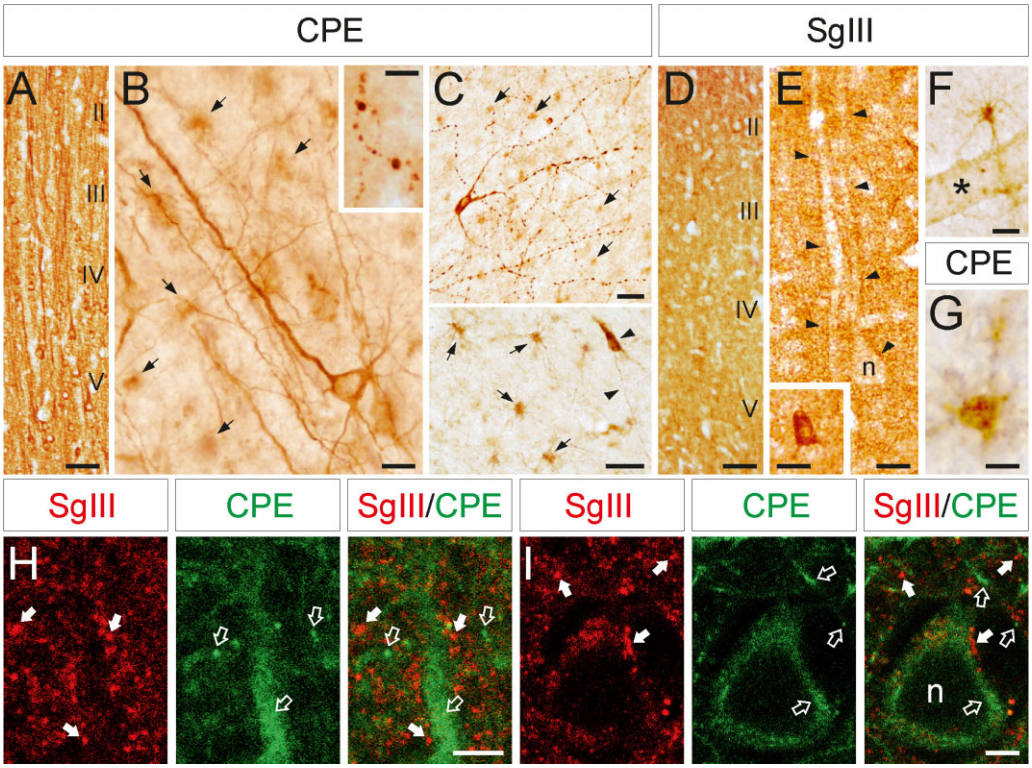

Figure 1. CPE and SgIII protein expression in the neocortex. (**A,B**) In the gray matter, an intense CPE immunoreaction is abundantly located in dendrites and neuronal perikarya through all cortical layers (**A**), especially in inner levels (**B**), whereas varicose axons (inset in **B**) and glial-like cells (arrows in **B**) are occasionally and faintly labeled, respectively. (**C**) Two different images showing neuronal somata and processes (arrowheads) and numerous fibrous astrocytes (arrows) immunolabeled for CPE in the white matter. (**D,E**) SgIII is detected in punctuate structures through the neuropil (**D**), outlining neuronal perykaria and proximal dendrites (arrowheads in **E**), and in interneuron somata (inset in **E**). (**F,G**) A granular immunoreaction for both SgIII (**F**) and CPE (**G**) is located in fibrous astroglial cell bodies and processes. (**H,I**) Confocal double immunofluorescence showing the location of SgIII (arrows) and CPE (open arrows) in the neuropil (**H**) and a neuronal soma (**I**). Note how most punctate structures and dendrite shafts are differentially labeled for SgIII and CPE. Scale bar in μm: **A** and **D**, 100; **B** and **E–G**, 25; **C**, 50; inset in **B**, 10; inset in **E**, 25; **H** and **I**, 5. n = nucleus; asterisk = blood vessel.

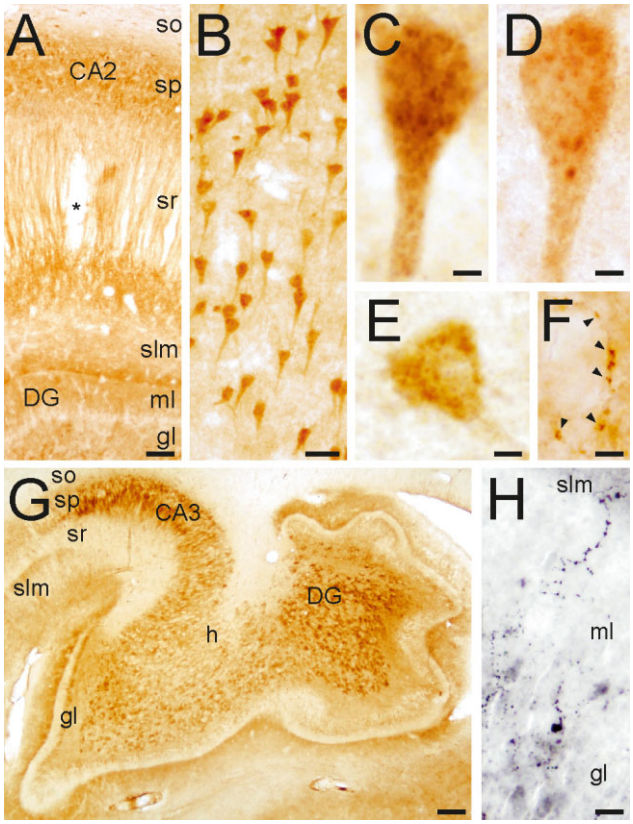

Figure 2. CPE and SgIII protein expression in the hippocampus. (**A**) CPE distribution in the hippocampus. (**B**) Pyramidal cell bodies labeled for SgIII. (**C**,**D**) Granule-like compartments stained for SgIII (**C**) and CPE (**D**) in CA1 pyramidal neurons. (**E**) A CPE-positive interneuron in the stratum oriens. (**F**) CPE-labeled terminal-like buttons on a negative soma in the hilus. (**G**) Pattern of SgIII immunolabeling in CA3 and the dentate gyrus. (**H**) SgIII varicose fibers in the inner portion of the molecular layer of the dentate gyrus. Scale bars in μm: **A**, 150; **B**, 50; **C-F**, 5; **G**, 1000, **H**, 25. Abbreviations: so = stratum oriens; sp = stratum pyramidale; sr = stratum radiatum; slm = stratum lacunosum-moleculare; ml = molecular layer; gl = granular layer; h = hilus; DG = dentate gyrus.

the cortex (Figure 1A). The strongest immunoreactive somata were located in inner cortical layers, including pyramidal and multipolar neurons. CPE immunoreactivity was also detected in some varicose axons and slightly in glial-like cells (Figure 1B). In the white matter, scattered pyramidal/polymorphic and fusiform neurons displayed high levels of CPE in the superficial and deep regions, respectively (Figure 1C). Neuronal varicose processes and numerous astroglial-like cells were positive for CPE in different myelinated areas (Figure 1C,G).

Of note, a differential immunolabeling pattern was found in the gray matter of neocortex for SgIII compared with CPE. Faint SgIII labeling was detected within large pyramidal cell bodies (Figure 1D). Somatic SgIII was mainly restricted to perinuclear secretory organelles, whereas labeling in dendritic shaft was weak or absent (Figure 1E). Characteristically, SgIII was found as immunoreactive puncta throughout the neuropil, occasionally outlining neuronal perykaria and proximal dendrites (Figure 1E). Scattered interneurons exhibited intense SgIII immunoreactivity (inset in Figure 1E). Some glial-like cells and processes in the outer layers also displayed this granin. In the white matter, astrocyte-like cells and deep fusiform neurons were weakly labeled for SgIII (Figure 1F).

The differential distribution of CPE and SgIII in neuronal microdomains of the isocortex was further substantiated by double confocal immunofluorescence. Numerous SgIII-containing puncta were detected in the neuropil and frequently opposite CPE-positive somata and dendrites of pyramidal neurons (Figure 1H,I). Only a few SgIII-immunofluorescent puncta also exhibited CPE signal. Moreover, a differential location was also detected inside large pyramidal cell bodies. CPE entirely filled the perikaryon, whereas SgIII antibodies faintly labeled structures around the nucleus, apparently not overlapping with CPE (Figure 1I).

In the entorhinal cortex, subicular complex and the hippocampus, the immunolabeling pattern of CPE was similar to that detected in the neocortex. Pyramidal and nonpyramidal neurons displayed intense CPE staining in dendritic shafts and perikarya (Figure 2A,D,E). In dentate gyrus and CA regions CPE was mainly detected in dendrites with a prominent laminar distribution, whereas perikarya and proximal dendrites of subiculum and entorhinal cortex were strongly labeled (Figure 2A). Subcellular structures labeled for CPE included somatic and dendritic granular compartments, varicose fibers and terminal-like buttons

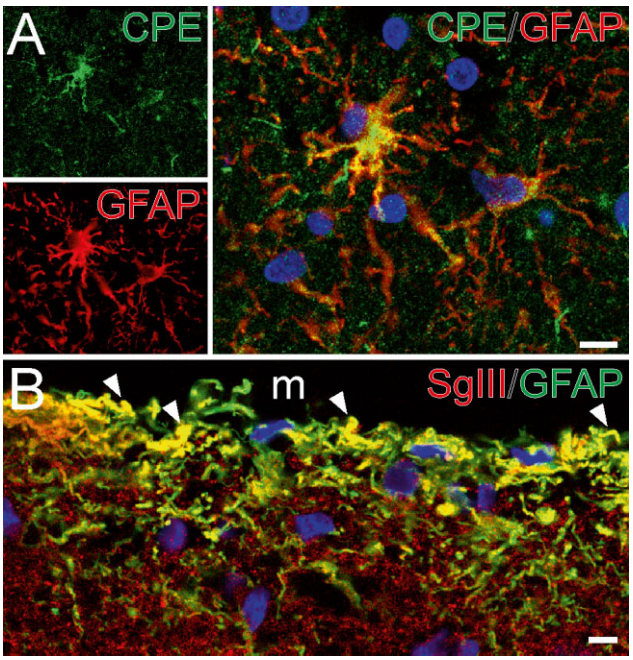

Figure 3. Astroglial-identified cells express CPE and SgIII in the cerebral cortex. (**A, B**) Confocal images illustrating double immunofluorescence of CPE and SgIII with GFAP in the white matter (**A**) and the upper layers of the parietal cortex (**B**). Note the location of CPE in the perinuclear area and processes of astrocytes. In **B**, SgIII decorates punctuate structures and thin processes exhibiting GFAP. Arrowheads indicate yellow color in merge images. Nuclei are in blue color. Scale bar in μm: **A**, 10; **B**, 5. M = meninge.

(Figure 2D–F). The pattern of SgIII immunolabeling in the entorhinal cortex was equivalent to that of the isocortex, where neural somata and dendrites lacked this granin. In the hippocampus, mossy fibers and the hilus were strongly labeled for SgIII (Figure 2G). Neuronal perykaria contained abundant SgIII in CA and subicular regions (Figure 2B,C). Marked SgIII immunoreaction was detected in varicose fibers located in the inner portion of the molecular layer of the dentate gyrus and the pyramidal layer of CA2 (Figure 2H). Typically, puncta immunoreactive for SgIII outlined pyramidal dendrites in CA2 (data not shown). Glial-like cells positive for CPE and SgIII were mainly detected in the white matter.

Finally, we determined whether non-neuronal cells labeled for CPE and SgIII in the human brain corresponded with astrocytes by using double immunofluorescence. Star-shaped cells displaying CPE were consistently decorated with the astroglial marker GFAP in several cortical areas (Figure 3A). This colocalization was particularly obvious in fibrous astrocytes of the white matter (Figure 3A). CPE labeling was located in astroglial cell bodies and processes, occasionally detected as a granule-like structure (Figure 1G). Similar results were obtained for SgIII in GFAP-identified astrocytes, however, as occurs in neurons, SgIII labeling in astrocytes was weaker than that found for CPE. Characteristically, many glial processes in the outer layers of the cortex, most likely glia limitants and interlaminar astrocytes, were differentially labeled for SgIII (Figure 3B).

Taken together, these results show that CPE and SgIII are widely expressed by neuronal and astroglial cell populations in the human cerebral cortex. Moreover, a differential targeting of these sorting receptors is strikingly evidenced in microdomains of specific neuronal subsets.

CPE and SgIII are aberrantly accumulated in cortical plaques of AD patients

To investigate alterations in CPE and SgIII in AD, we performed immunological analyses of the cerebral cortex of patients and age-matched controls. With Western blotting, a robust band around 55 kDa for CPE was detected in cortical tissues, whereas SgIII mainly displayed two greater bands corresponding to the precursor and mature forms (Figure 4A). No differences were found in the intensity or the electrophoretical mobility of the bands in the hippocampus (Figure 4A) and neocortex (data not shown) of AD patients (n = 6) compared to controls (n = 6).

Although total levels of CPE and SgIII were preserved in the AD cortices, dramatic changes in these two proteins were revealed in the AD cerebral cortex (n = 6) compared with controls (n = 7) with immunocytochemistry (Figure 4B–F). In general, distribution patterns of CPE and SgIII appeared normal in nonplaque areas of AD brains. Some sample-to-sample variability in the labeling intensity was detected in pyramidal cell bodies, likely related to differences in specimen processing. A striking accumulation of sorting receptors was widely found in senile plaques (Figure 4C,D). CPE- and SgIII-positive plaques were detected in the neocortex, mainly in superficial layers. In

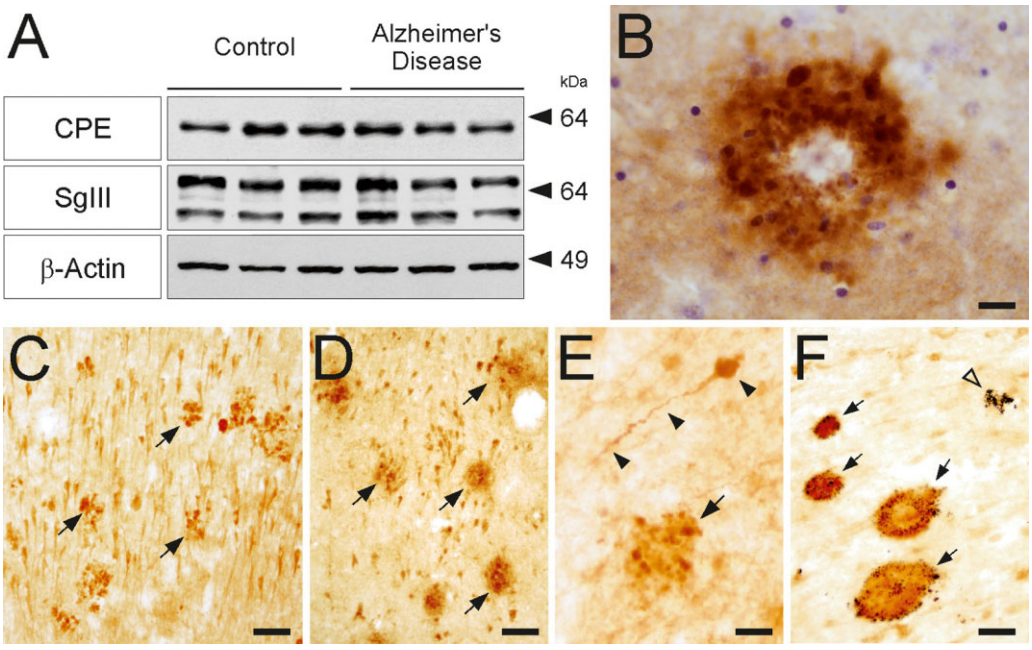

Figure 4. CPE and SgIII are accumulated in senile plaques of AD patients. (**A**) Western blots showing protein levels of CPE and SgIII in homogenates of hippocampus from AD patients and age-matched controls. Densitometric analyses revealed no significant differences among groups in protein expression levels, normalized to β-actin ($P > 0.05$). The mobility of molecular mass markers (in kDa) is indicated. (**B**–**F**) Aberrant accumulation of SgIII (**B**,**D**,**F**) and CPE (**C**,**E**) are consistently detected in AD plaques of different areas. (**B**) SgIII-labeled corona plaque in upper layers of the neocortex, Nissl counterstaining in blue. (**C**,**D**) Arrows indicate numerous plaques in the CA1 region of the hippocampus. (**E**) CPE-positive dystrophic neurite (arrowheads) and a plaque (arrow) in the white matter. (**F**) Double immunostaining against SgIII (brown) and Aβ (blue) in the hippocampus showing four double-labeled senile plaques (arrows) and one lacking SgIII. Scale bar in μm: **B**, 20; **C**,**D** and **F**, 50; **E**, 15.

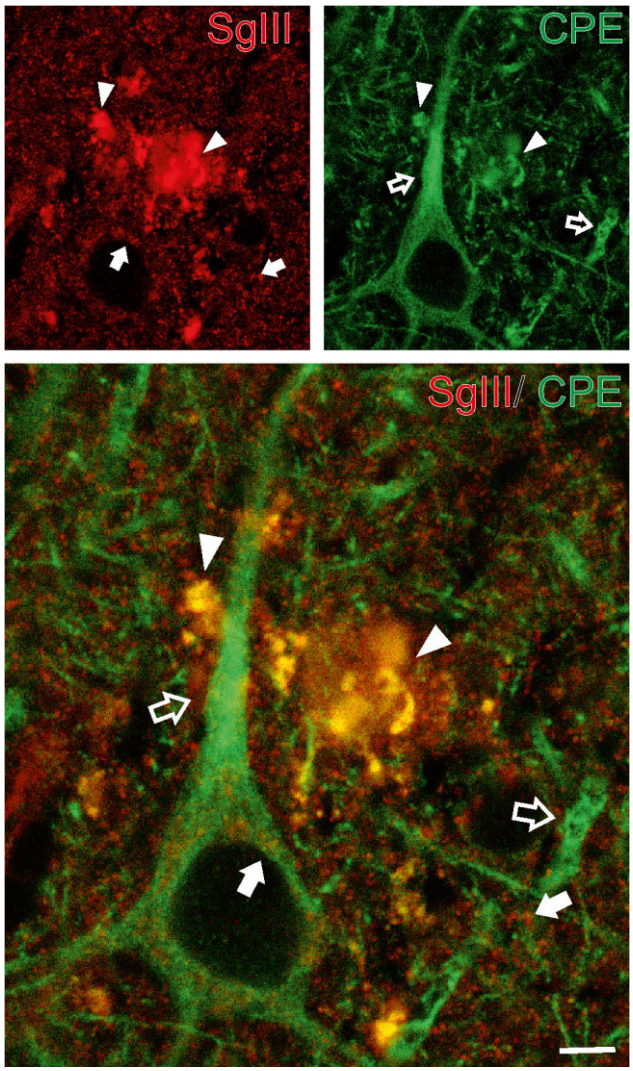

Figure 5. Colocalization of SgIII with CPE in AD senile plaques. Confocal images showing double immunofluorescence of SgIII and CPE in layer V of the parietal cortex. Aberrant plaque structures display a high grade of overlapping (yellow color in merge image, arrowheads). Note the differential distribution of SgIII (arrows) and CPE (open arrows) in the neuropil and subcelullar locations around the nucleus. Scale bar: 5 μm.

decreasing order, the sorting receptors were also observed in the entorhinal cortex, subiculum, CA1 hippocampal region, molecular layer of the dentate gyrus and myelinated tracts. Double immunocytochemistry showed that more than 90% the Aβ-labeled plaques were positive for CPE and SgIII (Figure 4F). We observed different degrees of colocalization of CPE and SgIII in senile plaques. Major overlapping between these proteins was frequently detected in the same plaque (Figure 5), although low colocalization and even single-labeled plaques were also observed (data not shown).

To identify structures accumulating secretory sorting receptors in AD plaques, different markers were used (Figures 6,7). Only a small amount of CPE and SgIII labeling colocalized with Aβ deposits (Figure 6). Because an array of proteins destined for secretion has been shown to co-deposit with Aβ in senile plaques (46), extracellular accumulation of secreted CPE and SgIII is conceivable. Most of the aberrant CPE and SgIII signal in plaques was associated with cellular structures in the vicinity of both diffuse and focal Aβ deposits (Figure 6). Typically, focal Aβ deposits were surrounded by a CPE- and SgIII-immunoreactive corona (Figure 4B). Neuritic identity of CPE- and SgIII-containing structures was determined by AT8 and VDAC immunolabeling. Dystrophic neurites identified by the pathological phosphorylated form of tau, recognized by AT8 antibodies, were also decorated for CPE and SgIII (Figure 6). Moreover, both sorting receptors colocalized with the mitochondrial porin VDAC (Figure 6). Interestingly, CPE and SgIII colocalizations with dystrophic neurite markers were partial. This observation suggests that a subpopulation, or certain microdomains, of degenerating neurites specifically accumulates these sorting receptors. Because CPE and SgIII are also expressed by astrocytes, we performed double labeling with GFAP to determine alterations in plaque-surrounding activated glia. Detailed inspection of immunofluorescence revealed that levels of sorting receptor were occasionally increased in reactive astrocytes, mainly for SgIII (Figure 7).

Finally, we evaluated whether CPE and SgIII accumulate in the other hallmark of AD, the neurofibrillary tangles. As AT8 labeling evidenced, no changes in the level of sorting receptors were found in tangle-bearing neuronal somata (data not shown).

We conclude that CPE and SgIII are aberrantly accumulated in degenerating neurites and activated astroglia of AD plaques.

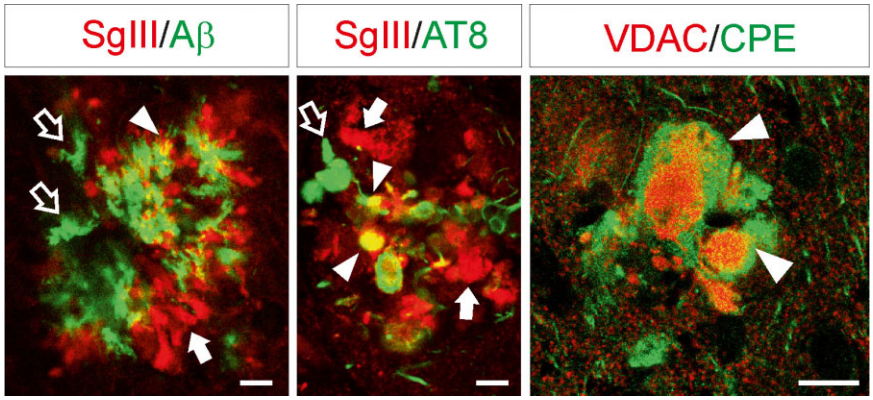

Figure 6. Dystrophic neurites aberrantly accumulate SgIII and CPE. Confocal double immunofluorescence of SgIII with Aβ and the dystrophic neurite markers AT8 and VDAC in senile plaques of the parietal cortex. SgIII poorly and moderately colocalize with Aβ and AT8, respectively (arrowheads). Arrows and open arrows indicate single labeling structures. Image on the right shows pathological enlarged neurites accumulating CPE, the core of which exhibits VDAC. Scale bar: 10 μm.

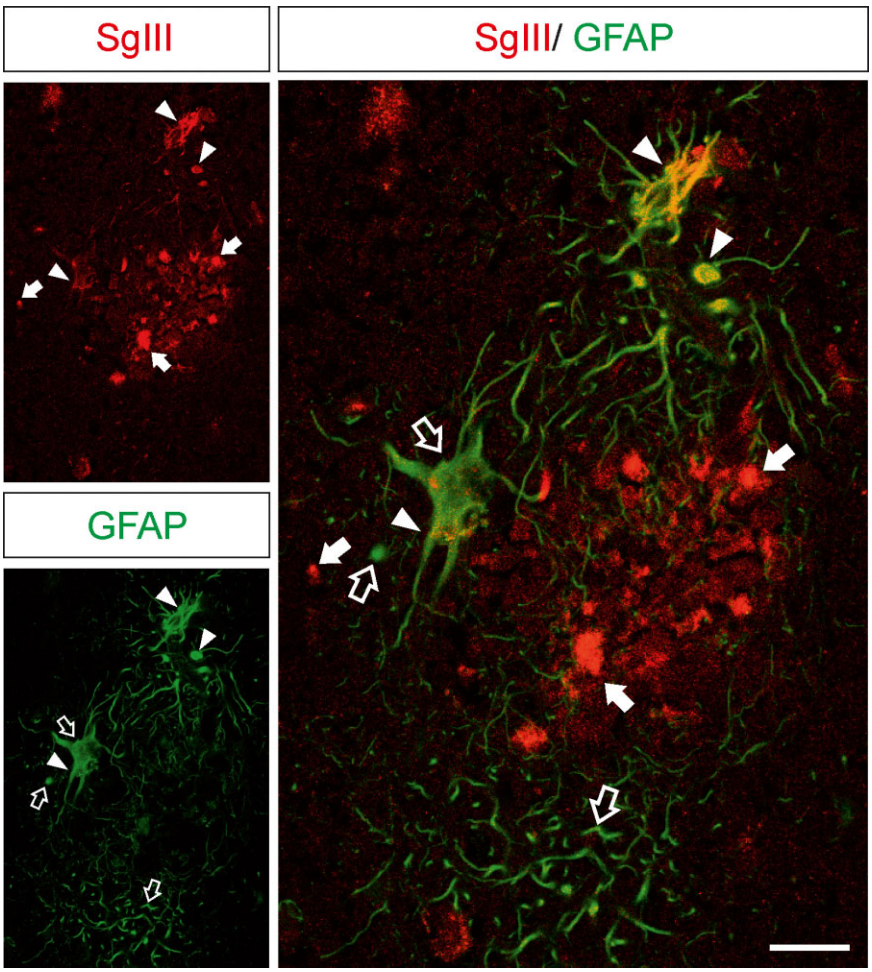

Figure 7. Increased levels of SgIII in plaque-surrounding reactive astrocytes. Confocal double immunofluorescence of SgIII and GFAP in the AD hippocampus. Hypertrophied GFAP-labeled astrocytes that surround an amyloid plaque aberrantly contain high levels of SgIII. Arrows and open arrows indicate single labeling structures. Yellow color in merge image indicates colocalization (arrowheads). Scale bar: 25 μm.

APPswe/PS1dE9 transgenic mice mimic the CPE and SgIII alterations found in AD subjects

Because Aβ plays a key role in contributing to the main alterations of AD, we next investigated the Aβ involvement in CPE and SgIII changes *in vivo*. We used amyloid-forming transgenic mice APPswe/PS1dE9. In these mice, the APPswe mutation causes Aβ deposits, whereas the dE9 variant of PS1 accelerates the amyloid pathology as early as 6 months of age (22). CPE and SgIII protein expression were analyzed in 12-month-old transgenic and wild-type animals. In general, the distribution pattern for both proteins in the mouse brain was similar to that in the human brain (data not shown). In control mice, strong CPE labeling was frequently detected in neuronal dendrites and perikarya, whereas a weaker signal for SgIII was observed mainly associated with punctate structures and fibers. Moreover, both SgIII and CPE were detected in astroglial cells. Of note, intense labeling for CPE and SgIII was found in numerous plaques through all the CNS of transgenic mice. These accumulations were evident in regions such as the cerebral cortex, striatum, thalamus and cerebellum (Figure 8). As in AD patients, CPE and SgIII were aberrantly accumulated in the same plaques, where a high degree of colocalization was frequently observed (Figure 9A,B). Double labeling of CPE and SgIII with AT8, VDAC and Aβ showed that sorting receptors were mainly accumulated in dystrophic neurites surrounding Aβ deposits (data not shown). To identify subcellular structures containing CPE and SgIII in degenerating neurites we performed immunogold labeling. At the ultrastructural level, dystrophic neurites were packed with heterogeneous collections of vesicular and vacuolar structures, including single- and double-membrane organelles, and they were commonly filled with dense or multilamellar contents (Figure 9C,D). CPE and SgIII labeling in dystrophic neurites was associated with enlarged and autophagic-like vesicles, indicating abnormal forms of vesicular compartments.

These results show that amyloid-forming transgenic mice accurately recapitulate the aberrant CPE and SgIII accumulation detected in AD dystrophic neurites.

DISCUSSION

In the present study, we show new and compelling evidence implicating the sorting receptors of the regulated secretory pathway in the Aβ-induced neurodegeneration of AD. We report for the first time the specific distribution of CPE and SgIII in neuronal and glial cells in the healthy human brain. Moreover, a dramatic accu-

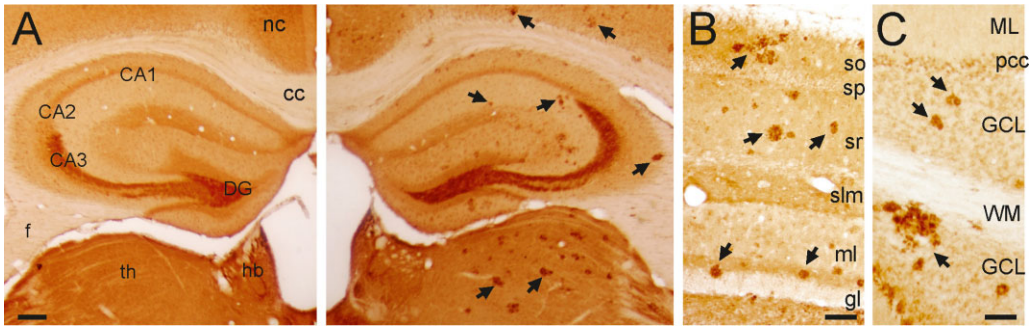

Figure 8. SgIII and CPE accumulation in APPswe/PS1dE9 mice. (**A**) SgIII distribution in wild-type (left) and transgenic (right) mice. Strong SgIII accumulation is associated in plaques through hippocampus, neocortex and thalamus of the APPswe/PS1dE9 mouse. In both genotypes, mossy fibers are intensely labeled. (**B**) Higher magnification of the transgenic hippocampus immunolabeled for SgIII. (**C**) CPE-positive accumulations in the APPswe/PS1dE9 cerebellar cortex. Scale bars: **A**, 250 µm; **B** and **C**, 100 µm. Abbreviations: nc = neocortex; cc = corpus callosum; CA = regions of the hippocampus; f = fimbria; hb = habenula; th = thalamus; DG = dentate gyrus; so = stratum oriens; sp = stratum pyramidale; sr = stratum radiatum; slm = stratum lacunosum-moleculare; ml = molecular layer; gl = granular layer.

mulation of these sorting receptors in senile plaques of AD patients and Aβ-forming transgenic mice is demonstrated.

CPE and SgIII in the human cerebral cortex

In general, the distribution patterns of CPE and SgIII shown in this study are in agreement with those formerly found in rodents (29, 34). However, some differential features were observed for the human brain. First, we found immunolabeling for these two proteins, robustly for CPE, in neuronal populations in both the superficial and the deep white matter, whereas no information of this kind has been reported for rodents. Moreover, human fibrous and interlaminar-like astrocytes widely display CPE and SgIII. In rodents, SgIII, but not CPE, was recently reported in astrocytes *in situ*, mainly protoplasmic cells (37). Although differences related to antibody cross-reactivity cannot be ruled out, species-specific features in CPE and SgIII expressions are suggested. In fact, several distinctions have been shown between human white matter neurons and astrocytes and those of rodents (17, 33).

One of the most striking observations of this study is the differential localization of CPE and SgIII in neuronal subsets. A nice study performed by Hosaka *et al* (21) demonstrated colocalization and functional interaction between SgIII and CPE to facilitate prohormone sorting in endocrine secretory granules. Therefore, an overlapping localization for these sorting receptors would be expected in subcellular neuronal domains. However, although both

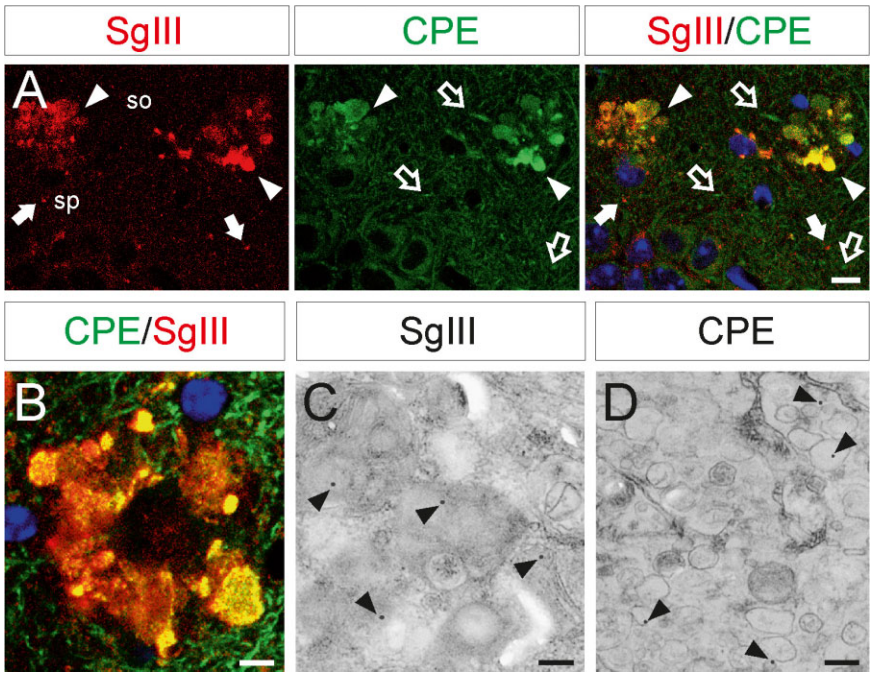

Figure 9. CPE and SgIII accumulation in dystrophic neurites of transgenic mice. CPE and SgIII colocalization in degenerating neurites in the CA1 region of the hippocampus (upper images) and somatosensorial cortex (lower image) by double confocal immunofluorescence. Blue color labels cell nuclei. Ultrastructural images show immunogold staining of SgIII and CPE in autophagic-like (left) and enlarged (right) vesicles in cortical dystrophic neurites. Scale bars in µm: **A**, 10; **B**, 5; **C** and **D**, 0.5. Abbreviations: so = stratum oriens; sp = stratum pyramidale.

proteins were present in axons, a predominant location in dendrites was detected for CPE but not for SgIII. In contrast to what is found in endocrine cells, these observations suggest a differential targeting of DCV sorting receptors in neurons, at least for distinctive subpopulations. Although a lack of immunolabeling could reflect protein levels below the detection threshold, the present differences between CPE and SgIII argue for differential targeting. Previous studies have lent support to the idea of differential routing of DCV cargo in neurons. For instance, in Aplysia bag cells and hypothalamic neurons differential packaging and targeting toward dendrites and nerve endings has been shown for neuropeptides and their processing endopeptidases (10, 26, 28, 35, 43). Therefore, a potential role for CPE and SgIII in specialized sorting and processing of DCV cargo in neuronal microdomains is proposed.

The regulated secretory pathway in astrocytes

In recent years, a growing body of evidence has shown that astrocytes can release non-peptidic transmitters such as adenosine triphosphate (ATP), glutamate and D-serine in a regulated fashion, to influence excitability and plasticity of neuronal networks (2). Regulated secretion for peptidic gliotransmitters has also been reported in cultured astrocytes. For instance, *in vitro* release of the hormones and growth factors atrial natriuretic peptide, neuropeptide Y and BDNF is triggered from astrocytes by different stimuli (4, 25, 40). Moreover, signaling mechanisms, such as the cyclic adenosine monophosphate (cAMP) pathway and the RE1-silencing transcription factor/neuron-restrictive silencer factor transcription factor, have been revealed to control regulated peptide secretion from astroglial cells (36, 39). However, the identity and function of molecular components of this stimuli-dependent secretory pathway in astrocytes are largely unknown. The present results showing that CPE and SgIII are expressed by astrocytes in human brain sections support the competence of these glial cells for regulated secretion of peptidic messengers *in vivo*. Therefore, as what we might call "professional" secretory cells, we propose an important role for these two sorting receptors in the trafficking and secretion of peptidic transmitters in astroglial cells *in vivo*.

Involvement of CPE and SgIII in AD

Here, we show for the first time that CPE and SgIII are dramatically accumulated in senile plaques of AD patients and transgenic mice. Aberrant levels of secretory sorting receptors are occasionally located in plaque-surrounding astrocytes, whereas the main accumulation corresponds within dystrophic neurites. Because activated astrocytes overexpress SgIII in rodents (37), increased levels of secretory sorting receptors in reactive astrocytes around human senile plaques were expected. Moreover, the BDNF overexpression previously found in plaque-associated astrocytes of AD transgenic mice suggests that Aβ deposits coordinately alter the expression of trophic factors and their secretory components in glial cells (5).

Typically, CPE and SgIII were markedly accumulated in dystrophic neurites close to Aβ deposits in both AD patients and transgenic mice. The lack of overlapping observed in some aberrant neurites may be related to their differential distribution in neurons, mentioned above. The accumulation of sorting receptors in dystrophic neurites likely indicates retention of DCV. This suggestion is supported by previous reports showing accumulation of classical granins and DCV cargos in AD dystrophic neurites, such as CgA, Secretogranin II and BDNF (5, 15, 48). Because typical markers of synaptic vesicles, small clear vesicles, are defective in dystrophic neurites (ie, synapsin and synaptophysin) (14), a predominant accumulation of peptide-containing vesicles in plaque-associate neuronal projections is plausible. Interestingly, the aberrant intracellular increase of CPE and SgIII agrees with the extracellular downregulation reported in cerebrospinal fluid of AD patients (1, 38), which suggests impairment in trafficking and secretion of these proteins. Furthermore, as proposed for some classical granins (3), SgIII and CPE could serve as diagnostic biomarkers of AD.

Of note, the aberrant accumulation of CPE and SgIII detected in dystrophic neurites of AD patients was faithfully recapitulated by APPswe/PS1dE9 mice. Because transgenic animals produce Aβ and develop amyloid plaques, a critical role for Aβ leading to neuritic CPE and SgIII alterations in AD is suggested. In agreement, previous studies performed on cultured cells have shown that Aβ disrupts trafficking of BDNF-containing DCV, likely impairing neurite transport (12, 44). Recent *in vivo* observations, showing that amyloid deposition precedes neuritic pathology in APPswe/PS1dE9 mice, support a mediation of plaque-associated Aβ changing secretory sorting receptors in AD (30). Although CPE and SgIII accumulation may represent a late-stage effect of neuritic dystrophy in AD, a contribution of these proteins in the neuropathological progression of AD may be suggested. It has been shown that improving levels of growth factors and neuropeptides, typically decreased in AD and sorted to the regulated secretory pathway (ie, BDNF and somatostatin), partially recover AD-altered neural circuitries (32, 41). Therefore, beyond transcriptional mechanisms, we propose that aberrant accumulation of CPE and SgIII may participate in AD progression by altering sorting, processing and secretion of DCV cargos critical in this neurodegenerative disease. In this view, the elimination of CPE leads to abnormal dendritic pattering, neuronal degeneration and memory deficits (8, 49, 50).

In conclusion, we show here for the first time the differential distribution of CPE and SgIII in neuronal and astroglial microdomains in the human cerebral cortex. Moreover, Aβ-associated accumulation of CPE and SgIII in AD dystrophic neurites and activated astroglia is uncovered. These data implicate the processing enzymes and sorting receptors for the regulated secretion of neuropeptides and neurotrophins in AD neural degeneration.

COMPETING INTERESTS

The authors declare that they have no competing interests.

ACKNOWLEDGMENTS

We are grateful to Dr. Javier DeFelipe (Cajal Institute, Spain) for helpful discussions, Drs José Antonio del Rio and Vanessa Gil (Catalonian Institute for Bioengineering, Spain) for providing some human brain samples, Margarita Carmona for technical assistance and Tom Yohannan for editorial assistance. This work

was supported by grants from the Spanish Ministry of Science and Innovation (BFU2007-67889 and BFU2010-22132) and MAPFRE Foundation to FA and Seventh Framework Programme of the European Commission, grant agreement 278486: DEVELAGE to IF. EP is a researcher of the Ramón y Cajal program (MICINN-Spain).

REFERENCES

1. Abdi F, Quinn JF, Jankovic J, McIntosh M, Leverenz JB, Peskind E *et al* (2006) Detection of biomarkers with a multiplex quantitative proteomic platform in cerebrospinal fluid of patients with neurodegenerative disorders. *J Alzheimers Dis* **9**:293–348.
2. Araque A, Navarrete M (2010) Glial cells in neuronal network function. *Philos Trans R Soc Lond B Biol Sci* **365**:2375–2381.
3. Bartolomucci A, Possenti R, Mahata SK, Fischer-Colbrie R, Loh YP, Salton SR (2011) The extended granin family: structure, function, and biomedical implications. *Endocr Rev* **32**: 755–797.
4. Bergami M, Santi S, Formaggio E, Cagnoli C, Verderio C, Blum R *et al* (2008) Uptake and recycling of pro-BDNF for transmitter-induced secretion by cortical astrocytes. *J Cell Biol* **183**:213–221.
5. Burbach GJ, Hellweg R, Haas CA, Del Turco D, Deicke U, Abramowski D *et al* (2004) Induction of brain-derived neurotrophic factor in plaque-associated glial cells of aged APP23 transgenic mice. *J Neurosci* **24**:2421–2430.
6. Burgos-Ramos E, Hervás-Aguilar A, Aguado-Llera D, Puebla-Jiménez L, Hernández-Pinto AM, Barrios V, Arilla-Ferreiro E (2008) Somatostatin and Alzheimer's disease. *Mol Cell Endocrinol* **286**:104–111.
7. Burgoyne RD, Morgan A (2003) Secretory granule exocytosis. *Physiol Rev* **83**:581–632.
8. Carrel D, Du Y, Komlos D, Hadzimichalis NM, Kwon M, Wang B *et al* (2009) NOS1AP regulates dendrite patterning of hippocampal neurons through a carboxypeptidase E-mediated pathway. *J Neurosci* **29**:8248–8258.
9. Cawley NX, Wetsel WC, Murthy SR, Park JJ, Pacak K, Loh YP (2012) New roles of carboxypeptidase e in endocrine and neural function and cancer. *Endocr Rev* **33**:216–253.
10. Chun JY, Korner J, Kreiner T, Scheller RH, Axel R (1994) The function and differential sorting of a family of aplysia prohormone processing enzymes. *Neuron* **12**:831–844.
11. Cool DR, Normant E, Shen F, Chen HC, Pannell L, Zhang Y, Loh YP (1997) Carboxypeptidase E is a regulated secretory pathway sorting receptor: genetic obliteration leads to endocrine disorders in Cpe(fat) mice. *Cell* **88**:73–83.
12. Decker H, Lo KY, Unger SM, Ferreira ST, Silverman MA (2010) Amyloid-beta peptide oligomers disrupt axonal transport through an NMDA receptor-dependent mechanism that is mediated by glycogen synthase kinase 3beta in primary cultured hippocampal neurons. *J Neurosci* **30**:9166–9171.
13. Ferrer I (2012) Defining Alzheimer as a common age-related neurodegenerative process not inevitably leading to dementia. *Prog Neurobiol* **97**:38–51.
14. Ferrer I, Martí E, Tortosa A, Blasi J (1998) Dystrophic neurites of senile plaques are defective in proteins involved in exocytosis and neurotransmission. *J Neuropathol Exp Neurol* **57**:218–225.
15. Ferrer I, Marín C, Rey MJ, Ribalta T, Goutan E, Blanco R *et al* (1999) BDNF and full-length and truncated TrkB expression in Alzheimer disease. Implications in therapeutic strategies. *J Neuropathol Exp Neurol* **58**:729–739.
16. Fricker LD (1988) Carboxypeptidase E. *Annu Rev Physiol* **50**:309–321.
17. García-Marín V, Blazquez-Llorca L, Rodriguez JR, Gonzalez-Soriano J, DeFelipe J (2010) Differential distribution of neurons in the gyral white matter of the human cerebral cortex. *J Comp Neurol* **518**:4740–4759.
18. Golde TE, Petrucelli L, Lewis J (2010) Targeting Abeta and tau in Alzheimer's disease, an early interim report. *Exp Neurol* **223**:252–266.
19. Hosaka M, Watanabe T, Sakai Y, Uchiyama Y, Takeuchi T (2002) Identification of a chromogranin A domain that mediates binding to secretogranin III and targeting to secretory granules in pituitary cells and pancreatic beta-cells. *Mol Biol Cell* **13**:3388–3399.
20. Hosaka M, Watanabe T (2010) Secretogranin III: a bridge between core hormone aggregates and the secretory granule membrane. *Endocr J* **57**:275–286.
21. Hosaka M, Watanabe T, Sakai Y, Kato T, Takeuchi T (2005) Interaction between secretogranin III and carboxypeptidase E facilitates prohormone sorting within secretory granules. *J Cell Sci* **118**:4785–4795.
22. Jankowsky JL, Fadale DJ, Anderson J, Xu GM, Gonzales V, Jenkins NA *et al* (2004) Mutant presenilins specifically elevate the levels of the 42 residue beta-amyloid peptide *in vivo*: evidence for augmentation of a 42-specific gamma secretase. *Hum Mol Genet* **13**:159–170.
23. Kim T, Tao-Cheng JH, Eiden LE, Loh YP (2001) Chromogranin A, an "on/off" switch controlling dense-core secretory granule biogenesis. *Cell* **106**:499–509.
24. Kim T, Gondré-Lewis MC, Arnaoutova I, Loh YP (2006) Dense-core secretory granule biogenesis. *Physiology (Bethesda)* **21**:124–133.
25. Krzan M, Stenovec M, Kreft M, Pangrsic T, Grilc S, Haydon PG, Zorec R (2003) Calcium-dependent exocytosis of atrial natriuretic peptide from astrocytes. *J Neurosci* **23**:1580–1583.
26. Landry M, Vila-Porcile E, Hökfelt T, Calas A (2003) Differential routing of coexisting neuropeptides in vasopressin neurons. *Eur J Neurosci* **17**:579–589.
27. Lou H, Kim SK, Zaitsev E, Snell CR, Lu B, Loh YP (2005) Sorting and activity-dependent secretion of BDNF require interaction of a specific motif with the sorting receptor carboxypeptidase E. *Neuron* **45**:245–255.
28. Ludwig M, Leng G (2006) Dendritic peptide release and peptide-dependent behaviours. *Nat Rev Neurosci* **7**: 126–136.
29. Lynch DR, Braas KM, Hutton JC, Snyder SH (1990) Carboxypeptidase E (CPE): immunocytochemical localization in the rat central nervous system and pituitary gland. *J Neurosci* **10**:1592–1599.
30. Meyer-Luehmann M, Spires-Jones TL, Prada C, Garcia-Alloza M, de Calignon A, Rozkalne A *et al* (2008) Rapid appearance and local toxicity of amyloid-beta plaques in a mouse model of Alzheimer's disease. *Nature* **451**:720–724.
31. Mirra SS, Gearing M, McKeel DW Jr, Crain BJ, Hughes JP, van Belle G, Heyman A (1994) Interlaboratory comparison of neuropathology assessments in Alzheimer's disease: a study of the Consortium to Establish a Registry for Alzheimer's Disease (CERAD). *J Neuropathol Exp Neurol* **53**:303–3015.
32. Nagahara AH, Merrill DA, Coppola G, Tsukada S, Schroeder BE, Shaked GM *et al* (2009) Neuroprotective effects of brain-derived neurotrophic factor in rodent and primate models of Alzheimer's disease. *Nat Med* **15**:331–337.
33. Oberheim NA, Takano T, Han X, He W, Lin JH, Wang F *et al* (2009) Uniquely hominid features of adult human astrocytes. *J Neurosci* **29**:3276–3287.

34. Ottiger HP, Battenberg EF, Tsou AP, Bloom FE, Sutcliffe JG (1990) 1B1075: a brain- and pituitary-specific mRNA that encodes a novel chromogranin/secretogranin-like component of intracellular vesicles. *J Neurosci* **10**:3135–3147.
35. Ovsepian SV, Dolly JO (2011) Dendritic SNAREs add a new twist to the old neuron theory. *Proc Natl Acad Sci U S A* **108**:19113–19120.
36. Paco S, Margelí MA, Olkkonen VM, Imai A, Blasi J, Fischer-Colbrie R, Aguado F (2009) Regulation of exocytotic protein expression and Ca2+-dependent peptide secretion in astrocytes. *J Neurochem* **110**:143–156.
37. Paco S, Pozas E, Aguado F (2010) Secretogranin III is an astrocyte granin that is overexpressed in reactive glia. *Cereb Cortex* **20**:1386–1397.
38. Perrin RJ, Craig-Schapiro R, Malone JP, Shah AR, Gilmore P, Davis AE *et al* (2011) Identification and validation of novel cerebrospinal fluid biomarkers for staging early Alzheimer's disease. *Plos ONE* **6**:e16032.
39. Prada I, Marchaland J, Podini P, Magrassi L, D'Alessandro R, Bezzi P, Meldolesi J (2011) REST/NRSF governs the expression of dense-core vesicle gliosecretion in astrocytes. *J Cell Biol* **193**:537–549.
40. Ramamoorthy P, Whim MD (2008) Trafficking and fusion of neuropeptide Y-containing dense-core granules in astrocytes. *J Neurosci* **28**:13815–13827.
41. Saito T, Iwata N, Tsubuki S, Takaki Y, Takano J, Huang SM *et al* (2005) Somatostatin regulates brain amyloid beta peptide Abeta42 through modulation of proteolytic degradation. *Nat Med* **11**:434–439.
42. Serrano-Pozo A, Frosch MP, Masliah E, Hyman BT (2011) Neuropathological alterations in Alzheimer disease. *Cold Spring Harb Perspect Med* **1**:a006189.
43. Sossin WS, Sweet-Cordero A, Scheller RH (1990) Dale's hypothesis revisited: different neuropeptides derived from a common prohormone are targeted to different processes. *Proc Natl Acad Sci U S A* **87**:4845–4848.
44. Stokin GB, Goldstein LS (2006) Axonal transport and Alzheimer's disease. *Annu Rev Biochem* **75**:607–627.
45. Tanzi RE, Bertram L (2005) Twenty years of the Alzheimer's review disease amyloid hypothesis: a genetic perspective. *Cell* **120**:545–555.
46. Timmer NM, Kuiperij HB, de Waal RM, Verbeek MM (2010) Do amyloid β-associated factors co-deposit with Aβ in mouse models for Alzheimer's disease? *Alzheimers Dis* **22**:345–355.
47. Wenk GL (2006) Neuropathologic changes in Alzheimer's disease: potential targets for treatment. *J Clin Psychiatry* **67**:3–7.
48. Willis M, Leitner I, Jellinger KA, Marksteiner J (2011) Chromogranin peptides in brain diseases. *J Neural Transm* **118**:727–735.
49. Woronowicz A, Koshimizu H, Chang SY, Cawley NX, Hill JM, Rodriguiz RM *et al* (2008) Absence of carboxypeptidase E leads to adult hippocampal neuronal degeneration and memory deficits. *Hippocampus* **18**:1051–1063.
50. Woronowicz A, Cawley NX, Chang SY, Koshimizu H, Phillips AW, Xiong ZG, Loh YP (2010) Carboxypeptidase E knockout mice exhibit abnormal dendritic arborization and spine morphology in central nervous system neurons. *J Neurosci Res* **88**:64–72.
51. Zuccato C, Cattaneo E (2009) Brain-derived neurotrophic factor in neurodegenerative diseases. *Nat Rev Neurol* **5**:311–322.

4.2 CHAPTER 2: AMYLOID-ß IMPAIRS VESICULAR SECRETION IN NEURONAL AND ASTROCYTE PEPTIDERGIC TRANSMISSION

frontiers in Molecular Neuroscience

ORIGINAL RESEARCH
published: 28 June 2017
doi: 10.3389/fnmol.2017.00202

Amyloid-β Impairs Vesicular Secretion in Neuronal and Astrocyte Peptidergic Transmission

Virginia Plá[1,2], *Neus Barranco*[1,2], *Esther Pozas*[1] *and Fernando Aguado*[1,2]*

[1]Department of Cell Biology, Physiology and Immunology, University of Barcelona, Barcelona, Spain,
[2]Institute of Neurosciences, University of Barcelona, Barcelona, Spain

Regulated secretion of neuropeptides and neurotrophic factors critically modulates function and plasticity of synapses and circuitries. It is believed that rising amyloid-β (Aβ) concentrations, synaptic dysfunction and network disorganization underlie early phases of Alzheimer's disease (AD). Here, we analyze the impact of soluble $A\beta_{1–42}$ assemblies on peptidergic secretion in cortical neurons and astrocytes. We show that neurons and astrocytes differentially produce and release carboxypeptidase E (CPE) and secretogranin III (SgIII), two dense-core vesicle (DCV) markers belonging to the regulated secretory pathway. Importantly, $A\beta_{1–42}$, but not scrambled $A\beta_{1–42}$, dramatically impairs basal and Ca^{2+}-regulated secretions of endogenously produced CPE and SgIII in cultured neurons and astrocytes. Additionally, KCl-evoked secretion of the DCV cargo brain-derived neurotrophic factor (BDNF) is lowered by $A\beta_{1–42}$ administration, whereas glutamate release from synaptic vesicle (SVs) remains unchanged. In agreement with cell culture results, $A\beta_{1–42}$ effects on CPE and SgIII secretion are faithfully recapitulated in acute adult brain slices. These results demonstrate that neuronal and astrocyte secretion of DCV cargos is impaired by Aβ *in vitro* and *in situ*. Furthermore, Aβ-induced dysregulated peptidergic transmission could have an important role in the pathogenesis of AD and DCV cargos are possible candidates as cerebrospinal fluid (CSF) biomarkers.

Keywords: Alzheimer's disease, BDNF, cerebral cortex, dense-core vesicles, exocytosis

OPEN ACCESS

Edited by:
Detlev Boison,
Legacy Health, United States

Reviewed by:
Ursula Susan Sandau,
Oregon Health & Science University, United States
Samaneh Maysami,
University of Manchester, United Kingdom

***Correspondence:**
Fernando Aguado
faguado@ub.edu

Received: *25 April 2017*
Accepted: *08 June 2017*
Published: *28 June 2017*

Citation:
Plá V, Barranco N, Pozas E and Aguado F (2017) Amyloid-β Impairs Vesicular Secretion in Neuronal and Astrocyte Peptidergic Transmission. Front. Mol. Neurosci. 10:202. doi: 10.3389/fnmol.2017.00202

INTRODUCTION

Alzheimer's disease (AD) is by far the most common cause of dementia in the elderly. The characteristic clinical phenotype of AD is a gradual and progressive loss of memory and cognition (Scheltens et al., 2016). Accumulation of abnormally folded amyloid-β (Aβ) peptides in extracellular plaques and hyperphosphorylated tau proteins in intracellular tangles are two major pathological hallmarks of AD. However, neuritic plaques and neurofibrillary tangles are only weakly correlated with the degree of dementia in AD patients (Selkoe and Hardy, 2016). In contrast, decreased synapse number is the major quantitative correlate of loss of memory and cognition in AD brain (DeKosky and Scheff, 1990). Accordingly, a growing body of electrophysiological, biochemical and behavioral evidence suggests that synaptic dysfunction and network disorganization centrally underlie the progressive cognitive manifestations of the clinical AD occurring before the onset of symptoms (Mucke and Selkoe, 2012; Palop and Mucke, 2016).

It has been shown that the concentration of soluble Aβ, but not insoluble Aβ deposits, is a predictor of synaptic changes in AD and tracks the disease progression and cognitive decline

(Lue et al., 1999; Koss et al., 2016). In fact, soluble Aβ species, mainly $A\beta_{1-42}$ oligomers, exert a pivotal role in the pathogenesis of the synaptic damage at early stages of AD (Ferreira et al., 2015; Viola and Klein, 2015; De Strooper and Karran, 2016). Binding of Aβ to neuronal and glial plasma membranes causes multiple aberrant effects that could trigger synaptic failure, such as dysfunction of Ca^{2+} homeostasis, axonal transport, neurotransmitter receptors and transporters and mitochondria. Moreover, several studies have proposed that Aβ peptides can affect synaptic function by altering vesicular release of classical transmitters (i.e., glutamate) from neurons and astrocytes (Arias et al., 1995; Abramov et al., 2009; Parodi et al., 2010; Brito-Moreira et al., 2011; Talantova et al., 2013; Hascup and Hascup, 2016). In this regard, two recent studies showing that Aβ oligomers directly impair SNARE complex formation and synaptic vesicle (SV) exocytosis further support a deleterious function of aberrant Aβ on transmitter secretion (Russell et al., 2012; Yang et al., 2015).

Besides SVs, the so-called dense-core vesicle (DCVs, secretory granules in endocrine cells) store a wide array of neuropeptides, hormones and growth factors that enable peptidegic transmission. In neurons, and as recently proposed astrocytes, DCVs-containing transmitters budding from trans-Golgi network mature during transport along microtubules toward the cell surface and secrete their cargos by Ca^{2+}-triggered exocytosis (Gondré-Lewis et al., 2012; Araque et al., 2014). Although structure and function of synapses and networks critically depend on the adjusted peptidergic transmission (van den Pol, 2012), secretory features of DCVs in the normal and pathological central nervous system have been little studied. Here, we determined the impact of Aβ on secretion of DCV cargos in cortical neurons and astrocytes. Therefore, we analyzed *in vitro* and *in situ* release of carboxypeptidase E (CPE) and secretogranin III (SgIII), two established DCVs markers which are aberrantly accumulated in neurons and astrocytes in the cerebral cortex of AD patients and amyloid-forming transgenic mice (Plá et al., 2013). First, we show that neurons and astrocytes produce distinctive forms of CPE and SgIII, which undergo release via differential mechanisms. Importantly, basal and regulated secretions of endogenously produced CPE and SgIII, as well as brain-derived neurotrophic factor (BDNF), are dramatically impaired by Aβ both in cultured dispersed cells and acute brain slices. The present results indicate that DCVs secretion is a significant target of amyloidogenic Aβ forms. Moreover, a participation of Aβ-induced peptidergic secretion alterations in the pathogenesis of AD and its potential use as a cerebrospinal fluid (CSF) biomarker are suggested.

MATERIALS AND METHODS

Antibodies and Reagents

Monoclonal and polyclonal antibodies against CPE were obtained from BD Transduction Laboratories (San Jose, CA, USA) and GeneTex (Irvine, CA, USA). Polyclonal antibodies against SgIII were purchased from Sigma-Aldrich (Madrid, Spain). Aβ monoclonal antibodies, clones 4G8 and 6E10, were from Covance (Emeryville, CA, USA). Polyclonal PC1/3 and PC2 were from Thermo Fisher Scientific (Madrid, Spain) and kindly provided by Dr I. Lindberg (University of Maryland), respectively. Antibodies against GFAP, MAP-2, CD11b, Tuj1, β-actin and Iba1 were from Millipore Iberica (Madrid, Spain), Serotec (Oxford, UK), Sigma-Aldrich and Wako GmbH (Neuss, Germany). DL-*threo*-β-benzyloxyaspartic acid (TBOA) was from Tocris Bioscience (Bristol, UK). Most chemicals and cell culture reagents were obtained from Sigma-Aldrich and Gibco (Thermo Fisher Scientific), respectively.

Animals and Ethics Statement

CD1 mice were provided by Envigo Rms (Sant Feliu de Codines, Spain), kept under controlled temperature (22 ± 2°C), humidity (40%–60%), and light (12-h cycles). All animals were handled in accordance with the guidelines for animal research set out in the European Community Directive 2010/63/EU, and all procedures were approved by the Ethics Committee for Animal Experimentation (CEEA), University of Barcelona (Barcelona, Spain). All efforts were made to minimize the number used and animal suffering.

Primary Cell Cultures and Acute Brain Slices

Astroglial and neuronal cultures were obtained from CD1 mice and prepared as described previously (Paco et al., 2009). Astrocyte cultures were prepared from the whole cerebral cortex of P0-P1-day-old mice. Cortical tissues were isolated, meninges were carefully dissected away, minced and incubated in 0.5% trypsin and 0.01% DNase. Dissociated cells were seeded in flasks and grown in high-glucose Dulbecco's Modified Eagle's Medium and F-12 (1:1) containing 10% fetal bovine serum, 10 mM HEPES and penicillin/streptomycin at 37°C in a 5% CO_2 incubator. At confluence (10–12 days), flasks were shaken overnight and the cells were rinsed, detached and subcultured at 1×10^5 cells/cm^2 onto poly-D-lysine-coated plastic culture dishes and glass coverslips. Under these conditions, cell cultures were essentially formed by astrocytes (>95% GFAP+), a small percentage of microglia (<5% CD11b+) and virtually devoid of neurons (<0.5% Tuj-1+). Neuronal cultures were grown from either whole cerebral cortex (including hippocampus) or isolated hippocampus of E16-E17 mouse embryos. After trypsin and DNase treatment, dissociated cells were seeded at 1.5×10^5 cells/cm^2 onto poly-D-lysine-coated culture plates and glass coverslips. Neurons were grown in Neurobasal A medium containing B27 and 1% FBS (Thermo Fisher Scientific), glutamine and penicillin/streptomycin at 37°C in a 5% CO_2 atmosphere for 10 days. During the first 4 days, cultures were also supplemented with 20 μg/mL 5-Fluoro-2′-deoxyuridine and 50 μg/mL Uridine (Sigma-Aldrich) to inhibit mitotic activity of glial cells. Tuj-1 and MAP2 immunostaining showed that more than 95% of the cells were neurons, whereas a <5% were GFAP+ astrocytes.

Brain slices were obtained from anesthetized adult mice (ketamine 120 μg/g and xylazine 6 μg/g i.p.), as described previously (Aguado et al., 2002). Their brains were removed and placed in cold artificial CSF (ACSF) containing (in mM): NaCl

120, KCl 3, D-glucose 10, $NaHCO_3$ 26, NaH_2PO_4 2.25, $CaCl_2$ 2, $MgSO_4$ 1, pH 7.4, bubbled with 95% O_2 and 5% CO_2. Horizontal tissue slices (300 μm thick) were cut with a vibratome, stabilized and transferred to a release chamber. All the experiments were conducted in ACSF bubbled continuously with 95% O_2 and 5% CO_2 at room temperature (22–25°C).

Aβ Aggregation and Cell Viability

Synthetic human Amyloid-β_{1-42} (Aβ) peptide (H-1368), and peptide comprised of the same amino acid composition of but in a randomized sequence, Scrambled Amyloid-β_{1-42} (H-7406; ScAβ), used as a control, were purchased from Bachem (Bubendorf, Switzerland) and prepared as described previously (Dahlgren et al., 2002). Lyophilized Aβ or ScAβ peptides were initially dissolved to 1 mM in 1,1,1,3,3,3-Hexafluoro-2-propanol (Sigma-Aldrich) and separated into aliquots in sterile microcentrifuge tubes. Then, hexafluoroisopropanol was evaporated under low temperature vacuum in a Speed Vac, and the peptide film was stored desiccated at −80°C until use. For the assembly, the peptide was first resuspended in anhydrous sterile dimethylsulfoxide (Sigma-Aldrich) to a concentration of 5 mM, diluted to a final concentration of 100 μM in 10 mM HCl and incubated for 24 h at 37°C. Aggregated species in Aβ stocks were identified by western blotting. Cultured cells and brain slices were treated with either 5 μM Aβ/ScAβ preparation or an equal volume of vehicle solution (controls). Cell viability was determined by WST-1 (Roche, Basel, Switzerland), lactate dehydrogenase (Roche) and propidium iodide/Hoechst (Sigma-Aldrich) assays. Levels of reduced WST-1 and released lactate dehydrogenase were measured with an ELISA plate reader (Tecan, Männedorf, Switzerland) at 450 nm and 492 nm, respectively. Propidium iodide/Hoechst uptake was analyzed by fluorescence microscopy and analyzed with ImageJ software.

Release Assays

Secretion in cultured cells was assayed in 12-well culture plates except for BDNF, for which it was done in 100 mm dishes and for glutamate, for which 48-well plates were used. Poly-D-lysine-attached cells were serum and supplement starved prior to release experiments. Release assays in brain slices were performed in superfused or static chambers (displaying the same results). Secretion from cultured cells was performed in commercial media and, when K^+ and Ca^{2+} concentrations were modified, in ACSF, whereas the release from brain slices was always carried out in ACSF. The composition of the 55 mM K^+ ACSF was adjusted to maintain the osmolarity with a corresponding NaCl decrease. In cultured cells, conditioned media were collected and cells were washed in phosphate buffer saline (PBS) and homogenized in lysis buffer (see below). Cell media and superfusate and static ACSF from brain slices were centrifuged at 600 *g* for 5 min to remove dislodged cells and all samples were stored at −20°C. Proteins in all release samples were precipitated with 5% trichloroacetic acid, using sodium deoxycholate as a carrier, or concentrated by Amicon® Ultra-15 and −0.5 Centrifugal filter devices (Merck Millipore, Madrid, Spain).

CPE and SgIII were detected by western blotting (see below) and Prep Cell Protein Standard was used as a control for the precipitation protocol for conditioned media (Bio-Rad Laboratories, Hercules, CA, USA). In cell culture media, β-actin was used to normalize the secretion in order to minimize variations in cell quantity. Levels of BDNF were quantified using the BDNF EMAX® ImmunoAssay System according to the manufacturer's instructions (Promega Corporation, Madison, WI, USA). Glutamate levels were measured using Amplex Red Glutamic Acid/Glutamate Oxidase Assay kit (Molecular Probes, Eugene, OR, USA) following the manufacturer's protocol. BDNF and glutamate levels were normalized by total protein levels.

Western Blotting

Cultured cells and tissues were homogenized in ice-cold lysis buffer containing 50 mM Tris-HCl pH 7.4, 150 mM NaCl, 5 mM $MgCl_2$, 1 mM ethyleneglycol-bis(2-aminoethylether)-N,N,N′,N′-tetra acetic acid (EGTA), 1% Triton X-100, and protease inhibitor cocktail (Roche Diagnostics). Samples of conditioned media and postnuclear lysates were electrophoresed in 8%–12% sodium dodecyl sulfate-polyacrylamide gel electrophoresis (SDS-PAGE; Bio-Rad Laboratories) and then transferred to PVDF membranes (Bio-Rad Laboratories). The membranes were activated and blocked in a solution containing 5% nonfat milk powder in tris-buffered saline tween-20 (140 mM NaCl, 10 mM Tris-HCl, pH 7.4, and 0.1% Tween 20; TBS-Tween) for 1 h at room temperature and then incubated with primary antibodies in blocking buffer for 2 h at room temperature or overnight at 4°C. After several washes in TBS-Tween solution, the membranes were incubated for 1 h with horseradish peroxidase-conjugated secondary antibodies (Bio-Rad Laboratories). Bound antibodies were visualized with enhanced chemiluminescence reagents (Bio-Rad Laboratories). Blot images were scanned and densitometric analyses were performed using ImageJ software.

Immunocytochemistry

Cells grown on glass coverslips were washed in ice-cold PBS and fixed with 4% paraformaldehyde in PB for 15 min. Animals were perfused transcardially under deep ketamine/xylacine anesthesia with 4% paraformaldehyde in 0.1 M PB, pH 7.4. The brains were removed from skulls, postfixed for 4 h in the same fixative solution, and cryoprotected overnight at 4°C by immersion in a 30% sucrose solution in 0.1 M PB. Forty-micrometer thick frozen sections were obtained with a cryostat and collected in PBS. Sections processed for the peroxidase method were soaked for 30 min in PBS containing 10% methanol and 3% H_2O_2 and subsequently washed in PBS. To suppress nonspecific binding, cell cultures and brain sections were incubated in 10% serum-PBS containing 0.1% Triton X-100, 0.2% glycine and 0.2% gelatin for 1 h at room temperature. Incubations with primary antibodies were carried out overnight at 4°C in PBS containing 5% fetal bovine serum, 0.1% Triton X-100 and 0.2% gelatin. Some histological sections were processed using the avidin-biotin-peroxidase method (Vectastain ABC kit, VECTOR, Burlingame, CA, USA). The peroxidase complex was visualized by incubating the sections with 0.05% diaminobenzidine and

0.01% H_2O_2 in PBS. Sections were mounted, dehydrated and coverslipped in Eukitt. Cell cultures and some brain sections were processed for immunofluorescence using secondary fluorochrome-conjugated antibodies (Alexa Fluor 488 and Alexa Fluor 568, Molecular Probes, Eugene, OR), and cell nuclei were stained with 4′,6-diamidino-2-phenylindole (DAPI, Molecular Probes, Eugene, OR, USA). Cell-containing coverslips and histological sections were mounted with Mowiol. The specificity of the immunostaining was tested by omitting the primary antibodies or by replacing them with an equivalent concentration of nonspecific IgG. No immunostaining was observed in these conditions. Bright field and fluorescent images were obtained with the Olympus fluorescent BX-61 and Leica TCS SPE scanning confocal microscopes.

Quantitative Real-Time PCR

RNA from cells was isolated by treatment with Trizol® reagent (Invitrogen) following the manufacturer's instructions and the quantity and quality were determined with a NanoDrop ND-1000 (NanoDrop Technologies, Wilmington, DE, USA) and Bioanalyzer 2100 (Agilent, Waldbronn, Germany). cDNA was synthesized using the Superscript III Reverse Transcriptase kit (Invitrogen) from 1 μg of total RNA. Reactions were incubated at 25°C for 10 min, 50°C for 30 min, 85°C for 5 min, chilled on ice and finally *E. coli* RNAse H was added and incubated at 37°C for 20 min. Quantitative real-time PCR (qPCR) was performed using the StepOneTM Real-Time PCR System (Applied Biosystems) using TaqMan Probes Mm00516341_m1 (CPE), Mm00485961_m1 (SgIII) and Mm01277042_m1 (TBP, as housekeeping gene). The 20 μl PCR included 0.01 μl RT product, 1× PerfeCTa® qPCR FastMix® II with ROX (Quanta BioSciences, Inc.) and 1 μL TaqMan probe. The reactions were incubated in a 48-well plate at 95°C for 5 min, followed by 42 cycles of 95°C for 15 s, 58°C for 15 s and 72°C for 30 s. All reactions were run in triplicate. The threshold cycle (C_T) is defined as the fractional cycle number at which the fluorescence passes the fixed threshold.

Statistical Analysis

Data are shown as the mean ± Standard Error of the Mean (SEM) summarizing three or more independent experiments, performed at least in triplicates. Non-parametric one-way ANOVA were calculated to determine significant effects of treatments, using Kruskal-Wallis or Friedman test when appropriate. Changes were calculated in relation to the average of controls using Mann–Whitney or Wilcoxon tests as *post hoc* analysis. Significance was set at $^{*}p < 0.05$, $^{**}p < 0.01$ and $^{***}p < 0.001$.

RESULTS

Differential Mechanisms Underlie CPE and SgIII Secretion from Neurons and Astrocytes

First, we determined the *in situ* cellular location of the DCV markers CPE and SgIII in the mouse cerebral cortex by immunohistological methods. High levels of both proteins were found in processes and cell bodies of pyramidal and non-pyramidal neurons and astrocyte-like glial cells (**Figure 1**). For neuronal CPE and SgIII, we detected differential location patterns at the regional and subcellular levels. In general, CPE immunostaining was more intense and more extended than for SgIII (**Figure 1**). Both proteins were present in perikarya, but only CPE was associated with dendritic shafts. Characteristically, SgIII was found abundantly as immunoreactive puncta throughout the neuropil, resembling axon terminals (**Figure 1**). Differential location of these two DCV proteins in neurons was apparent for the CA3 region of the hippocampus, where CPE- and SgIII-labeled projections corresponded with dendrites and mossy fibers, respectively (**Figure 1**). Regarding glial cells, most cortical astrocyte-like somata through the gray and white matters copiously displayed both CPE and SgIII (**Figure 1**). Double immunofluorescence showed that non-neuronal CPE and SgIII were associated with virtually all GFAP+ astrocytes and absent in Iba1+ microglial cells (data not shown), in agreement with our previous report (Paco et al., 2010).

To study peptidergic secretion from astrocytes and neurons, we prepared cortical primary cultures highly enriched in each cell type. Astrocyte cultures were virtually devoid of neurons, while a small number of astrocytes (<5%) was present in neuronal cultures which improved survival. In cultured astrocytes, CPE and SgIII were associated with secretory organelles showing a non-overlapping location, mainly for distal vesicles (**Figure 2A**). CPE- and SgIII-immunolabeled vesicular compartments were also evident in astrocytes grown within neuronal cultures (**Figure 2B**). GFAP co-labeling was used to validate astroglial identity. Careful analysis of media and cell lysates of glial cultures by western blotting revealed that astrocyte CPE and SgIII proteins corresponded to the nonprocessed forms (∼55 kDa for CPE and ∼80–75 kDa for precursor SgIII, pSgIII; **Figure 2C**). Because glial-produced proteins likely corresponded to the uncleaved precursor forms, we determined whether astrocytes lacked the corresponding PC1/3 and PC2 processing prohormone convertases. Double immunocytochemical labeling and Western blotting showed that *in vitro* astrocytes did not express either PC1/3 or PC2 proteins (data not shown).

As previously reported for SgIII (Paco et al., 2010), we show here that cultured astrocytes displayed high rates of basal release of both CPE and SgIII (**Figure 2C**). To analyze secretory kinetics of *de novo* synthesized CPE and SgIII in astrocytes, extracellular and intracellular protein pools were analyzed during cycloheximide (CHX) chase. As expected for secretory proteins, untreated cells showed rising extracellular levels and steady intracellular pools of CPE and SgIII over time. When protein synthesis was blocked by CHX, decreasing levels of intracellular CPE and SgIII were coupled with an almost invariable secreted pool (**Figure 2C**). These observations show that newly generated DCVs-like in astrocytes are poorly retained and rapidly undergo exocytosis, independently of stimuli. Next, we evaluated the regulated secretion of glial CPE and SgIII triggering $[Ca^{2+}]_i$ elevation by ionophores. Noteworthy, exposure to 1 μM ionomycin over 15 min gave variable responses from one culture set to another. Compared to unstimulated cultures, released

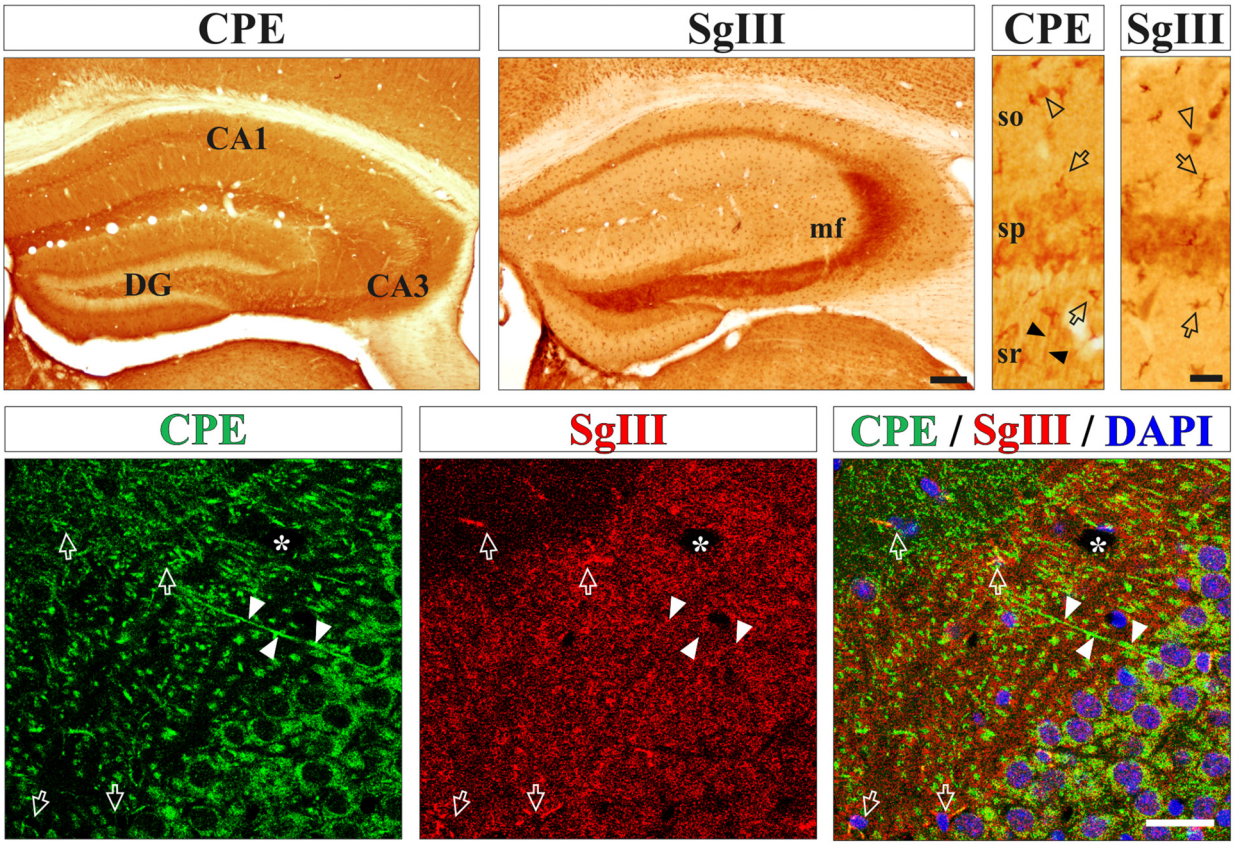

FIGURE 1 | Neurons and astrocytes abundantly express carboxypeptidase E (CPE) and SgIII proteins in the cerebral cortex *in vivo*. Upper boxes illustrate immunoperoxidase staining for CPE and SgIII in panoramic (left) and CA1 region (right) views of the hippocampal formation. Both proteins display a remarkable area specific and laminar distribution. Neuronal CPE is primarily found in dendritic shafts (filled arrowheads) and perikarya, where mossy fibers robustly exhibit SgIII. Intense immunolabeling for SgIII and CPE is detected in astroglial cell bodies and processes (arrows). Bottom boxes show confocal images of CPE (green) and SgIII (red) double immunofluorescences in the hippocampal CA3 region. Both proteins are mainly associated with different neuronal domains. CPE is largely located in somatodendritic compartments and SgIII is mainly distributed in terminal-like buttons of mossy fibers. Intense SgIII and CPE immunofluorescences colocalize in the same astrocyte processes (arrows). Nuclei are stained in blue. Arrows and arrow-heads point to astroglial cells and interneurons, respectively. Filled arrow-heads outline dendrites and asterisk indicates blood vessels. Scale bars in μm: upper-left, 250; upper-right and bottom, 50. Abbreviations: CA, regions of the hippocampus; DG, dentate gyrus; mf, mossy fibers; so, stratum oriens; sp, stratum pyramidale; sr, stratum radiatum.

CPE was higher after ionophore administration (181.4 ± 29.8% over basal; p = 0.03), while no statistically significant changes were observed for SgIII during stimulation (146.1 ± 25.4% over basal; p = 0.3). Moreover, CPE and SgIII intracellular levels were decreased after treatment (**Figure 2D**). Finally, the addition of 55 mM KCl to the media did not substantially change the levels of CPE nor SgIII secreted from astrocytes (**Figure 2D**). We conclude that cultured astrocytes robustly produce unprocessed forms of CPE and SgIII and largely release them in a stimulus-independent fashion.

In neuronal cultures, CPE and SgIII were associated with secretory organelles of pyramidal- and stellate-shaped neurons (**Figure 3A**). In agreement with the above *in vivo* data, a preferential location in dendrites was observed for CPE, whereas SgIII was mainly associated with axon-like projections and terminals. Neuronal and dendritic identities were confirmed by double immunolabeling with MAP2. In contrast to glial cells, cultured neurons produce and release both the precursor and mature forms of CPE (∼55 and 53 kDa) and SgIII (∼75 and 55 kDa; pSgIII and mSgIII respectively; **Figure 3B**). Moreover, as anticipated by the mature form occurrence of CPE and SgIII, cultured neurons abundantly displayed the DCV-associated convertases PC1/3 and PC2 (**Figure 3A**).

Opposite to astrocytes, cultured neurons showed a very low basal and high stimulus-triggered secretion of CPE and SgIII (**Figures 3B–D**). Therefore, forcing Ca^{2+} entry during 15 min by 1 μM ionomycin addition increased up to fivefold secretion from neuronal cells (**Figure 3D**). Depolarization by KCl for 15 min resulted in a dramatic enhancement of CPE and SgIII release (**Figure 3C**). Although shorter stimulation times, such as 5 min, offered similar results, 15 min of depolarization was maintained to ensure detection of released proteins by Western blotting. K^+-evoked secretion of CPE

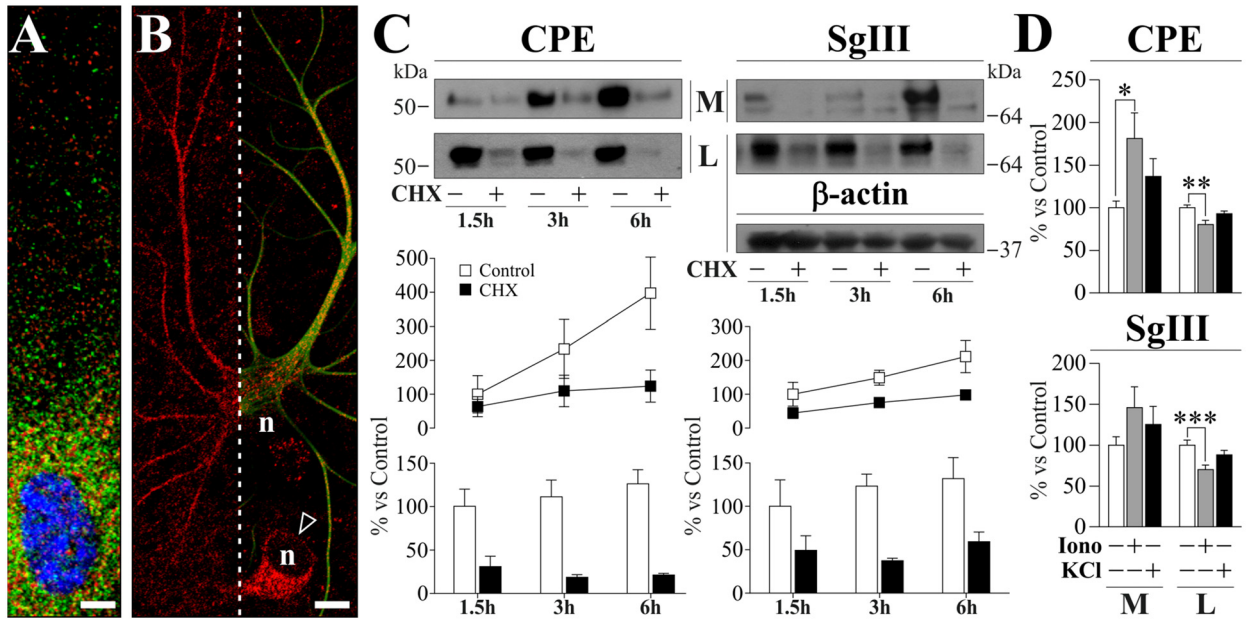

FIGURE 2 | Localization and release of CPE and SgIII in cultured cortical astrocytes. **(A,B)**. Confocal immunofluorecence images in astrocytes grown in glial **(A)** and neuronal **(B)** enriched cultures. High magnification in **(A)** shows a poor co-localization (yellow signal) of CPE (green) and SgIII (red) around the nucleus (blue). The astrocyte identity of a process-bearing cell positive for SgIII (red) is revealed by GFAP (green) co-staining (right in **B**). In **(B)**, arrow-head points to a neuronal soma displaying SgIII (red) and *n* indicates nucleus location. Scale bars in μm: **(A)** 5; **(B)** 15. **(C)** Immunoblots illustrate cellular content (lysates, L) and basal secretion into the medium (M) of CPE and SgIII in astrocyte cultures treated or not with 7.5 μM CHX during 1.5 h, 3 h and 6 h. β-actin was used as loading control. The graphs below summarize percent variation of the extracellular (lines) and intracellular (bars) levels of CPE and SgIII after CHX administration compared to controls. Data are presented as the mean ± standard error of the mean (SEM) of a representative experiment performed in quadruplicates. **(D)** Histograms summarizing the effect of 1 μM ionomycin (Iono) and 55 mM KCl incubations over 15 min on release (M) and cell content (L) of CPE and SgIII. Values represent percent variation compared with controls and are presented as the mean ± SEM. All the data (M and L) was normalized by intracellular levels of β-actin. $^{*}p < 0.05$; $^{**}p < 0.01$; $^{***}p < 0.001$, Mann-Whitney test.

was enhanced by a 279% over basal, whereas a 289% was observed for SgIII forms. Because nominally Ca^{2+}-free medium virtually abolished DCVs release, K^{+}-induced release of CPE and SgIII in cultured neurons entirely depended on the influx of this cation (**Figure 3C**). Interestingly, Ca^{2+}-evoked SgIII secretion was stronger for mature forms than for precursors in both ionomycin (1.7 m/p ratio) and KCl (2.0 m/p ratio) stimulations. These data indicate that neuronal and astroglial DCVs undergo differential proteolytic processing and exocytotic profiles.

Aβ Alters Production and Release of CPE and SgIII in Cultured Astrocytes

To determine whether Aβ alters glial and neuronal DCVs secretion, we prepared Aβ assemblies incubating $Aβ_{1-42}$ peptides for 24 h at 37°C. Immunoblotting with 6E10 and 4G8 Aβ antibodies revealed that Aβ preparations contained a broad mixture of low- (20–50 kDa) and high-molecular-weight (>50 kDa) aggregates, as well as the Aβ monomers, trimers and tetramers (**Figure 4**). Consistent with previous reports (Moreth et al., 2013), mono-tetrameric species were instantaneously formed, whereas larger oligomeric aggregates appeared over time of aging. No immunoreactive bands were detected from ∼200 kDa to the top/entrance of the gels (**Figure 4**).

Cell viability of cultured cells incubated with 5 μM Aβ was evaluated at 24 h for astrocytes and 16 h for neurons. Cellular membrane integrity was analyzed by a propidium iodide/Hoechst uptake test. No changes were observed between Aβ-treated and untreated cell cultures (Aβ vs. control: 99.6 ± 0.7%, $p = 0.8$ for neurons and 100.2 ± 0.8%, $p = 0.9$ for astrocytes). Due to the vulnerability of neurons, 2 additional tests were performed. WST-1 reduction was evaluated to detect variations in the mitochondrial metabolic rate, finding no significant changes (111.7 ± 4.7% of the control, $p = 0.14$). Additionally, the release of the cytoplasmic enzyme lactate dehydrogenase was analyzed in neuronal supernatant, showing no increase in response to Aβ (97.7 ± 3.6% of the control, $p = 0.6$). Because no differences were found between Aβ- and vehicle-treated cultures in any of the tests performed, no toxicity was found at the incubation times used.

Next, we analyzed the effect of Aβ on astrocyte CPE and SgIII secretion. Because the weak regulated release of these proteins in glia, we focused on their basal secretion at 8 and 24 h. Incubation of astrocytes with 5 μM Aβ caused a significant reduction in the extracellular levels of SgIII and CPE, mainly at 8 h (65% for SgIII and 41% for CPE) compared with controls (vehicle-treated cells; **Figures 5A,B**). The unchanged

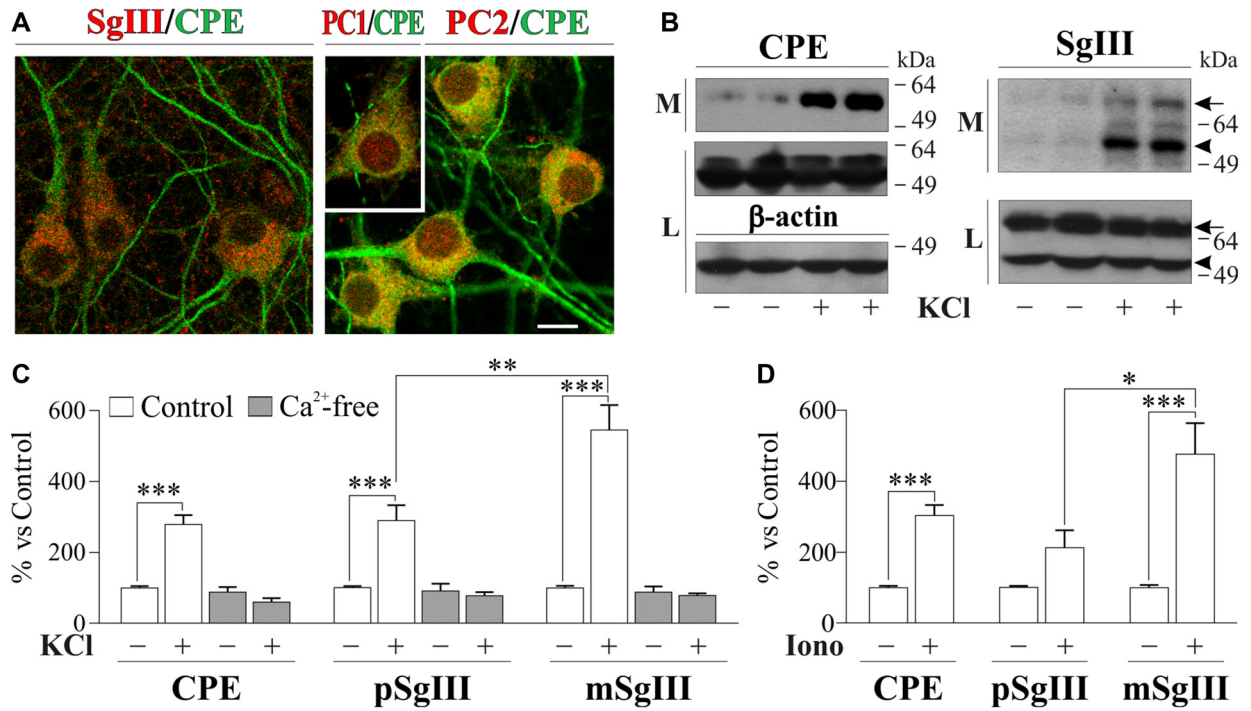

FIGURE 3 | Cellular distribution and release of CPE and SgIII in cultured neurons of the cerebral cortex. **(A)** Confocal immunofluorescence shows a prominent dendritic location for CPE (green) in pyramidal- and stellate-shaped neurons, while SgIII (red, left) is found in cell bodies and axon-like processes. No apparent colocalization was observed for the 2 proteins. Abundant signal shows the presence of the PC1/3 (red, inset) and PC2 (red, right) in the cultured neurons, with a broad somatic distribution. Scale bar in μm: 10. **(B)** Western blots show a very low basal secretion for CPE and SgIII, which were abundantly released in response to depolarization by KCl 55 mM for 15 min. Both forms of SgIII (arrow: proform, p and arrowhead: mature, m) were found in the extracellular media (M). No changes were found at intracellular levels in the lysate fraction (L). β-actin was used as loading control. **(C)** Release in response to KCl-depolarization was significant for CPE and both *p*- and mSgIII, the latter being especially high. In all cases, evoked secretion was abolished in absence of Ca^{2+}, showing a Ca^{2+} dependance. **(D)** 1 μM Ionomycin was used to trigger the CPE and SgIII release. Graphs show the percent variation compared with controls and are presented as the mean ± SEM normalized by intracellular levels of β-actin. $^{*}p < 0.05$; $^{**}p < 0.01$; $^{***}p < 0.001$, Mann-Whitney test.

CPE and SgIII levels in culture media of astrocytes incubated with a scrambled amino acid sequence of $A\beta_{1-42}$ (5 μM ScAβ) substantiated the specific effect of the aberrant amyloid on released glial proteins. To assess whether decreased levels into the media correlated with a diminished production or an impaired release, intracellular SgIII and CPE levels were assayed in Aβ- and ScAβ-treated cells. Concomitantly with a reduction in secreted CPE and SgIII, Aβ markedly increased their cellular content, mainly for SgIII (320% at 8 h and 257% at 24 h, $p < 0.0001$). No differences were detected after incubation with ScAβ peptides (**Figures 5A,B**). In addition to an impaired secretion, an Aβ-induced transcriptional dysregulation could contribute to change extra- and intracellular levels of secretory proteins. Therefore, we performed qPCR analysis for CPE and SgIII mRNA in Aβ-treated and control astrocytes. We found that levels of CPE transcripts were upregulated by amyloid species (158.1 ± 18.7% of control, $p = 0.03$), whereas SgIII mRNA expression was declined (70.2 ± 7.8% of control, $p = 0.004$; **Figure 5C**). Taking together, these results indicate that Aβ differentially regulates CPE and SgIII transcription and consistently impairs their protein secretion in astrocytes.

Regulated Secretion of DCV Cargos from Cultured Neurons is Impaired by Aβ

To evaluate the impact of Aβ on neuronal DCV release, primary cultures were exposed to vehicle (control) and 5 μM Aβ and ScAβ preparations for 16 h, then basal and K^+-evoked release were analyzed by immunoblotting. A representative experiment in **Figure 6A** illustrates no differences in the intracellular levels of CPE, SgIII forms and β-actin after Aβ-treatments (data quantification not shown). However, a significant decrease of basal secretion was detected for CPE (73% of control, $p < 0.0001$) and precursor (75% of control, $p = 0.007$) and mature (66% of control, $p = 0.0005$) SgIII forms in Aβ-exposed neurons, but not in cells incubated with ScAβ (**Figures 6A,B**). Importantly, Aβ specifically impaired K^+-depolarized release of CPE (Aβ 203.3% vs. control 363.2%, $p < 0.0001$), pSgIII (Aβ 190.0% vs. control 302.1%, $p = 0.006$) and mSgIII (Aβ 245.3% vs. control 426.0%, $p < 0.0001$) but not ScAβ (**Figures 5A,B**). Furthermore, an immunocytochemical analysis was performed on MAP2-identified neurons to examine subcellular distribution. Comparing neurons exposed to amyloid with vehicle (control), aberrant immunoreactive accumulations around the nuclei were detected in Aβ-treated cultures. This

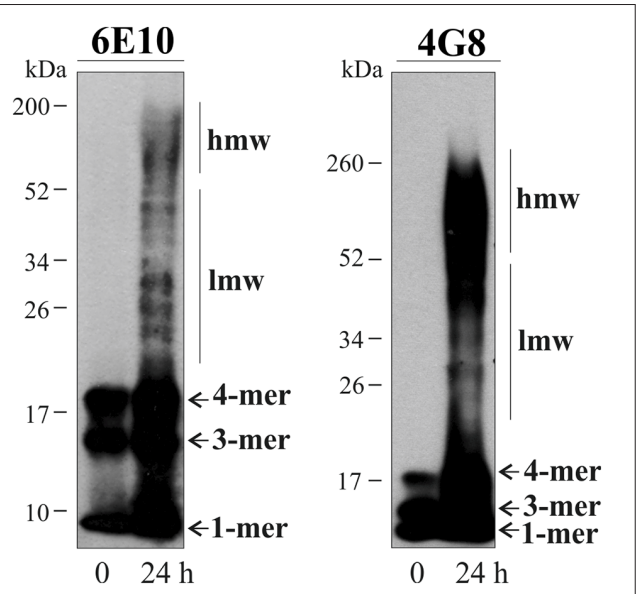

FIGURE 4 | Characterization of aggregates present in the Aβ preparations. Immunoblots illustrate 6E10- and 4G8-immunoreactive soluble $A\beta_{1-42}$ peptide before and after 24 h incubation at 37°C. Monomeric (1-mer), trimeric (3-mer) and tetrameric (4-mer) forms of Aβ are detected in both preparations, whilst low molecular weight (lmw) and high molecular weight (hmw) aggregates are only detected after the 24 h-incubation.

abnormal distribution was mainly associated with pyramidal-shaped cells and principally occurred for SgIII (**Figure 6C**). The present observations evidence that Aβ strongly alters the regulated secretory pathway in neurons, impairing the evoked release of CPE and SgIII.

Probably, the most studied DCV protein in brain-related diseases is the pleiotrophic growth factor BDNF (Adachi et al., 2014). With the aim to analyze whether release of physiologically relevant DCV cargos is affected by Aβ, we investigated secretion of endogenously produced BDNF by a sensitive sandwich immunoassay. First, we assessed BDNF levels in the same cortical-derived neuronal cultures used for CPE and SgIII analysis. However, cellular content of BDNF in cultured whole cortices was very low (8.6 ± 2.7 pg per 5×10^6 cells). Therefore, although K^+-evoked secretion could be determined, basal secretion was under detectable levels. In order to achieve detectable basal levels, we prepared BDNF-enriched cultures by isolating hippocampal neurons (Chen et al., 2006). Intracellular BDNF in hippocampal neurons was around four-fold higher than in whole cortical cultures (38.8 ± 4.9 pg per 5×10^6 cells). No significant differences were found in intracellular BDNF levels in untreated and 5 μM Aβ treated cells for 16 h (control 0.61 vs. Aβ 0.53 pg BDNF/μg protein, $p = 0.6$). As shown in **Figure 7**, depolarization-stimulated secretion of BDNF in hippocampal neurons was greatly impaired by Aβ exposure (Aβ 439.6% vs. control 1055.0%, $p = 0.003$), whereas basal release levels were unchanged (94.8% of control, $p = 0.5$). Furthermore, immunoblot examination of CPE and SgIII secretion patterns in Aβ-treated hippocampal neurons offered similar results to those obtained in whole cortical cultures. Decrease in basal secretion was 44% for CPE ($p = 0.0002$), 23% for pSgIII ($p = 0.003$) and 53% for mSgIII ($p = 0.01$) in Aβ-treated hippocampal cultures, whereas K^+-depolarized release was impaired by a 64.7% ($p = 0.007$),

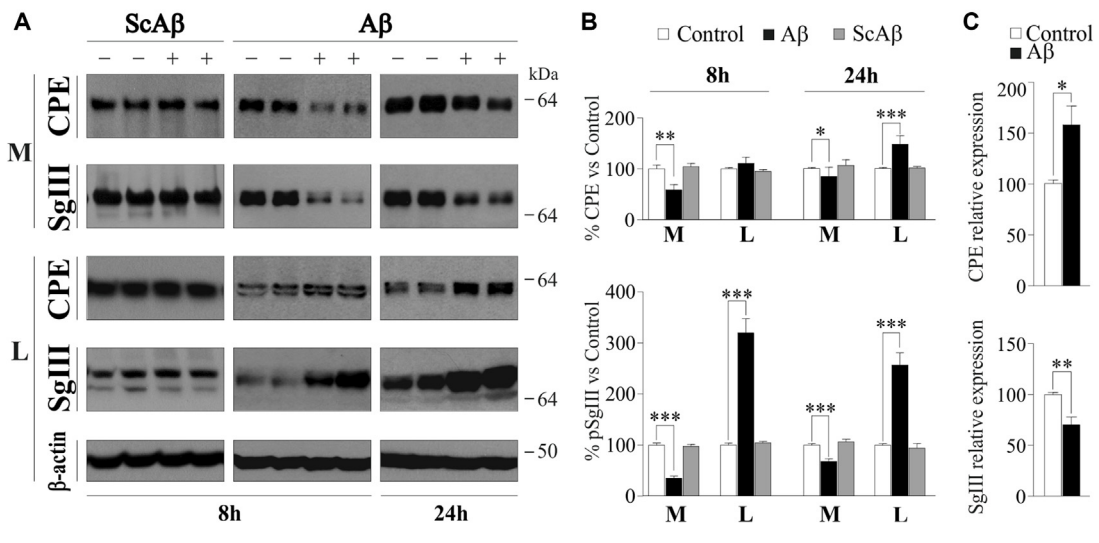

FIGURE 5 | Basal release and production of CPE and SgIII is altered in Aβ-treated cultured astrocytes. **(A)** Western blots showed basal release from cortical astrocytes treated with 5 μM Aβ during 8 or 24 h. A marked reduction in the extracellular levels (media, M) of SgIII and CPE compared with controls and an intracellular (lysates, L) accumulation is found in response to treatment with Aβ. No changes were found in response to ScAβ, either in the extracellular medium or the content. β-actin was used as loading control. **(B)** Graphical representation of the levels of CPE and SgIII compared with the vehicle-treated levels. Data are presented as the β-actin-normalized mean ± SEM. **(C)** mRNA quantification by Quantitative Real-Time PCR (qPCR) of CPE and SgIII of Aβ-treated cells (16 h) compared with the vehicle-treated levels. Values represent percent variation compared with controls and are presented as the mean ± SEM. *$p < 0.05$; **$p < 0.01$; ***$p < 0.001$, Mann-Whitney test.

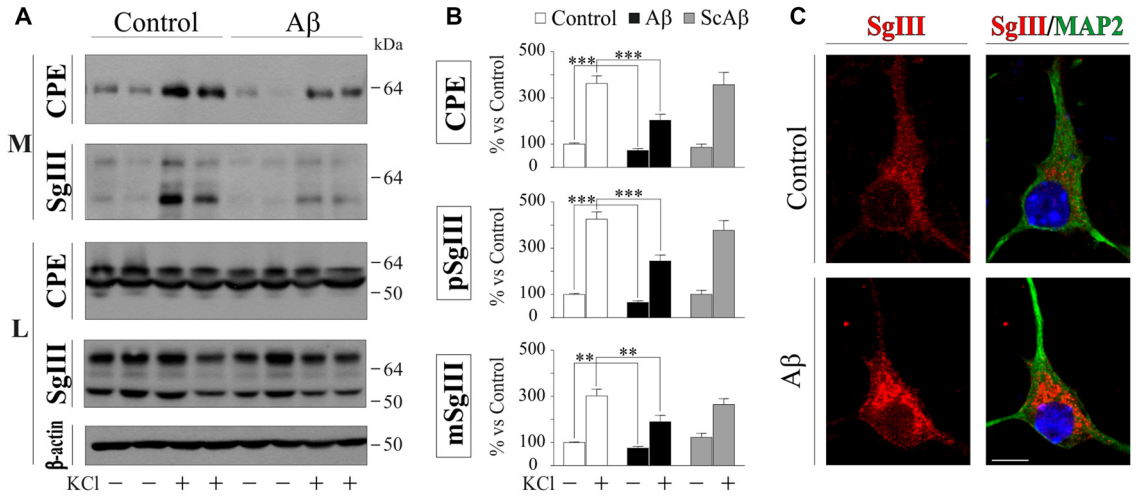

FIGURE 6 | Aβ impairs regulated secretion of CPE and SgIII in cultured cortical neurons. **(A)** Western Blot analysis shows a decrease in the release of CPE and SgIII both in basal and stimulated conditions in response to β-amyloid compared with vehicle-treated controls. Intracellular levels were unaffected by the treatment. β-actin was used as loading control. **(B)** Summary of Aβ and ScAβ effects on basal and evoked secretion of CPE, pSgIII and mSgIII. Data are presented as the β-actin-normalized mean ± SEM. $^{**}p < 0.01$; $^{***}p < 0.001$, Mann-Whitney test. **(C)** Confocal immunofluorescent images show an aberrant intracellular accumulation of SgIII in Aβ-treated neurons, mainly localized around the nucleus. Scale bar in μm: 10.

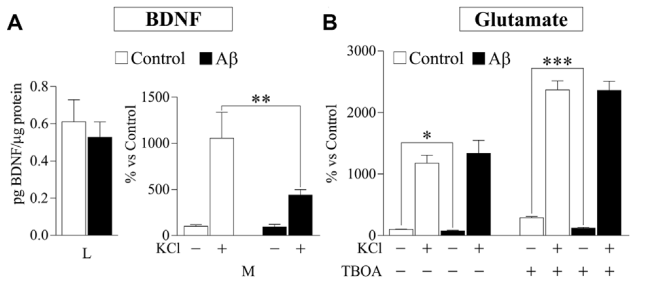

FIGURE 7 | Aβ effects on brain-derived neurotrophic factor (BDNF) and glutamate release in hippocampal cultured neurons. **(A)** Intracellular BDNF content (lysates, L) in neuronal cultures was no affected by 5 μM Aβ during 16 h, whereas K^+-stimulated release was decreased (media, M). **(B)** Extracellular glutamate levels were decreased in basal media of neurons treated with 5 μM Aβ during 16 h, whereas no changes were observed after KCl stimulation. Inhibiting glutamate re-uptake by TBOA shows that released neurotransmitter was unchanged during depolarization but decreased at basal conditions. Values were normalized by total proteins levels and represent percent variation compared with controls and are presented as the mean ± SEM. $^{*}p < 0.05$; $^{**}p < 0.01$; $^{***}p < 0.001$, Wilcoxon test.

50.9% ($p = 0.01$) and 43.4% ($p = 0.03$) for CPE, pSgIII and mSgIII, respectively.

Finally, to compare Aβ effects on neuronal DCV secretion with those on SV exocytosis, we determined glutamate release in hippocampal neurons exposed to 5 μM Aβ for 16 h by a fluorometric assay. Compared to unstimulated conditions, glutamate levels in the media were robustly increased during K^+-evoked depolarization (1176% over basal). Incubation of Aβ caused a significant decrease in extracellular glutamate levels at basal conditions (78.1% of control), whereas no changes were observed during stimulation (**Figure 7**). To ascertain the reliable contribution of secretion in extracellular glutamate levels, its re-uptake was blocked by addition of the excitatory amino acid transporter inhibitor TBOA (75 μM). In all TBOA-treated samples, extracellular glutamate concentrations were higher than in non-blocked conditions. Similar to the results obtained without the transporter inhibitor, in absence of glutamate re-uptake, Aβ reduces levels of glutamate released in unstimulated cells (41.4% of control) but does not influence secretion in KCl-depolarized neurons (**Figure 7**). Taken together, these results show that Aβ specifically impairs Ca^{2+}-regulated secretion of DCVs in neuronal populations.

Aβ Impairs DCV Secretion in Adult Neural Cells *In Situ*

To gain further insight into the impact of Aβ on regulated secretory pathway in neural cells, we next performed experiments on acute brain slices from adult mice. A major advantage of slice preparations is that cells *in situ* largely retain the states of differentiation, cytoarchitecture, extracellular matrix and synaptic circuits of the intact adult brain. First, we characterized CPE and SgIII secretion in horizontal adult brain slices under different conditions by western blot analysis (**Figure 8**). Low levels of both proteins were detected in unstimulated slices. However, CPE and SgIII release markedly increased after 10 min of a depolarizing stimulus (55 mM $[K^+]_0$). Cell integrity in the slice was confirmed by the lack of vesicular integral and cytosolic proteins, such as synaptophysin and actin, in the extracellular media. As occurred in cultured neurons (**Figure 3C**), KCl-evoked secretion of mSgIII form was stronger than for precursors (**Figure 8B**). To determine the involvement of Ca^{2+} in the evoked secretion of CPE and SgIII, we performed similar experiments in

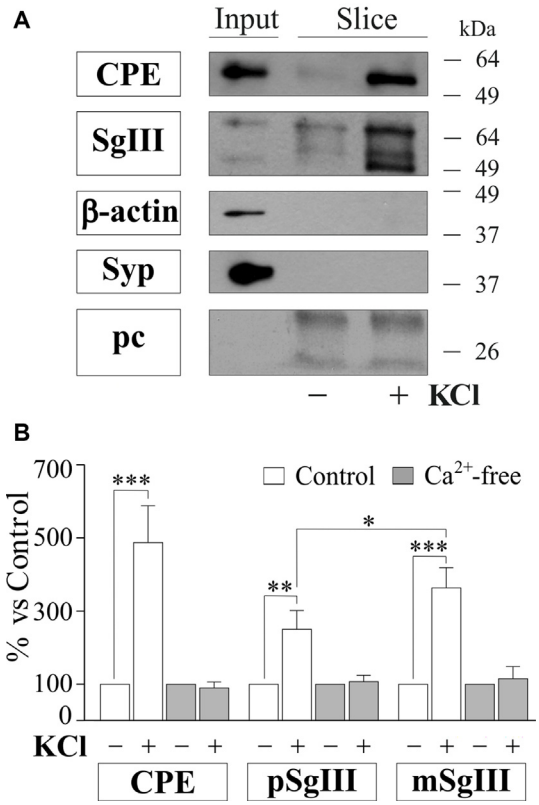

FIGURE 8 | Basal and depolarization-evoked release of CPE and SgIII from adult acute brain slices. **(A)** Representative immunoblots detecting different proteins in the perfused artificial CSF (ACSF) of the same slice after 15 min of basal (–) and 55 mM KCl (+) conditions. β-actin and synaptophysin (Syp) were used to confirm slice integrity and prestained proteins were added to ensure correct sample concentration (precipitation control, pc). Forebrain homogenates were used as input. **(B)** Histograms summarize variations of released CPE, pSgIII and mSgIII after KCl stimulation in normal (2mM $[Ca^{2+}]_0$) and nominally Ca^{2+}-free (0 mM $[Ca^{2+}]_0$, 2 mM EGTA) ACSF compared with basal conditions, showing mean ± SEM. *$p < 0.05$; **$p < 0.01$; ***$p < 0.001$, Mann-Whitney test.

a nominally Ca^{2+}-free ACSF. Lack of extracellular Ca^{2+} totally prevented the K^+-induced CPE and SgIII secretion (**Figure 8B**). These results show that *in situ* adult neural cells of the brain release CPE and SgIII in a depolarization- and Ca^{2+}-dependent manner.

To compare DCV secretion in the same cell populations between control and Aβ-treated brain slices, we split horizontal brain slices into left and right hemispheres (**Figure 9A**), minimizing the variability associated with cellular composition and responsiveness inherent to each slice. Each pair of hemispheres was incubated with vehicle (control) and 5 μM Aβ or 5 μM ScAβ for 8 h and basal and K^+-evoked secretion of CPE and SgIII were analyzed by immunoblotting and statistical analysis was performed using a Wilcoxon test (**Figures 9B,C**). Aβ notably reduced depolarization-evoked release of CPE (Aβ 334% vs. control 475.9%, $p = 0.0005$), pSgIII (Aβ 232.9% vs. control 348.3%, $p = 0.0068$) and mSgIII (Aβ 299.1% vs. control 456.2%, $p = 0.0015$). Moreover, basal secretion of CPE and mSgIII was also impaired by Aβ (88.0% and 89.1% of controls, respectively). No changes were observed in hemispheric slices incubated with ScAβ (**Figures 9B,C**).

In summary, these results evidence that Aβ impairs DCV secretion in cultured cortical cells and adult neural networks *in situ*.

DISCUSSION

The major finding of this study is that aberrant Aβ markedly impairs neuronal and astrocyte secretion of endogenously-produced DCV cargos *in vitro* and *in situ*. CPE and SgIII are two established DCV markers that belong to the regulated secretory pathway of neurons and endocrine cells with recognized roles in sorting, trafficking and processing of peptidic cargos and proposed new functions as intercellular transmitters (Bartolomucci et al., 2011; Cawley et al., 2012; Cheng et al., 2014). Here we show that neurons and astrocytes produce specific CPE and SgIII forms which are released in a cell type specific manner. CPE, SgIII and BDNF secretion, but not glutamate release, is dramatically impaired by Aβ in dispersed neurons and astrocytes in culture. Furthermore, similar detrimental effects of Aβ assemblies on basal and evoked release of DCV cargos are observed on treated acute brain slices.

Secretion of DCV Cargos in Neurons and Astrocytes

As well as their known expression by neurons, CPE and SgIII are also abundantly produced by astrocytes *in vitro* and *in vivo* (Paco et al., 2010). In agreement with a previous study performed in human brains (Plá et al., 2013), we found a segregate location of CPE and SgIII in DCV subsets in mouse neurons and astrocytes. Irrespective whether neurons were analyzed in cultures o *in situ*, a preferential somatodendritic location was observed for CPE, whereas SgIII was mainly associated with axons and terminal-like buttons. A non-overlapping vesicular location of these proteins was also found in cultured astrocytes. These observations lend support to the idea of differential routing and release of DCV cargos in the same secretory cell (Fisher et al., 1988; Zhang et al., 2011). Furthermore, the separate vesicular distribution of CPE and SgIII noticed here may imply differences in sorting mechanisms of neural cells compared with those described in endocrine cells (Hosaka et al., 2005; Cawley et al., 2016).

Although both CPE and SgIII are indeed expressed by neurons and astrocytes, we found important differences in the forms produced and their release dynamics comparing cultures of each cell type. First, probably due to the lack of the prototypical prohormone convertases of the regulated secretory pathway (PC1/3 and PC2; Winsky-Sommerer et al., 2000), astrocyte CPE and SgIII forms correspond to nonprocessed precursors. Additionally, a differential secretory profile was observed between neurons and astrocytes. Stimuli that evoked robust CPE and SgIII release in neurons barely provoked a response in astrocytes. In good agreement with a seminal work analyzing secreted CPE enzymatic activity from Fricker's lab

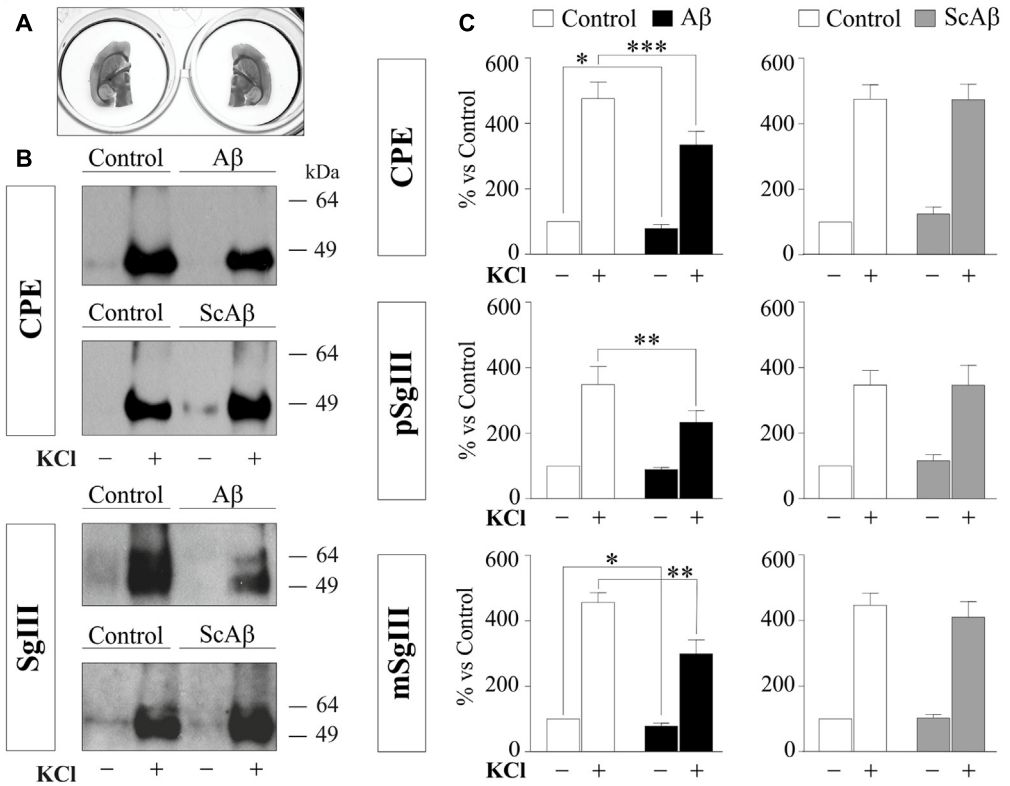

FIGURE 9 | Aβ impairs CPE and SgIII secretion in acute adult brain slices. **(A)** Left and right hemispheres of the same slice were incubated in parallel with vehicle and Aβ or vehicle and ScAβ for 8 h. **(B)** Immunoblots showing released CPE and SgIII from representative paired hemispheres after 15 min of basal (–) and 55 mM KCl (+) conditions. **(C)** Summary of Aβ and ScAβ effects on basal and evoked secretion of CPE, pSgIII and mSgIII. Values represent percent variation compared with basal release of controls (mean ± SEM). Statistical significance: $*p < 0.05$; $**p < 0.01$; $***p < 0.001$, Wilcoxon test.

(Vilijn et al., 1989), we observed no response of released CPE and SgIII to elevated $[KCl]_o$ from astrocytes. In addition, increasing $[Ca^{2+}]_i$ by ionophores caused variable and weak release responses in glial cells. Furthermore, we show that newly synthesized CPE and SgIII in non-stimulated astrocytes are poorly retained and rapidly released. Taken together, these observations would suggest that although bonafide CPE and SgIII are produced in astrocytes, they are not sorted and stored in typical DCVs. Based essentially on cell cultures, recent studies have proposed the occurrence of DCVs in astrocytes (Verkhratsky et al., 2016). However, several typical hallmarks of neuronal and endocrine DCVs (e.g., size, core density, long residence in cytoplasm, presence of synaptobrevin2, robust stimulus-dependent exocytosis) have hardly been demonstrated in cultured astrocytes (Crippa et al., 2006; Potokar et al., 2008; Paco et al., 2009). Because astrocytes *in vitro* display a partially immature phenotype and they do not accurately reproduce their *in vivo* attributes, DCV features in astroglial cells may be higher *in situ* than in culture. In fact, regulated gliosecretion of DCV components in cultured cells is enhanced under differentiating conditions, such as activation of the cAMP pathway and tone attenuation of the REST/NRSF transcription factor (Paco et al., 2009, 2016; Prada et al., 2011). On this basis, the typical size and dense core characteristics of neuroendocrine DCVs have been evidenced in granin-containing vesicles of human astrocytes *in vivo* (Hur et al., 2010).

Peptidergic Secretion as a New Target for Aβ

Aβ dramatically impairs neuronal and astrocyte secretion of DCV cargos *in vitro* and *in situ*. In unstimulated astrocyte cultures Aβ exposure dramatically reduced levels of CPE and SgIII released over 8–24 h. Conversely, intracellular amounts were increased without an apparent correlation with transcriptional mechanisms. Due to the poor cytoplasm retention observed for exocytic vesicles, CPE and SgIII secretion decrease and intracellular accumulation induced by Aβ in astrocytes probably reflects an impairment of the secretory pathway. In neuronal cultures, overnight incubation with Aβ did not provoke apparent changes in intracellular levels of the DCV cargos CPE, SgIII and BDNF, but did affect their basal and KCl-stimulated secretion. Interestingly, basal release of the SV transmitter glutamate was also impaired by Aβ, while its evoked discharge was largely preserved. Because Aβ incubations reduce spontaneous neuronal activity of recurrent networks

in primary cultures (Rönicke et al., 2011; Lee et al., 2013; Zurita et al., 2013), it is possible that the intrinsic activity-driven exocytosis of both SVs and DCVs decreases as Aβ lowers activation rates. In contrast to basal secretion, when release was forced by K^+-induced depolarization, Aβ selectively impairs secretion of cargos from DCVs but not from SVs. Although the cell type source of secreted cargos cannot be addressed in intact neuro-glial circuitries, alterations in CPE and SgIII release in treated acute slices from adult brains further substantiate the notion that Aβ impairs peptidergic secretion in cortical cells. The present conclusion is supported by previous studies showing secretion failures in exogenous (ANP.emd) and endogenous (cystatin C and thrombospondin 1) vesicular cargos in cultured astrocytes and neurons expressing presenilins carrying mutations linked to familial Alzheimer disease and incubated with Aβ (Ghidoni et al., 2007; Rama Rao et al., 2013; Stenovec et al., 2016).

Because Aβ can induce dysfunctions in different factors and stages involved in the secretory pathway, how amyloidogenic peptides affect neural vesicular secretion is uncertain. Aβ could alter peptidergic secretion influencing vesicular biogenesis, trafficking and exocytosis. It has been shown that soluble Aβ forms induce key changes which could compromise the integrity of the secretory pathway at early stages, such as endoplasmic reticulum stress, Golgi fragmentation and autophagy (Alberdi et al., 2013; Joshi et al., 2014; Son et al., 2015). Moreover, Aβ can also impair transport, docking and discharge of secretory vesicles. Recent evidence has shown that Aβ disrupts regulated exocytosis through its direct interaction with SNARE proteins (Russell et al., 2012; Yang et al., 2015). However, given that DCVs and SVs share the basic SNARE machinery for Ca^{2+}-evoked secretion (Gondré-Lewis et al., 2012), the Aβ-induced impairment in DCV cargo release from KCl-depolarized neurons and not for glutamate makes a major contribution of SNAREs unlikely. On the contrary, a failure of vesicular trafficking could underlie the secretion changes reported here. A large body of evidence indicates that defects in microtubule-mediated transport contribute to the initiation or progression of neurodegenerative diseases, including AD (Encalada and Goldstein, 2014; Llorens-Martín et al., 2014). Specifically, soluble Aβ species impair dendritic and axonal BDNF transport in cultured neurons (Decker et al., 2010; Gan and Silverman, 2015). Moreover, spontaneous and Ca^{2+}-dependent mobility of ANP.emd-containing vesicles was diminished in astrocytes expressing mutated presenilin 1 (Stenovec et al., 2016). Although a dysregulation of Ca^{2+} homeostasis and mitochondrial function could also participate in secretion failure (Ferreira et al., 2015; Viola and Klein, 2015; De Strooper and Karran, 2016), we propose that impaired trafficking exerts a central role in the Aβ-mediated secretion alterations showed in this study. Furthermore, the aberrant accumulation of granin family members and CPE detected in dystrophic neurites and neuronal and astrocyte somata in the cerebral cortex of AD patients and amyloid-forming transgenic mice strongly supports an Aβ-induced impairment of vesicular transport and secretion in the peptidergic transmission (Willis et al., 2011; Plá et al., 2013). Lastly, which Aβ species are affecting neural peptidergic secretion is an intricate issue. In our Aβ preparation we virtually detected aggregates under 200 kDa. However, the array of different forms and the complex equilibrium among them at physiological conditions over time make difficult to ascertain the specific identity of the Aβ assemblies involved in peptidergic secretion failure (Jan et al., 2011; Moreth et al., 2013; Yang et al., 2017).

Pathophysiologic Implication of Impaired Peptidergic Transmission in AD

Due to critical functions of CPE, SgIII and BDNF together with their wide distribution in the cerebral cortex, it is expected that the Aβ-induced release impairment showed here is involved in the AD pathophysiology. It has been shown that CPE and SgIII sort granins, proneuropeptides, prohormones and pro-BDNF to DCVs (Cool et al., 1997; Hosaka et al., 2005; Lou et al., 2005). Therefore, it is likely that proteins belonging to the regulated secretory pathway, at least those interacting with CPE and SgIII, are aberrantly co-secreted in the presence of Aβ. In addition, a dysregulated secretion could disturb the new extracellular functions attributed to CPE (alternatively named neurotrophic factor-alpha 1, NF-α1; Cheng et al., 2014). Moreover, the association of an uncovered CPE/NF-α1 gene mutation with AD comorbidity further connects CPE with this neurodegenerative disease (Cheng et al., 2016). Because BDNF has powerful and recognized effects on synaptic transmission, plasticity and neuronal survival and is strongly linked with AD, independently of transcriptional defects, the impact of an impaired release on neural network functions is anticipated (Adachi et al., 2014).

Beyond secretion failures for CPE, SgIII and BDNF and based on a common vesicular trafficking impairment, we suggest a more general effect of Aβ on both neuronal and astroglial peptidergic secretion. Because a rise in of soluble Aβ concentrations in early phases of AD is linked with synaptic dysfunction and network disorganization, it is conceivable that alteration of peptidergic transmission, which controls circuitry function and homeostasis, is involved in AD progression. It is worth noting that improving levels of DCV cargos (i.e., BDNF and somatostatin) partially recover AD-altered networks, preventing cognitive deficits and favoring Aβ clearance (Saito et al., 2005; Nagahara et al., 2009; Zhang et al., 2015). Moreover, the aberrant secretion and intracellular accumulation of CPE and SgIII observed in Aβ-treated and AD mouse and human brains (Plá et al., 2013) are in line with the low levels found in the CSF of AD patients by quantitative proteomics (Fagan and Perrin, 2012). Taking into account the importance of CSF biomarkers for clinical practice and trial design (Lleó et al., 2015), CSF changes based on peptidergic secretion failures could reflect synaptic dysfunction and serve as complementary diagnostic biomarkers of AD at early stages.

In summary, this study demonstrates that neuronal and astrocyte secretion of endogenous DCV proteins is impaired by Aβ *in vitro* and *in situ*. Additionally, Aβ-induced dysregulated peptidergic transmission could play an important role in the pathogenesis of AD and DCV cargos are possible candidates as CSF biomarkers.

AUTHOR CONTRIBUTIONS

VP planned and conducted all the experiments, data analysis and interpretation. NB contributed to performing some experiments and figure preparation. EP provided materials and contributed to data analysis. FA conceived, planned, interpreted and supervised the study and wrote the manuscript. All authors read and approved its final manuscript.

FUNDING

This work was supported (FA) by grants from Spanish Ministry of Economy and Competitiveness (BFU2013-48822-R and BFU2016-80868-R; MINECO/FEDER) and from Catalonian Government (2014SGR-01178). VP and NB are grateful to the Universitat de Barcelona (APIF) and Generalitat de Catalunya (FI) for their financial support, respectively.

ACKNOWLEDGMENTS

We are grateful to Dr I. Lindberg (University of Maryland) for PC2 antibody, Drs I. Ferrer, J.A. del Rio and J. Pérez-Clausell (Universitat de Barcelona), T. Fernández (Universidad Rey Juan Carlos) and A. Lleó and D Alcolea (Hospital de la Santa Creu i Sant Pau) for helpful discussions, V. Fagetti for technical assistance and H. Evans for editorial assistance.

REFERENCES

Abramov, E., Dolev, I., Fogel, H., Ciccotosto, G. D., Ruff, E., and Slutsky, I. (2009). Amyloid-β as a positive endogenous regulator of release probability at hippocampal synapses. *Nat. Neurosci.* 12, 1567–1576. doi: 10.1038/nn.2433

Adachi, N., Numakawa, T., Richards, M., Nakajima, S., and Kunugi, H. (2014). New insight in expression, transport and secretion of brain-derived neurotrophic factor: implications in brain-related diseases. *World J. Biol. Chem.* 5, 409–428. doi: 10.4331/wjbc.v5.i4.409

Aguado, F., Espinosa-Parrilla, J. F., Carmona, M. A., and Soriano, E. (2002). Neuronal activity regulates correlated network properties of spontaneous calcium transients in astrocytes in situ. *J. Neurosci.* 22, 9430–9444.

Alberdi, E., Wyssenbach, A., Alberdi, M., Sánchez-Gómez, M. V., Cavaliere, F., Rodríguez, J. J., et al. (2013). Ca^{2+}-dependent endoplasmic reticulum stress correlates with astrogliosis in oligomeric amyloid β-treated astrocytes and in a model of Alzheimer's disease. *Aging Cell* 12, 292–302. doi: 10.1111/acel.12054

Araque, A., Carmignoto, G., Haydon, P. G., Oliet, S. H. R., Robitaille, R., and Volterra, A. (2014). Gliotransmitters travel in time and space. *Neuron* 81, 728–739. doi: 10.1016/j.neuron.2014.02.007

Arias, C., Arrieta, I., and Tapia, R. (1995). β-Amyloid peptide fragment 25–35 potentiates the calcium-dependent release of excitatory amino acids from depolarized hippocampal slices. *J. Neurosci. Res.* 41, 561–566. doi: 10.1002/jnr.490410416

Bartolomucci, A., Possenti, R., Mahata, S. K., Fischer-Colbrie, R., Loh, Y. P., and Salton, S. R. J. (2011). The extended granin family: structure, function, and biomedical implications. *Endocr. Rev.* 32, 755–797. doi: 10.1210/er.2010-0027

Brito-Moreira, J., Paula-Lima, A. C., Bomfim, T. R., Oliveira, F. F., Sepúlveda, F. J., De Mello, F. G., et al. (2011). Aβ oligomers induce glutamate release from hippocampal neurons. *Curr. Alzheimer Res.* 8, 552–562. doi: 10.2174/156720511796391917

Cawley, N. X., Rathod, T., Young, S., Lou, H., Birch, N., and Loh, Y. P. (2016). Carboxypeptidase E and secretogranin III coordinately facilitate efficient sorting of proopiomelanocortin to the regulated secretory pathway in AtT20 cells. *Mol. Endocrinol.* 30, 37–47. doi: 10.1210/me.2015-1166

Cawley, N. X., Wetsel, W. C., Murthy, S. R. K., Park, J. J., Pacak, K., and Loh, Y. P. (2012). New roles of carboxypeptidase E in endocrine and neural function and cancer. *Endocr. Rev.* 33, 216–253. doi: 10.1210/er.2011-1039

Chen, Z.-Y., Jing, D., Bath, K. G., Ieraci, A., Khan, T., Siao, C.-J., et al. (2006). Genetic variant BDNF (Val66Met) polymorphism alters anxiety-related behavior. *Science* 314, 140–143. doi: 10.1126/science.1129663

Cheng, Y., Cawley, N. X., and Loh, Y. P. (2014). Carboxypeptidase E (NF-α1): a new trophic factor in neuroprotection. *Neurosci. Bull.* 30, 692–696. doi: 10.1007/s12264-013-1430-z

Cheng, Y., Cawley, N. X., Yanik, T., Murthy, S. R. K., Liu, C., Kasikci, F., et al. (2016). A human carboxypeptidase E/NF-α1 gene mutation in an Alzheimer's disease patient leads to dementia and depression in mice. *Transl. Psychiatry* 6:e973. doi: 10.1038/tp.2016.237

Cool, D. R., Normant, E., Shen, F., Chen, H. C., Pannell, L., Zhang, Y., et al. (1997). Carboxypeptidase E is a regulated secretory pathway sorting receptor: genetic obliteration leads to endocrine disorders in Cpe(fat) mice. *Cell* 88, 73–83. doi: 10.1016/s0092-8674(00)81860-7

Crippa, D., Schenk, U., Francolini, M., Rosa, P., Verderio, C., Zonta, M., et al. (2006). Synaptobrevin2-expressing vesicles in rat astrocytes: insights into molecular characterization, dynamics and exocytosis. *J. Physiol.* 570, 567–582. doi: 10.1113/jphysiol.2005.094052

Dahlgren, K. N., Manelli, A. M., Stine, W. B. Jr., Baker, L. K., Krafft, G. A., and LaDu, M. J. (2002). Oligomeric and fibrillar species of amyloid-β peptides differentially affect neuronal viability. *J. Biol. Chem.* 277, 32046–32053. doi: 10.1074/jbc.M201750200

Decker, H., Lo, K. Y., Unger, S. M., Ferreira, S. T., and Silverman, M. A. (2010). Amyloid-β peptide oligomers disrupt axonal transport through an NMDA receptor-dependent mechanism that is mediated by glycogen synthase kinase 3β in primary cultured hippocampal neurons. *J. Neurosci.* 30, 9166–9171. doi: 10.1523/JNEUROSCI.1074-10.2010

DeKosky, S. T., and Scheff, S. W. (1990). Synapse loss in frontal cortex biopsies in Alzheimer's disease: correlation with cognitive severity. *Ann. Neurol.* 27, 457–464. doi: 10.1002/ana.410270502

De Strooper, B., and Karran, E. (2016). The cellular phase of Alzheimer's disease. *Cell* 164, 603–615. doi: 10.1016/j.cell.2015.12.056

Encalada, S. E., and Goldstein, L. S. B. (2014). Biophysical challenges to axonal transport: motor-cargo deficiencies and neurodegeneration. *Annu. Rev. Biophys.* 43, 141–169. doi: 10.1146/annurev-biophys-051013-022746

Fagan, A. M., and Perrin, R. J. (2012). Upcoming candidate cerebrospinal fluid biomarkers of Alzheimer's disease. *Biomark. Med.* 6, 455–476. doi: 10.2217/bmm.12.42

Ferreira, S. T., Lourenco, M. V., Oliveira, M. M., and De Felice, F. G. (2015). Soluble amyloid-β oligomers as synaptotoxins leading to cognitive impairment in Alzheimer's disease. *Front. Cell. Neurosci.* 9:191. doi: 10.3389/fncel.2015.00191

Fisher, J. M., Sossin, W., Newcomb, R., and Scheller, R. H. (1988). Multiple neuropeptides derived from a common precursor are differentially packaged and transported. *Cell* 54, 813–822. doi: 10.1016/s0092-8674(88)91131-2

Gan, K. J., and Silverman, M. A. (2015). Dendritic and axonal mechanisms of Ca^{2+} elevation impair BDNF transport in Aβ oligomer-treated hippocampal neurons. *Mol. Biol. Cell* 26, 1058–1071. doi: 10.1091/mbc.e14-12-1612

Ghidoni, R., Benussi, L., Paterlini, A., Missale, C., Usardi, A., Rossi, R., et al. (2007). Presenilin 2 mutations alter cystatin C trafficking in mouse primary neurons. *Neurobiol. Aging* 28, 371–376. doi: 10.1016/j.neurobiolaging.2006.01.007

Gondré-Lewis, M. C., Park, J. J., and Loh, Y. P. (2012). Cellular mechanisms for the biogenesis and transport of synaptic and dense-core vesicles. *Int. Rev. Cell. Mol. Biol.* 299, 27–115. doi: 10.1016/B978-0-12-394310-1.00002-3

Hascup, K. N., and Hascup, E. R. (2016). Soluble amyloid-β42 stimulates glutamate release through activation of the α7 nicotinic acetylcholine receptor. *J. Alzheimers Dis.* 53, 337–347. doi: 10.3233/JAD-160041

Hosaka, M., Watanabe, T., Sakai, Y., Kato, T., and Takeuchi, T. (2005). Interaction between secretogranin III and carboxypeptidase E facilitates prohormone

sorting within secretory granules. *J. Cell Sci.* 118, 4785–4795. doi: 10.1242/jcs.02608

Hur, Y. S., Kim, K. D., Paek, S. H., and Yoo, S. H. (2010). Evidence for the existence of secretory granule (dense-core vesicle)-based inositol 1,4,5-trisphosphate-dependent Ca^{2+} signaling system in astrocytes. *PLoS One* 5:e11973. doi: 10.1371/journal.pone.0011973

Jan, A., Adolfsson, O., Allaman, I., Buccarello, A.-L., Magistretti, P. J., Pfeifer, A., et al. (2011). Aβ42 neurotoxicity is mediated by ongoing nucleated polymerization process rather than by discrete Aβ42 species. *J. Biol. Chem.* 286, 8585–8596. doi: 10.1074/jbc.M110.172411

Joshi, G., Chi, Y., Huang, Z., and Wang, Y. (2014). Aβ-induced Golgi fragmentation in Alzheimer's disease enhances Aβ production. *Proc. Natl. Acad. Sci. U S A* 111, E1230–E1239. doi: 10.1073/pnas.1320192111

Koss, D. J., Jones, G., Cranston, A., Gardner, H., Kanaan, N. M., and Platt, B. (2016). Soluble pre-fibrillar tau and β-amyloid species emerge in early human Alzheimer's disease and track disease progression and cognitive decline. *Acta Neuropathol.* 132, 875–895. doi: 10.1007/s00401-016-1632-3

Lee, S., Zemianek, J., and Shea, T. B. (2013). Rapid, reversible impairment of synaptic signaling in cultured cortical neurons by exogenously-applied amyloid-β. *J. Alzheimers Dis.* 35, 395–402. doi: 10.3233/JAD-122452

Lleó, A., Cavedo, E., Parnetti, L., Vanderstichele, H., Herukka, S. K., Andreasen, N., et al. (2015). Cerebrospinal fluid biomarkers in trials for Alzheimer and Parkinson diseases. *Nat. Rev. Neurol.* 11, 41–55. doi: 10.1038/nrneurol.2014.232

Llorens-Martín, M., Jurado, J., Hernández, F., and Avila, J. (2014). GSK-3β, a pivotal kinase in Alzheimer disease. *Front. Mol. Neurosci.* 7:46. doi: 10.3389/fnmol.2014.00046

Lou, H., Kim, S.-K., Zaitsev, E., Snell, C. R., Lu, B., and Loh, Y. P. (2005). Sorting and activity-dependent secretion of BDNF require interaction of a specific motif with the sorting receptor carboxypeptidase e. *Neuron* 45, 245–255. doi: 10.1016/j.neuron.2004.12.037

Lue, L. F., Kuo, Y. M., Roher, A. E., Brachova, L., Shen, Y., Sue, L., et al. (1999). Soluble amyloid-β peptide concentration as a predictor of synaptic change in Alzheimer's disease. *Am. J. Pathol.* 155, 853–862. doi: 10.1016/s0002-9440(10)65184-x

Moreth, J., Kroker, K. S., Schwanzar, D., Schnack, C., von Arnim, C. A. F., Hengerer, B., et al. (2013). Globular and protofibrillar aβ aggregates impair neurotransmission by different mechanisms. *Biochemistry* 52, 1466–1476. doi: 10.1021/bi3016444

Mucke, L., and Selkoe, D. J. (2012). Neurotoxicity of amyloid β-protein: synaptic and network dysfunction. *Cold Spring Harb. Perspect. Med.* 2:a006338. doi: 10.1101/cshperspect.a006338

Nagahara, A. H., Merrill, D. A., Coppola, G., Tsukada, S., Schroeder, B. E., Shaked, G. M., et al. (2009). Neuroprotective effects of brain-derived neurotrophic factor in rodent and primate models of Alzheimer's disease. *Nat. Med.* 15, 331–337. doi: 10.1038/nm.1912

Paco, S., Hummel, M., Plá, V., Sumoy, L., and Aguado, F. (2016). Cyclic AMP signaling restricts activation and promotes maturation and antioxidant defenses in astrocytes. *BMC Genomics* 17:304. doi: 10.1186/s12864-016-2623-4

Paco, S., Margelí, M. A., Olkkonen, V. M., Imai, A., Blasi, J., Fischer-Colbrie, R., et al. (2009). Regulation of exocytotic protein expression and Ca^{2+}-dependent peptide secretion in astrocytes. *J. Neurochem.* 110, 143–156. doi: 10.1111/j.1471-4159.2009.06116.x

Paco, S., Pozas, E., and Aguado, F. (2010). Secretogranin III is an astrocyte granin that is overexpressed in reactive glia. *Cereb. Cortex* 20, 1386–1397. doi: 10.1093/cercor/bhp202

Palop, J. J., and Mucke, L. (2016). Network abnormalities and interneuron dysfunction in Alzheimer disease. *Nat. Rev. Neurosci.* 17, 777–792. doi: 10.1038/nrn.2016.141

Parodi, J., Sepúlveda, F. J., Roa, J., Opazo, C., Inestrosa, N. C., and Aguayo, L. G. (2010). β-amyloid causes depletion of synaptic vesicles leading to neurotransmission failure. *J. Biol. Chem.* 285, 2506–2514. doi: 10.1074/jbc.M109.030023

Plá, V., Paco, S., Ghezali, G., Ciria, V., Pozas, E., Ferrer, I., et al. (2013). Secretory sorting receptors carboxypeptidase E and secretogranin III in amyloid β-associated neural degeneration in Alzheimer's disease. *Brain Pathol.* 23, 274–284. doi: 10.1111/j.1750-3639.2012.00644.x

Potokar, M., Stenovec, M., Kreft, M., Kreft, M. E., and Zorec, R. (2008). Stimulation inhibits the mobility of recycling peptidergic vesicles in astrocytes. *Glia* 56, 135–144. doi: 10.1002/glia.20597

Prada, I., Marchaland, J., Podini, P., Magrassi, L., D'Alessandro, R., Bezzi, P., et al. (2011). REST/NRSF governs the expression of dense-core vesicle gliosecretion in astrocytes. *J. Cell Biol.* 193, 537–549. doi: 10.1083/jcb.201010126

Rama Rao, K. V., Curtis, K. M., Johnstone, J. T., and Norenberg, M. D. (2013). Amyloid-β inhibits thrombospondin 1 release from cultured astrocytes: effects on synaptic protein expression. *J. Neuropathol. Exp. Neurol.* 72, 735–744. doi: 10.1097/NEN.0b013e31829bd082

Rönicke, R., Mikhaylova, M., Rönicke, S., Meinhardt, J., Schröder, U. H., Fändrich, M., et al. (2011). Early neuronal dysfunction by amyloid β oligomers depends on activation of NR2B-containing NMDA receptors. *Neurobiol. Aging* 32, 2219–2228. doi: 10.1016/j.neurobiolaging.2010.01.011

Russell, C. L., Semerdjieva, S., Empson, R. M., Austen, B. M., Beesley, P. W., and Alifragis, P. (2012). Amyloid-β acts as a regulator of neurotransmitter release disrupting the interaction between synaptophysin and VAMP2. *PLoS One* 7:e43201. doi: 10.1371/journal.pone.0043201

Saito, T., Iwata, N., Tsubuki, S., Takaki, Y., Takano, J., Huang, S.-M., et al. (2005). Somatostatin regulates brain amyloid-β peptide Aβ42 through modulation of proteolytic degradation. *Nat. Med.* 11, 434–439. doi: 10.1038/nm1206

Scheltens, P., Blennow, K., Breteler, M. M. B., de Strooper, B., Frisoni, G. B., Salloway, S., et al. (2016). Alzheimer's disease. *Lancet* 388, 505–517. doi: 10.1016/s0140-6736(15)01124-1

Selkoe, D. J., and Hardy, J. (2016). The amyloid hypothesis of Alzheimer's disease at 25 years. *EMBO Mol. Med.* 8, 595–608. doi: 10.15252/emmm.201606210

Son, S. M., Nam, D. W., Cha, M.-Y., Kim, K. H., Byun, J., Ryu, H., et al. (2015). Thrombospondin-1 prevents amyloid β-mediated synaptic pathology in Alzheimer's disease. *Neurobiol. Aging* 36, 3214–3227. doi: 10.1016/j.neurobiolaging.2015.09.005

Stenovec, M., Trkov, S., Lasič, E., Terzieva, S., Kreft, M., Rodríguez Arellano, J. J., et al. (2016). Expression of familial Alzheimer disease presenilin 1 gene attenuates vesicle traffic and reduces peptide secretion in cultured astrocytes devoid of pathologic tissue environment. *Glia* 64, 317–329. doi: 10.1002/glia.22931

Talantova, M., Sanz-Blasco, S., Zhang, X., Xia, P., Akhtar, M. W., Okamoto, S.-I., et al. (2013). Aβ induces astrocytic glutamate release, extrasynaptic NMDA receptor activation, and synaptic loss. *Proc. Natl. Acad. Sci. U S A* 110, E2518–E2527. doi: 10.1073/pnas.1306832110

van den Pol, A. N. (2012). Neuropeptide transmission in brain circuits. *Neuron* 76, 98–115. doi: 10.1016/j.neuron.2012.09.014

Verkhratsky, A., Matteoli, M., Parpura, V., Mothet, J.-P., and Zorec, R. (2016). Astrocytes as secretory cells of the central nervous system: idiosyncrasies of vesicular secretion. *EMBO J.* 35, 239–257. doi: 10.15252/embj.201592705

Vilijn, M. H., Das, B., Kessler, J. A., and Fricker, L. D. (1989). Cultured astrocytes and neurons synthesize and secrete carboxypeptidase E, a neuropeptide-processing enzyme. *J. Neurochem.* 53, 1487–1493. doi: 10.1111/j.1471-4159.1989.tb08542.x

Viola, K. L., and Klein, W. L. (2015). Amyloid β oligomers in Alzheimer's disease pathogenesis, treatment, and diagnosis. *Acta Neuropathol.* 129, 183–206. doi: 10.1007/s00401-015-1386-3

Willis, M., Leitner, I., Jellinger, K. A., and Marksteiner, J. (2011). Chromogranin peptides in brain diseases. *J. Neural Transm.* 118, 727–735. doi: 10.1007/s00702-011-0648-z

Winsky-Sommerer, R., Benjannet, S., Rovère, C., Barbero, P., Seidah, N. G., Epelbaum, J., et al. (2000). Regional and cellular localization of the neuroendocrine prohormone convertases PC1 and PC2 in the rat central nervous system. *J. Comp. Neurol.* 424, 439–460. doi: 10.1002/1096-9861(20000828)424:3<439::AID-CNE4>3.0.CO;2-1

Yang, Y., Kim, J., Kim, H. Y., Ryoo, N., Lee, S., Kim, Y., et al. (2015). Amyloid-β oligomers may impair SNARE-mediated exocytosis by direct binding to syntaxin 1a. *Cell Rep.* 12, 1244–1251. doi: 10.1016/j.celrep.2015.07.044

Yang, T., Li, S., Xu, H., Walsh, D. M., and Selkoe, D. J. (2017). Large soluble oligomers of amyloid β-protein from Alzheimer brain are far less neuroactive than the smaller oligomers to which they dissociate. *J. Neurosci.* 37, 152–163. doi: 10.1523/JNEUROSCI.1698-16.2016

Zhang, L., Fang, Y., Lian, Y., Chen, Y., Wu, T., Zheng, Y., et al. (2015). Brain-derived neurotrophic factor ameliorates learning deficits in a rat model of Alzheimer's disease induced by aβ1–42. *PLoS One* 10:e0122415. doi: 10.1371/journal.pone.0122415

Zhang, Z., Wu, Y., Wang, Z., Dunning, F. M., Rehfuss, J., Ramanan, D., et al. (2011). Release mode of large and small dense-core vesicles specified by different synaptotagmin isoforms in PC12 cells. *Mol. Biol. Cell* 22, 2324–2336. doi: 10.1091/mbc.E11-02-0159

Zurita, M. P., Muñoz, G., Sepúlveda, F. J., Gómez, P., Castillo, C., Burgos, C. F., et al. (2013). Ibuprofen inhibits the synaptic failure induced by the amyloid-β peptide in hippocampal neurons. *J. Alzheimers Dis.* 35, 463–473. doi: 10.3233/JAD-122314

Conflict of Interest Statement: The authors declare that the research was conducted in the absence of any commercial or financial relationships that could be construed as a potential conflict of interest.

4.3 Chapter 3: Dense Core Vesicle Markers Decline in Cerebrospinal Fluid and Accumulate in Dystrophic Neurites and Granulovacuolar Degeneration Bodies in Alzheimer's Disease

DENSE CORE VESICLE MARKERS DECLINE IN CEREBROSPINAL FLUID AND ACCUMULATE IN DYSTROPHIC NEURITES AND GRANULOVACUOLAR DEGENERATION BODIES IN ALZHEIMER'S DISEASE

Virginia Plá [1,2,*], Neus Barranco [1,2,*], Daniel Alcolea[3,4], Iris Lindberg[5], Reiner Fischer-Colbrie[6], Isidro Ferrer[4,7], Alberto Lleó[3,4] and Fernando Aguado[1,2]

(1) Department of Cell Biology, Physiology and Immunology, University of Barcelona, Barcelona E-08028, Spain. (2) Institute of Neurosciences, University of Barcelona. (3) Memory Unit, Department of Neurology, Sant Pau Biomedical Research Institute. Sant Pau Hospital, Autonomous University of Barcelona, Barcelona.(4) Centro de Investigaciones en Red en Enfermedades Neurodegenerativas (CIBERNED), Spain (5) Department of Anatomy and Neurobiology, University of Maryland Medical School, Baltimore, MD, 21201, USA. (6) Medical University of Innsbruck, Institute of Pharmacology, Innsbruck, Austria (7) Institute of Neuropathology, Bellvitge Biomedical Research Institute, Bellvitge University Hospital, University of Barcelona, Hospitalet de Llobregat, Spain.

(*) These authors contributed equally

Running head: DCV cargos in AD brain and CSF

Keywords: Alzheimer’s disease, amyloid, biomarkers, cerebral cortex, cerebrospinal fluid, dense-core vesicles, glia, granulovacuolar degeneration, PCSK2, synapse, tau protein.

INTRODUCTION

Alzheimer's disease (AD) is the most prevalent neurodegenerative disorder in the elderly (Scheltens et al., 2016). Because no effective treatments or prevention for AD are currently available, understanding of the pathological mechanisms and identification of diagnostic biomarkers in early stages of this type of dementia are crucial to therapeutic developments (Canter at al., 2016; Lleó al., 2015). The main clinical symptoms of AD are gradual and progressive memory and cognitive impairments which strongly correlate with the cortical atrophy-related synapse and neuronal loss in all affected brain regions (DeKosky & Scheff, 1990; Terry et al., 1990; Selkoe et al., 2002). Pathologically, AD is characterized by two hallmark lesions, deposits of amyloid-β peptides (Aβ) in extracellular senile plaques and accumulation of hyperphosphorylated tau protein in somatic neurofibrillary tangles and plaque-surrounding dystrophic neurites. Besides circuitry and neuronal cell bodies loss, cerebral amyloid angiopathy, granulovacuolar degeneration (GVD) and Hirano bodies and glial activation have also been suggested as part of AD pathology (Serrano-Pozo et al., 2011; Vinters, 2015).

Over the last years, an intensive effort is under way to identify AD fluid biomarkers uncovering the different neuropathological changes for clinical practice and trial design (Zetterberg, 2017). Reliable cerebrospinal fluid (CSF) signatures have been developed for plaque and tangle pathologies and for neurodegenerative processes (reduced $A\beta_{1–42}$ and increased phosphorylated tau (P-tau) and total tau (T-tau) levels, respectively). These so-called core CSF biomarkers are currently used for diagnosis of AD and also in patients at the mil cognitive impairment (MCI) stage of the disease (Olsson et al., 2016). Additionally, recent reports have proposed several microglial and astrocyte proteins, such as Trem-2 and YKL-40,

as biomarkers of glial activation in AD (Suárez-Calvet et al., 2016; Craig-Schapiro et al., 2010). Importantly, because decreased synapse number is the major quantitative correlate of loss of memory and cognition in AD brain (Selkoe et al., 2002), much interest is currently focusing on biomarkers detecting the degree of synaptic dysfunction and degeneration in early stages of AD. Novel CSF biomarkers candidates for synaptic pathology include membrane-associated presynaptic proteins involved in neurosecretion, such as SNAP-25 and synaptotagmin-1, the post-synaptic cytosolic neurogranin and the cytoskeletal component neurofilament light (Brinkmalm et al., 2014; Öhrfelt et al., 2016; Mattsson et al., 2016). Increased CSF levels of all these proteins in AD dementia likely reflects neurodegenerative processes. Other group of potential biomarkers for synapse loss and degeneration comprises released cargos of dense core vesicles (DCVs) that belong to the regulated secretory pathway. In fact, DCV-containing chromogranin A (CgA) was one of the first biochemical marker candidates for AD synaptic degeneration, which has been consistently identified in many studies, both in its intact form and as proteolytic fragments (Blennow et al., 1995; Fagan and Perrin 2012). CSF levels of CgA and other DCV proteins, such as chromogranin B and Secretogranin II, have been identified in proteomics screens of AD patients, offering variable results (Fagan and Perrin 2012). Moreover, no validating analysis of most of these proteomic-generated candidates are available. Here, we analyze the abundant DCV cargos processing prohormone convertases 1·and 2 (PC1/3 and PC2), carboxypeptidase E (CPE) and Secretogranin III (SgIII) in the cerebral cortex and CSF of AD patients by immunological methods. We show that most DCV proteins are aberrantly accumulated in dystrophic neurites and in GVD bodies in AD cortices. Interestingly, MCI-AD patients display decreased levels of all of these secretory proteins in the CSF. Furthermore, CSF levels of processed PC2 in AD

patients correlated inversely with those of T-tau and directly with the mini-mental state examination (MMSE) score. The present results showing marked alterations of DCV proteins in AD brain and CSF propose their use as fluid CNS biomarkers of cortical degeneration in early stage AD.

MATERIAL AND METHODS

Brain tissues

Post-mortem human AD (n=11) and non-AD (n=13) brain samples (aged 49–81; post-mortem delays between 2.15 and 8.5h) originated from the Institute of Neuropathology Brain Bank IDIBELL Hospital Universitari de Bellvitge (Hospitalet de Llobregat, Spain) in agreement with the local ethics committee. Individuals were selected according to post-mortem diagnosis of AD following the Consortium to Establish a Registry for Alzheimer's Disease (CERAD) criteria (Mirra et al., 1991). AD diagnosed subjects corresponded to Braak stages V and VI. No neurological symptoms or signs were noted in control cases.

Lumbar CSF samples

Human CSF samples were obtained from patients of the Hospital de la Santa Creu i Sant Pau (Barcelona). Extractions were carried out at the same center by routine diagnostic lumbar puncture and samples were regularly analyzed to minimize intervention-derived inflammation. Biopsied CSF samples were collected from diseased patients (n=33) clinically diagnosed as incipient AD/ mild cognitive impairment (MCI) and from non-demented control subjects (n=33). CSF core AD biomarkers were determined by ELISA and secretory proteins were analyzed by SDS-PAGE and immunoblotting, as explained below.

Antibodies

Polyclonal antibodies against SgIII and monoclonal anti β-actin peroxidase antibodies were purchased from Sigma (Sigma-Aldrich, Diesenhofen, Germany). Monoclonal and polyclonal antibodies against CPE were obtained from BD Biosciences (BD Transduction Laboratories, San Jose, CA, USA) and GeneTex (GeneTex Inc, Irvine, CA, USA), respectively. Polyclonal antibodies against PC1/3 were purchased from Abcam (Abcam Plc, Cambridge, UK) and Thermo (Thermo Fisher Scientific, Waltham, MA, USA), Cell Signaling (Cell Signaling Technology Inc, Leiden, The Netherlands) and Santa Cruz (Santa Cruz Biotechnology Inc, Heidelberg, Germany). Two polyclonal antibodies anti PC2 were from GeneTex Inc and from Dr. Iris Lindberg (Maryland, Baltimore, USA). SgII were kindly provided by Dr. Reiner Fischer-Colbrie (Innsbruck, Austria). Polyclonal antibodies against Cystatin C (CysC) and monoclonal antibodies against GFAP were obtained from Millipore Iberica (Madrid, Spain). Monoclonal anti LAMP-1 and NFL antibodies were obtained from Developmental Studies Hybridoma Bank at the University of Iowa (Iowa City, Iowa, USA) and Cell Signaling (Cell Signaling Technology Inc, Leiden, The Netherlands), respectively. Antibodies against Aβ and AT8 were from DAKO (Glostrup, Denmark) and Innogenetics (Gent, Belgium).

Immunohistochemistry

Human brain samples were fixed in 4% paraformaldehyde in 0.1 M phosphate buffer, pH 7.4, by immersion. After being cryoprotected in a 30% sucrose solution, samples were frozen and sectioned with a cryostat. For peroxidase immunohistochemistry, histological sections were blocked for 30min in 10% methanol and 3% H_2O_2 supplemented phosphate buffered saline (PBS) and afterwards washed in PBS. Pretreatment with formic acid was used to enhance labeling of plaques. To avoid nonspecific binding, brain sections were blocked in PBS

containing 10% serum, 0.2% glycine, 0.1% Triton X-100 and 0.2% gelatin for 1h at room temperature (RT). Incubations with the primary antibodies were carried out overnight at 4°C in PBS containing 1% fetal bovine serum, 0.1% Triton X-100 and 0.2% gelatin. Bound antibodies were detected using the avidin-biotin-peroxidase system (Vectastain ABC kit, Vector Laboratories Inc., Burlingame, CA, USA). PBS containing 0.05% diaminobenzidine and 0.01% H_2O_2 was used to visualize the peroxidase complex. Sections were mounted, dehydrated and coverslipped in Eukitt® (Sigma-Aldrich, Diesenhofen, Germany). Double-labeling fluorescent immunohistochemistry was carried out incubating with different fluorochrome-conjugated secondary antibodies (Alexa Fluor 488 and Alexa Fluor 568, Molecular Probes, Eugene, OR, USA), and cell nuclei were stained with Hoechst (Sigma-Aldrich, Diesenhofen, Germany). Endogenous autofluorescence was avoided using Sudan Black B (Sigma-Aldrich, Diesenhofen, Germany). Sections were mounted in Mowiol (Merk Chemicals Ltd., Nottingham, UK) and visualized with a Leica TCS SPE scanning confocal microscope. The specificity of the immunolabeling was checked using a previous incubation of the primary antibodies with an excess of antigen (Proteintech Group Inc., Deansgate, Manchester, UK), using nonspecific IgG instead of the primary antibodies and omitting them. No immunostaining was observed in these conditions.

Western blotting and radioimmunoassay

Human lumbar CSF samples were collected into vials at equal volume and human brain tissues were homogenized in ice-cold lysis buffer containing 50mM Tris-HCl pH 7.4, 150mM NaCl, 5mM MgCl2,1mM EGTA, 1% Triton X-100 and protease inhibitor cocktail (Roche Diagnostics GmbH, Mannheim, Germany). CSF samples and post nuclear brain lysates were mixed up with sample buffer 3x (Tris-HCl 188mM, Glycerol 30%, SDS 3%, Bromophenol

Blue 0.01%, β-mercaptoethanol 15%), electrophoresed in 10-12% SDS-acrylamide gels (Bio-Rad Laboratories, Hercules, CA, USA) and then transferred to polyvinylidene difluoride (PVDF) immobilization membranes (Whatman® Schleicher & Schuell, NH, USA). Membranes were blocked in a 5%-nonfat milk powder solution in Tris-buffered saline and Tween 20 (TBST; 140mM NaCl, 10mM Tris/HCl, pH 7.4 and 0.1% Tween 20) for 1h at RT and then incubated with primary antibodies in blocking solution overnight at 4°C. After numerous washes in blocking buffer, membranes were incubated during 1h with horseradish peroxidase-conjugated secondary antibodies (Bio-Rad Laboratories, Hercules, CA, USA). Enhanced chemiluminescence reagents ECL™ (GE Healthcare, Buckinghamshire, UK) were used to visualize bound antibodies. Blot images were taken with a scanner. Secretogranin II/secretoneurin (SN) radioimmunoassay was performed as described previously (Kirchmair et al., 1993). In brief, samples were denaturalized to avoid protein degradation and antiserum was added in RIA buffer and incubated for 24 h at 4ºC. SN antiserum generated with synthetic rat SN (SgII 154–186) as antigen, regardless of their length. Then iodinated SN (200 cpm/µL) was added and samples were incubated for an additional 24 h at 4ºC. The non-binded tracer was separated by dextran-coated charcoal absorption and pulled down by centrifugation. The iodinated tracer remaining in the supernatant fraction was quantified, with a detection limit of 1-2 fmol.

Statistical analysis

Quantitative data were statistically analyzed using GraphPad Prism 6.01® software (GraphPad Software, CA, USA) by t-test and Mann-Whitney test. All data are presented as the standard error means (SEM). Correlations of the measured values were examined using the Bonferroni-corrected Spearman correlation coefficient. Significance was set at $P<0.05$.

RESULTS

Neuropathological alterations of DCV cargos in the AD cerebral cortex

To investigate alterations in levels of DCV cargos in AD samples, first we performed immunoblotting assays to compare band patterns for different DCV proteins in normal brain tissues and CSF samples. We focus this study in the two prohormone convertases belonged to the regulated secretory pathway, PC1/3 and PC2, a third DCV processing enzyme CPE and the abundant Secretogranin SgIII. We also analyzed the classical and widely studied granin SgII and the AD-involved vesicular protein Cystatin C (Kaur et al., 2012). All secretory proteins were abundantly detected in hippocampal tissues and in CSF samples (Fig 1). In brain samples, band patterns corresponded with precursor/unprocessed (p) and mature/processed (m) forms and different bands with high and low MW likely corresponding with aggregates and cleaved species. Interestingly, precursor and processed forms of DCV cargos were robustly detected in CSF. For instance, CSF volumes as small as 1 µL were enough to detect SgIII. We tried to detect the potential biomarker NFL and the ubiquitous cytosolic brain protein β actin in the same CSF volumes, but without success. Thus, besides their abundance in brain tissues, DCV proteins are copiously detected in CSF, likely corresponding with released species.

A previous work of our group showed no differences in the levels of CPE and SgIII in the cerebral cortex (parietal cortex and hippocampus) of AD patients and age-matched controls (Plá et al., 2013). Here, we performed a similar immunoblotting analysis for PC1/3, PC2 and CysC. Despite we used a low number of samples (n=3), we found increased levels of the PC2 precursor form (pPC2) in AD hippocampus ($p=0.026$), whereas no statistical changes were detected for PC1/3 (Figure 2). Additionally, trimeric CysC levels were decreased in the parietal cortex of AD patients ($p=0.035$).

Next, we analyzed cellular distribution of DCV proteins in histological brain sections by immunohistochemical methods. In general, distribution patterns of PC1/3, PC2, CPE and SgIII were similar through different neuronal populations in the normal brain, although a differential robust immunolabeling for CPE was detected filling dendritic shafts (Fig3A). PC1/3 and PC2 were absent in non-neuronal cells, whereas immunostaining for SgIII, CPE and CysC were also detected in GFAP+ astrocytes (Fig 3A). We observed a vesicular-like intracellular labeling for each DCV protein analyzed, which differs from CysC subcellular patterns (Fig 3A). Noteworthy, all the analyzed secretory proteins were aberrantly accumulated in AT8+ dystrophic neurites surrounding amyloid plaques in parietal cortex and hippocampus from all examined AD patients (Fig 3B). In some samples, intense immunolabeling for SgIII and CysC was detected in reactive astrocytes close to the amyloid deposits (data not shown). Unexpectedly, we found strong immunolabeling for PC2, and to a lesser extend CPE, occurring in typical GVD bodies of many CA1 neurons from AD samples, whereas only occasionally were detected in age-matched controls (Fig4). Interestingly, PC2 immunolabeling of GVD bodies was associated with AT8+ neurofibrillary tangle pathology in many, but not all, individual CA1 neurons (Fig 4).

Taken together, these results show that DCV proteins are aberrantly accumulated in dystrophic neurites and GVD bodies in the AD cerebral cortex.

MCI-AD patients display decreased levels of DCV cargos in the CSF

Next, we investigate DCV levels in the AD CSF samples by immunoblotting and RIA (Fig 5). Table 1 shows the clinical characteristics and CSF core AD biomarkers of the study cohort. Compared with non-AD controls, most DCV cargos were decreased in patients diagnosed with MCI-AD. The most dramatic significantly reduction was found for pPC1/3

(42%) and CPE (21%). Unprocessed and mature forms of PC2 were statistically diminished en AD samples (16%, p=0.024 and 12%, p=0,011, respectively). Precursor SgIII levels was also decreased in AD (p=0.047), whereas no significantly differences were detected for SgII (p=0.74). A 33% decrease was also found for CysC in disease patients (p=0.001).

Finally, we investigated the relationship between DCV protein forms and MMSE score and the core AD biomarkers in AD subjects (Fig 7). We found a strong correlation between mPC2 and MMSE score ($p = 0.0001$, $r = 0.6449$) and mPC2 and t-tau ($p = 0.0004$, $r = 0.5837$). Additionally, we found a positive correlation between CPE and P-tau and pSgIII and p-tau (Fig 7).

DISCUSSION

This study show an association between brain accumulation and CSF decline of DCV markers in AD patients. In agreement with previous studies (Ferrer et al., 1999; Willis et al., 2011; Plá et al., 2013), we found key components of the DCV molecular machinery (i.e. PC1/3 and PC2) markedly accumulated in dystrophic neurites. These alterations seem to be common to all DCV component, including chromogranins, secretogranins, processing enzymes and neuroactive cargos and likely correspond with an impairment of peptidergic vesicular transport (Encalada and Goldstein, 2014). In addition to dystrophic neurites, DCV components were found dramatically accumulated in GVD bodies. As far as we know, this is the first study showing components of the regulated secretory pathway in GVD bodies. These AD-associated aberrant structures contain proteins related to cytoskeleton, autophagy, signaling and stress, but no secretory components have been reported yet (Köhler, 2016). Pathological targeting of DCV component to GVD granules could imply an alteration of the secretory pathways in AD.

Taken together, the observed accumulation of DCV cargos in dystrophic neurites and GVD bodies in AD strongly suggest an important dysfunction of the regulated secretory pathway. Furthermore, the reported negative impact of Aβ on the regulated secretory pathway of neurons and astrocytes further support an impairment of DCV secretion in AD (Plá et al., submitted).

In addition to the brain accumulation, we show that DCV cargos are decreased in CSF of early stage AD. Similar results were detected for CgA in seminal reports (Blennow et al., 1995). More recently, several proteomic screen studies have identified other DCV components in CSF of AD patients (Abdi et al., 2006; Perrin et al., 2011; Fagan and Perrin, 2012). However, some proteomic results have been inconsistent and not validated. Here we substantiate by immunological methods a general decrease of DCV cargos in AD CSF. Additionally to synapse loss we suggest that DCV impairment in AD CSF could be related to alterations in DCV secretion. The main correlation between DCV proteins and the CSF core biomarkers in AD was PC2 and T-tau. Because the PC2 neuronal-specific convertase is widely expressed through the CNS and increased T-tau levels reflects neurodegenerative processes, we propose PC2 as a CSF biomarker in AD.

TABLE 1

	Age (years)	Gender	MMSE	APOE allelic frequency	CSF Aβ42 (pg/mL)	CSF tau (pg/mL)	CSF p-tau (pg/mL)	CSF glucose (mmol/L)
ND controls (n=33)	63,75 (±7,18)	13M/20 F	29,21 (±0,96)	ε2 = 0.05; ε3 = 0.83; ε4 = 0.12	836,09 (±154,72)	221,97 (±57,44)	43,38 (±10,39)	3,46 (±0,51)
MCI-AD (n=33)	66,94 (±6,13)	12M/21 F	21,58 (±4,39)	ε2 = 0.03; ε3 = 0.44; ε4 = 0.53	353,27 (±101,20)	905,32 (±457,94)	99,33 (±31,32)	3,39 (±0,51)

Table 1. Clinical characteristics and CSF core AD biomarkers of the study subjects. According to selection criteria, MCI-AD patients displayed reduced levels of CSF Aβ42 ($p<0.001$) and lower MMSE scores ($p<0.001$) and levels of CSF tau ($p<0.001$) and p-tau ($p<0.001$) were significantly higher in MCI-AD patients in comparison with the control group ($p<0.001$). No significant differences were observed in age and CSF glucose levels between groups. Data are shown as means and standard deviations for age, MMSE, CSF Aβ42, tau, p-tau and total protein. Statistically significant difference was calculated using a two-tailed Mann-Whitney test.

FIGURE 1

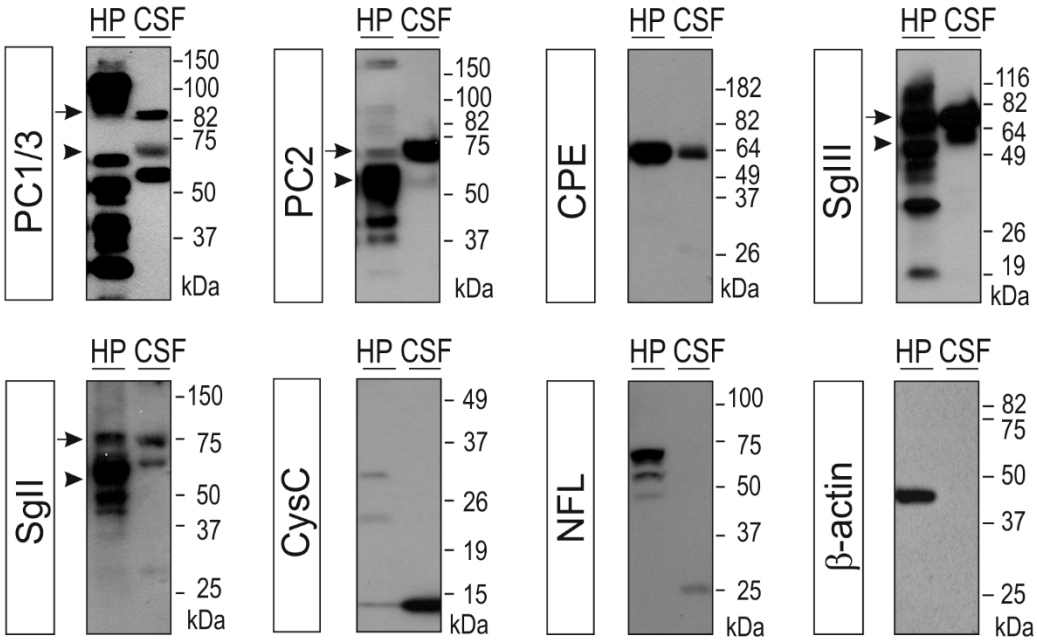

Figure 1. Brain secretory proteins are abundantly detected in the human CSF. Western blotting analysis of the secretory proteins PC1/3, PC2, CPE, SgIII, SgII, and CysC in human hippocampus (HP, 20µg) and CSF (6-10µL). In CSF, precursor forms (arrows) of granins and convertases are more abundant than their mature forms (arrow-heads). Additional bands in HP samples likely correspond to aggregates and cleaved forms. Brain tissues display monomeric, dimeric and trimeric CysC forms, while only monomers are detected in CSF. Cytosolic proteins such as NFL and β-actin are not detected in the CSF when performing analyses of the same samples at similar volumes and concentrations.

FIGURE 2

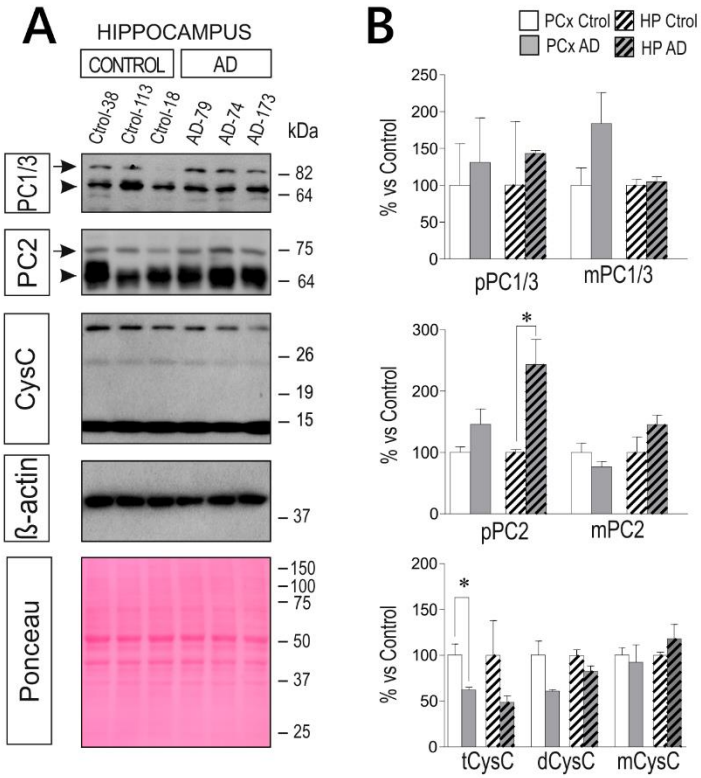

Figure 2. Levels of secretory proteins in the AD cerebral cortex. Hippocampal and parietal cortical samples of controls and AD patients (Braak stages V-VI) were analyzed by western blot. Representative immunoblots for some secretory proteins and a Ponceau S staining to establish content of total proteins are shown in A. In B, graphs summarize percent variation of secretory protein levels in the parietal cortex and hippocampus of AD patients compared to controls (n=3 for each tissue). A reduction of the trimeric form of CysC (tCysC; p=0.035) and an increase of the precursor form of PC2 (pPC2; p=0.026) is determined in the cortex and in the hippocampus of AD patients, respectively (mean ±SEM, two-tailed t-student test).

FIGURE 3

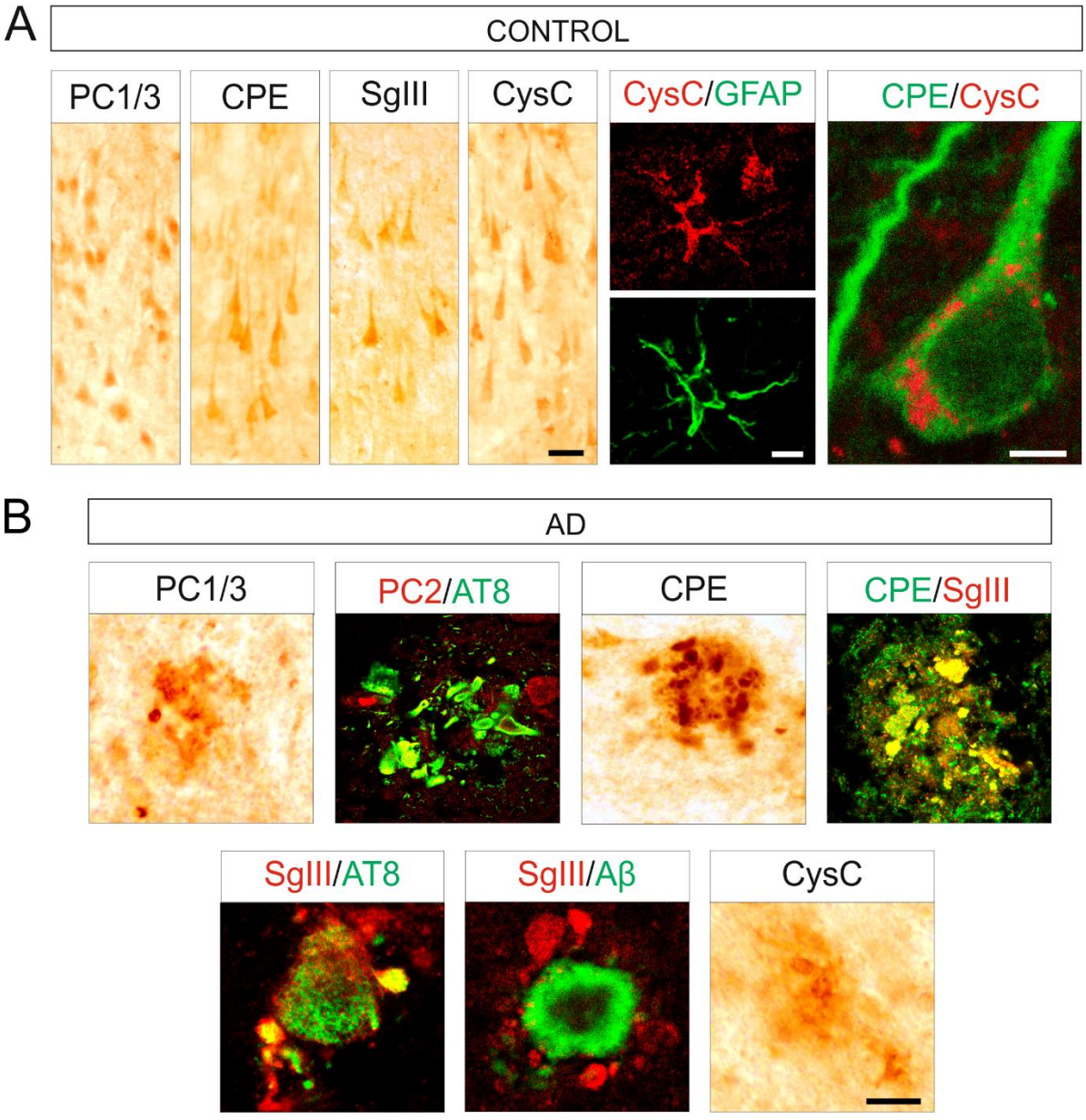

Figure 3. A. PC1/3, CPE, SgIII and CysC expression in the control hippocampus. Immunoreactivity is found mainly in pyramidal neurons. Double immunolabeling for CysC (red) and GFAP (green) confirms astroglial identity. CPE (green) and CysC (red) are located in different subcellular compartments in pyramidal neurons as shown by confocal fluorecent microscopy. B. PC1/3, PC2, CPE, SgIII and CysC are accumulated in senile plaques (Aβ; green) and dystrophic neurites (AT8; green) of AD patients. Scale bars in μm: 20; 10; 5; 20.

FIGURE 4

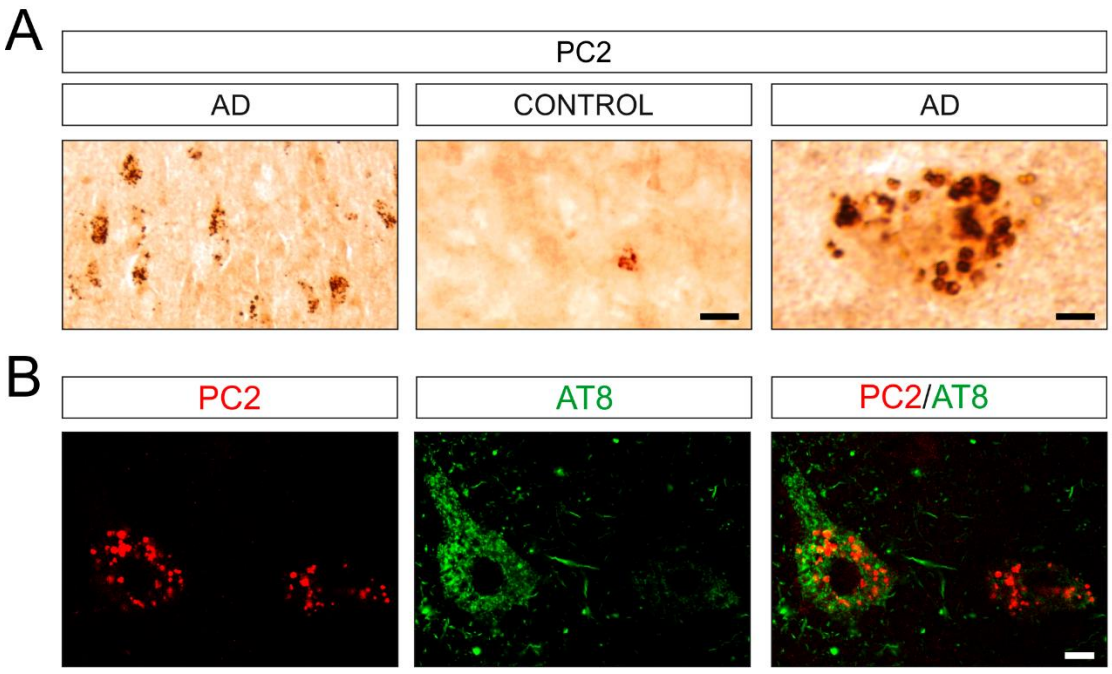

Figure 4. A. Immunohistochemical detection of PC2 in the hippocampal region CA1 of control and AD patients. B. Double immunolabeling in the CA1 of AD patients illustrating PC2-positive granulovacuolar degenerations (GVDs; red) in p-tau (AT8; green) positive or negative pyramidal neurons. Scale bars in µm: upper-left, 20; upper-right, 4; bottom, 7.

FIGURE 5

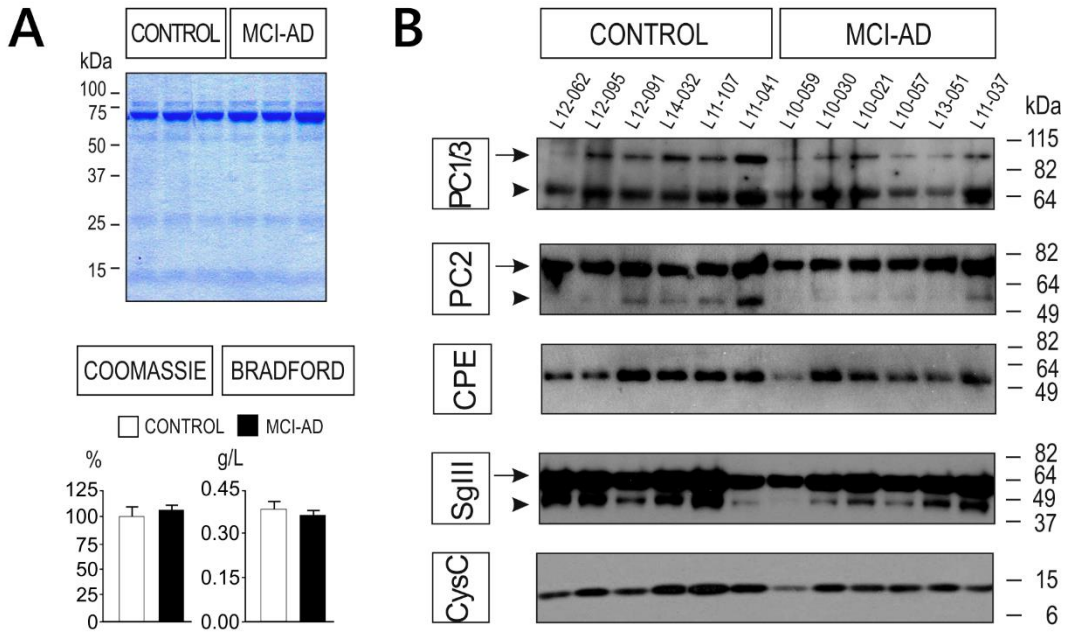

Figure 5. Western blot analysis of secretory proteins in the CSF of MCI-AD patients. Total protein content in control and MCI-AD CSF samples was determined by Coomassie staining and Bradford assay (A). Representative immunoblots show levels of CPE, PC1/3, PC2, SgIII and CysC forms in the same CSF control and MCI-AD samples (B).

FIGURE 6

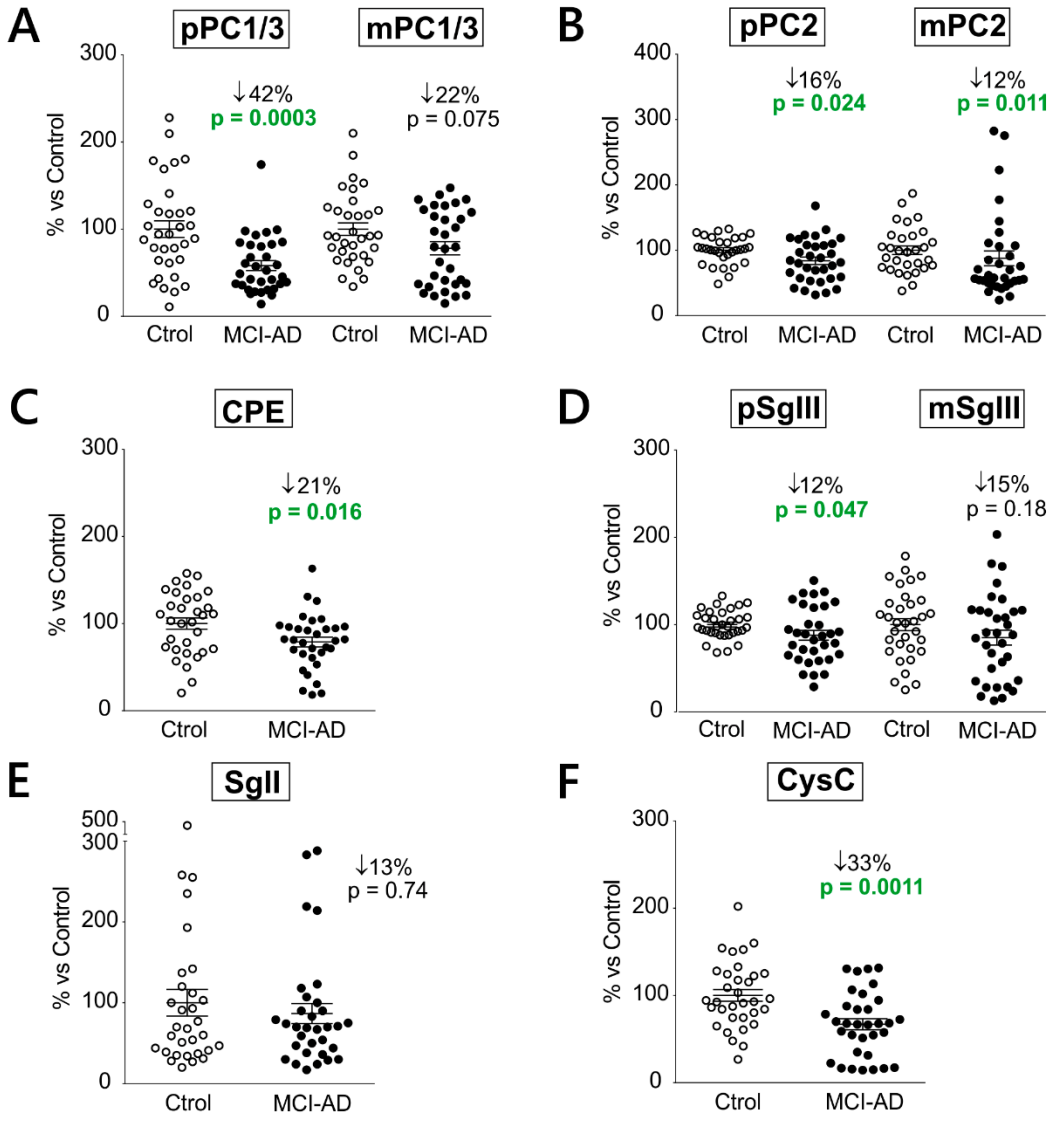

Figure 6. CSF samples of MCI-AD patients display decreased levels of secretory proteins. CPE, PC1/3, PC2, SgIII and CysC were analyzed by western blot and SgII by radioimmunoassay. Scatter dot-plots represent percent variation of secretory proteins levels in the CSF of MCI-AD patients (n=33) compared to controls (n=33). Arrows indicate percentage reduction and p values the statistic significances. Data are presented as the mean ± SEM of analysis performed in duplicate. Statistically significant difference was calculated using a two-tailed Mann-Whitney test.

FIGURE 7

A

vs CSF	pPC1/3		mPC1/3		pPC2		mPC2		CPE		pSgIII		mSgIII		SgII		CysC	
	r	p	r	p	r	p	r	p	r	p	r	p	r	p	r	p	r	p
Age	0,3137	0,0754	0,1852	0,3023	0,0635	0,7255	0,3436	0,0503	-0,2393	0,1798	-0,1280	0,4778	-0,0348	0,8477	0,0304	0,8687	-0,1156	0,5216
MMSE	0,3143	0,0749	0,4416	0,0101	-0,0517	0,7751	0,6449	0,0001	-0,1387	0,4413	0,0072	0,9681	0,1911	0,2867	0,1614	0,3775	-0,1197	0,5070
CSF Aβ42	-0,1945	0,2781	0,0239	0,8949	-0,1542	0,3914	0,2200	0,2186	0,0676	0,7086	0,1300	0,4709	0,2595	0,1448	0,0628	0,7328	0,1489	0,4083
CSF T-tau	-0,1896	0,2905	-0,4942	0,0035	0,0836	0,6438	-0,5837	0,0004	0,4717	0,0056	0,4326	0,0119	0,3010	0,0887	0,2073	0,2549	0,3714	0,0333
CSF P-tau	-0,0675	0,7089	-0,3660	0,0362	0,2094	0,2421	-0,4369	0,0110	0,5377	0,0013	0,5216	0,0019	0,4217	0,0145	0,2871	0,1111	0,2905	0,1010

B

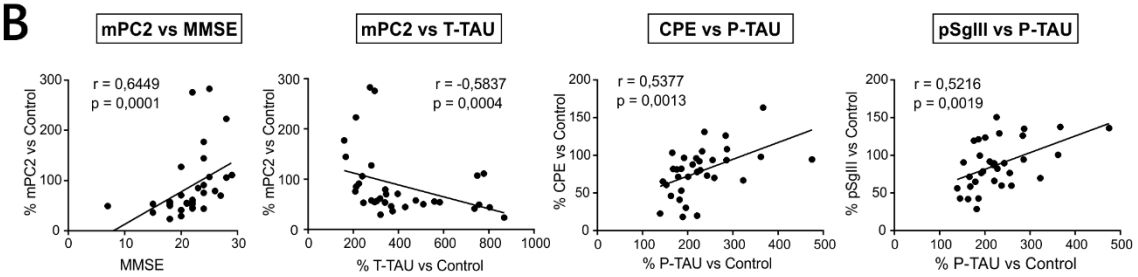

Figure 7. Correlation analysis of CSF secretory proteins with age, MMSE score and the CSF core-AD biomarkers in AD subjects. A. Table summarizing Bonferroni-corrected Spearman correlations between secretory proteins and age, MMSE score, Aβ42, tau and p-tau. Significant correlations ($p < 0.0019$) are highlighted in green and represented in correlation graphs (B).

REFERENCES

Abdi F, Quinn JF, Jankovic J, McIntosh M, Leverenz JB, Peskind E et al 2006 Detection of biomarkers with a multiplex quantitative proteomic platform in cerebrospinal fluid of patients with neurodegenerative disorders. J Alzheimers Dis 9:293–348.

Blennow K, Davidsson P, Wallin A, Ekman R. 1995. Chromogranin A in cerebrospinal fluid: a biochemical marker for synaptic degeneration in Alzheimer's disease? Dementia. 6:306-11.

Brinkmalm A1, Brinkmalm G, Honer WG, Frölich L, Hausner L, Minthon L, Hansson O, Wallin A, Zetterberg H, Blennow K, Öhrfelt A. 2014. SNAP-25 is a promising novel cerebrospinal fluid biomarker for synapse degeneration in Alzheimer's disease. Mol Neurodegener. ;9:53.

Canter RG, Penney J, Tsai LH1. 2016. The road to restoring neural circuits for the treatment of Alzheimer's disease. Nature. 539(7628):187-196. doi: 10.1038/nature20412.

Craig-Schapiro R, Perrin RJ, Roe CM, Xiong C, Carter D, Cairns NJ, Mintun MA, Peskind ER, Li G, Galasko DR, Clark CM, Quinn JF, D'Angelo G, Malone JP, Townsend RR, Morris JC, Fagan AM, Holtzman DM. 2010. YKL-40: a novel prognostic fluid biomarker for preclinical Alzheimer's disease. Biol Psychiatry. 68(10):903-12.

DeKosky, S. T., and Scheff, S. W. (1990). Synapse loss in frontal cortex biopsies in Alzheimer’s disease: correlation with cognitive severity. Ann. Neurol. 27, 457–64.

Encalada, S. E., and Goldstein, L. S. B. 2014. Biophysical challenges to axonal transport: motor cargo deficiencies and neurodegeneration. Annu. Rev. Biophys. 43, 141–69.

Ferrer I, Marín C, Rey MJ, Ribalta T, Goutan E, Blanco R, Tolosa E, Martí E,. 1999. BDNF and full-length and truncated TrkB expression in Alzheimer disease. Implications in therapeutic strategies. J Neuropathol Exp Neurol. 58:729-39.

Heywood WE, Galimberti D, Bliss E, Sirka E, Paterson RW, Magdalinou NK, Carecchio M, Reid E, Heslegrave A, Fenoglio C, Scarpini E, Schott JM, Fox NC, Hardy J, Bhatia K, Heales S, Sebire NJ, Zetterberg H, Mills K. 2015. Identification of novel CSF biomarkers for neurodegeneration and their validation by a high-throughput multiplexed targeted proteomic assay. Mol Neurodegener. 10:64.

Kaur G1, Levy E. 2012. Cystatin C in Alzheimer's disease. Front Mol Neurosci. 5:79.

Kirchmair, R., Hogue-Angeletti, R., Gutierrez, J., Fischer-Colbrie, R., and Winkler, H. 1993. Secretoneurin—a neuropeptide generated in brain, adrenal medulla and other endocrine tissues by proteolytic processing of secretogranin II (chromogranin C). Neuroscience 53, 359–365.

Köhler C. 2016. Granulovacuolar degeneration: a neurodegenerative change that accompanies tau pathology. Acta Neuropathol. 132:339-59.

Lleó A, Cavedo E, Parnetti L, Vanderstichele H, Herukka SK, Andreasen N, Ghidoni R, Lewczuk P, Jeromin A, Winblad B, Tsolaki M, Mroczko B, Visser PJ, Santana I, Svenningsson P, Blennow K, Aarsland D, Molinuevo JL, Zetterberg H, Mollenhauer B. 2015. Cerebrospinal fluid biomarkers in trials for Alzheimer and Parkinson diseases. Nat Rev Neurol. 11:41-55.

Mattsson N1, Insel PS2, Palmqvist S3, Portelius E4, Zetterberg H5, Weiner M6, Blennow K4, Hansson O1; Alzheimer's Disease Neuroimaging Initiative. 2016. Cerebrospinal fluid tau, neurogranin, and neurofilament light in Alzheimer's disease. EMBO Mol Med. 8):1184-1196.

Mirra SS, Heyman A, McKeel D, Sumi SM, Crain BJ, Brownlee LM, Vogel FS, Hughes JP, van Belle G, Berg L. 1991.The Consortium to Establish a Registry for Alzheimer's Disease (CERAD). Part II. Standardization of the neuropathologic assessment of Alzheimer's disease. Neurology. 41:479-86.

Plá V, Paco S, Ghezali G, Ciria V, Pozas E, Ferrer I, Aguado F. 2013. Secretory sorting receptors carboxypeptidase E and secretogranin III in amyloid β-associated neural degeneration in Alzheimer's disease. Brain Pathol. 2013 May;23(3):274-84.

Perrin RJ, Craig-Schapiro R, Malone JP, Shah AR, Gilmore P, Davis AE et al 2011 Identification and validation of novel cerebrospinal fluid biomarkers for staging early Alzheimer's disease. Plos ONE 6:e16032.

Öhrfelt A, Brinkmalm A, Dumurgier J, Brinkmalm G, Hansson O, Zetterberg H, Bouaziz-Amar E, Hugon J, Paquet C, Blennow K. 2016. The pre-synaptic vesicle protein synaptotagmin is a novel biomarker for Alzheimer's disease. Alzheimers Res Ther. 8:41.

Selkoe DJ. 2002. Alzheimer's disease is a synaptic failure. Science 298:789–791.

Terry RD, Masliah E, Salmon DP, Butters N, DeTeresa R, Hill R, Hansen LA, Katzman R. 1991. Physical basis of cognitive alterations in Alzheimer's disease: Synapse loss is the major correlate of cognitive impairment. Ann Neurol 30:572–580.

Willis, M., Leitner, I., Jellinger, K. A., and Marksteiner, J. 2011. Chromogranin peptides in brain diseases. J. Neural Transm. 118, 727–735.

Zetterberg H. 2017. Applying fluid biomarkers to Alzheimer's disease. Am J Physiol Cell Physiol. 2017 Apr 19:ajpcell.00007.2017.

4.4 Chapter 4: Dense Core Vesicle Cargos in Mouse Cerebral Cortex and Cerebrospinal Fluid During Aging and in a Model of Alzheimer's Disease

DENSE CORE VESICLE CARGOS IN MOUSE CEREBRAL CORTEX AND CEREBROSPINAL FLUID DURING AGING AND IN A MODEL OF ALZHEIMER'S DISEASE

Virginia Plá [1,2], Esther Aso[3], Reiner Fischer-Colbrie[3], Carla Rodríguez[1], Isidro Ferrer [2, 4, 5, 6] and Fernando Aguado[1,2]

1 Department of Cell Biology, Physiology and Immunology, University of Barcelona, Barcelona, Spain
2 Institute of Neurosciences of the University of Barcelona, Spain
3 Medical University of Innsbruck, Institute of Pharmacology, Innsbruck, Austria
4 Institute of Neuropathology, Pathologic Anatomy Service, Bellvitge University Hospital, IDIBELL, Hospitalet de Llobregat, Spain.
5 Department of Pathology and Experimental Therapeutics, University of Barcelona, Spain.
6 Biomedical Network Research Center on Neurodegenerative Diseases (CIBERNED), Institute Carlos III, Hospitalet de Llobregat, Spain.

ABSTRACT

Alzheimer's disease is a neurodegenerative disorder characterized by cognitive impairment and dementia that could be consequence of amyloid-β triggered synaptic dysfunction and network abnormalities. Here, we analyzed differently aged APPswe/PS1ΔE9 mice and wildtype littermates to determine progressive changes affecting the dense core vesicle secretory pathway. First, we show that peptidergic vesicle markers content in cerebral cortex and CSF undergo changes along progressive ageing, being accumulated in brain, which could reflect an age-associated modulation. Subsequently, we demonstrate a strikingly decrease in CSF levels of peptidergic transmitters, concurrent with an increase of the protein content in the brain tissue that start before the senile plaques occurrence and goes along with gradual Aβ accumulation. These results support that the DCV secretion undergoes age-related modulation and could be a possible target of Aβ toxicity, being RSP impairment an early event of the physiopathology of the disease. Moreover, a possible role of DCV proteins as biomarkers of the AD progression has been suggested.

2 INTRODUCTION

Alzheimer's disease (AD) is a progressive and irreversible neurodegenerative disorder, being the most common cause of dementia nowadays. The appearance of senile plaques, composed of aggregated forms of amyloid-β (Aβ), and neurofibrillary tangles (NFT), consequence of the hyperphosphorylation of the microtubule-associated protein Tau (Querfurth and LaFerla, 2010) are its main neurohistological hallmarks (Goedert and Spillantini, 2006). Age has been determined as the major risk factor for AD, but the huge number of factors possibly affecting the ongoing disease and the lack of consistent stage biomarkers to characterize the AD patients in clinical trials, make difficult to determine the concrete sequence of events occurring in the brain (Fjell et al., 2014). A growing body of evidence shows that pathological changes start decades before the onset of dementia and first outbreak of histologic signs of the disease (Sala Frigerio and De Strooper, 2016), reason for what is necessary to determine the initial events that could be involved in early stages of AD development.

Even when Aβ accumulation is assumed to be the major pathological trigger of the brain alterations (Barage and Sonawane, 2015; Hardy and Selkoe, 2002), recent findings have shown that cognitive decline symptoms could be consequence of the neuronal network abnormalities and synaptic loss detected in early stages of the disease (Palop and Mucke, 2016). Alteration in neuropeptides levels, which tightly regulate the neuronal function (van den Pol, 2012), have been extensively described in AD (Davies et al., 1980; Palop et al., 2007), being suggested an unbalance of these systems as a result of Aβ toxicity (Barage and Sonawane, 2015). Recent results have demonstrated an aberrant accumulation of dense core vesicle (DCV) proteins in dystrophic neurites and senile plaques of AD patients, which are reproduced in APP/PS1 mice (Plá et al., 2013). Moreover, the direct application of soluble amyloid to *in vitro* neuronal and glial cell cultures and *in situ* acute brain slices have shown an impairment of the regulated secretory pathway (RSP) (Plá et al, chapter 2). Also, a decrease of peptidergic vesicle markers has been found in cerebrospinal fluid (CSF) of early stage AD patients, correlating with the cognitive impairment progression (Plá et al, chapter 3). Taken together, these evidences point to an impairment of the RSP as an early event of AD neuropathology.

Although the peptidergic transmission plays and important role in cognitive and behavioural functions through the regulation of synapsis and networks, its implication in pathological processes have been poorly studied. Here, we analyzed differently aged mice cohorts of APPswe/PS1ΔE9 and wildtype littermates in order to ascertain the time-related and pathological changes affecting the DCV secretory pathway. First, we show that vesicle markers brain tissue and CSF content undergo changes along progressive ageing, which could reflect an age-associated modulation. Subsequently, we demonstrate a strikingly decrease in CSF levels of peptidergic transmitters,

concurrent with an increase of the protein content in the brain tissue along with gradual Aβ accumulation, which start before the senile plaques occurrence. Taken together, those results sustain that an impairment of the DCV pathway could be an early effect of the deleterious cascade triggered by neurotoxic species of Aβ, and may participate in physiopathology of AD, being their CSF levels potentially used as a stage biomarkers of AD.

3 METHODS

Antibodies and Reagents

Monoclonal and polyclonal antibodies against CPE were purchased from BD Transduction Laboratories (San Jose, CA, USA) and GeneTex (Irvine, CA, USA). Polyclonal antibodies against SgIII were obtained from Sigma-Aldrich (Madrid, Spain). Aβ monoclonal antibodies were from Covance (Emeryville, CA, USA). Polyclonal PC1/3 and PC2 were from Thermo Fisher Scientific (Madrid, Spain) and GeneTex (Irvine, CA, USA), respectively. Antibodies against GFAP and β-actin were from Millipore Iberica (Madrid, Spain), Serotec (Oxford, UK) and Sigma-Aldrich (Diesenhofen, Germany), while CysC was from Thermo Fisher Scientific (Madrid, Spain) and Iba1 antibodies was provided by Wako Chemicals (Neuss, Germany), respectively. Most chemicals were obtained from Sigma-Aldrich (Madrid, Spain).

Animals and ethics statement

Analysis were performed on APPswe/PS1ΔE9 mice and wildtype littermates with the same genetic substrate obtained from The Jackson Laboratory (Bar Harbor, ME, USA). The generation of the transgenic mice strain expressing chimeric mouse/human amyloid precursor protein (APPswe) and a human PSN1 (PS1dE9) has been described previously (Borchelt et al., 1996). Animals were kept under controlled temperature (22±2°C), humidity (40–60 %), and light (12-h cycles). Genotypes were identified by polymerase chain reaction (PCR) amplification of tail DNA. All animals were handled in accordance with the guidelines for animal research set out in the European Community Directive 2010/63/EU, and all procedures were approved by the Ethics Committee for Animal Experimentation (CEEA), University of Barcelona (Barcelona, Spain). All efforts were made to minimize the number used and animal suffering. To evaluate effects of aging and/or genotype, the following groups were used: Young, mice aged from 3.2 to 3.5 months; Mature, mice aged from 6.8 to 13.2 months and Old, mice aged from 15.9 to 20.3 months (at least, n=5).

Mouse CSF Extraction and Transcardial Perfusion

CSF was collected from the cisterna magna of profoundly ketamine/xylazine anesthetized mice as previously described (Liu and Duff, 2008). Briefly, anesthetized animals were placed on

the stereotaxic frame and CSF was collected within a capillary going through the dura, visible after a sagittal incision of the posterior head skin was done and subcutaneous tissue and neck muscles through the midline were separated. CSF volume typically arrived to 5 μL that were placed at -20ºC until the analysis. After the CSF collection was done, animals were transcardially perfused with 4% paraformaldehyde in 0.1 M phosphate buffer. Brains were removed and post-fixated overnight at 4ºC, cryoprotected in 30% sucrose in 0.1 M phosphate buffer and frozen until posterior histological analysis.

Western blotting

Tissues were homogenized in ice-cold lysis buffer containing 50 mM Tris-HCl pH 7.4, 150 mM NaCl, 5 mM MgCl2, 1 mM ethyleneglycol-bis(2-aminoethylether)-N, N, N', N'-tetra acetic acid (EGTA), 1% Triton X-100, and protease inhibitor cocktail (Roche Diagnostics). Post-nuclear tissue homogenates and CSF were electrophoresed in 8-12% sodium dodecyl sulfate-polyacrylamide gel electrophoresis (SDS-PAGE; Bio-Rad Laboratories) and then transferred in PVDF membranes (Bio-Rad Laboratories). The membranes were activated and blocked in a solution containing 5% nonfat milk powder in tris-buffered saline tween-20 (140 mM NaCl, 10 mM Tris-HCl, pH 7.4, and 0.1% Tween 20; TBS-Tween) for 1 h at room temperature and then incubated with primary antibodies in blocking buffer for 2 h at room temperature or overnight at 4ºC. After several washes in TBS-Tween solution, the membranes were incubated for 1 h with horseradish peroxidase-conjugated secondary antibodies (Bio-Rad Laboratories). Bound antibodies were visualized with enhanced chemiluminescence reagents (Bio-Rad Laboratories). Blot images were scanned and densitometric analyses were performed using ImageJ software.

Immunocytochemistry

Forty-micrometer thick frozen sections were obtained with a cryostat and collected in PBS. Sections processed for the peroxidase method were soaked for 30 min in PBS containing 10% methanol and 3% H_2O_2 and subsequently washed in PBS. To suppress nonspecific binding, brain sections were incubated in 10% serum-PBS containing 0.1% Triton X-100, 0.2% glycine and 0.2% gelatin for 1 h at room temperature. Incubations with primary antibodies were carried out overnight at 4ºC in PBS containing 5% fetal bovine serum, 0.1% Triton X-100 and 0.2% gelatin. Some histological sections were processed using the avidin-biotin-peroxidase method (Vectastain ABC kit, VECTOR, Burlingame, CA, USA). The peroxidase complex was visualized by incubating the sections with 0.05% diaminobenzidine and 0.01% H_2O_2 in PBS. Sections were mounted, dehydrated, and coverslipped in Eukitt. The specificity of the immunostaining was tested by omitting the primary antibodies or by replacing them with an equivalent concentration of nonspecific IgG. No immunostaining was observed in these conditions. Bright field images were obtained with the Olympus fluorescent BX-61 microscope.

RNA Purification

RNA was purification was carried out with RNeasy Lipid Tissue Mini Kit (Qiagen GmbH, Hilden, Germany) following the protocol provided by the manufacturer. Freshly isolated RNA quantity and quality was determined with Nanodrop 1000 (Thermo Scientific, Wilmington, DE) and BioAnalyzer (Agilent), respectively. Posterior retrotranscription reaction was done using a High-Capacity cDNA Archive Kit (Applied Biosystems, Foster City, CA) following the protocol provided by the supplier.

Quantitative Real-Time PCR

Quantitative Real-Time PCR (qPCR) was performed using the StepOneTM Real-Time PCR System (Applied Biosystems) using TaqMan Probes Mm00516341_m1 (CPE), Mm00485961_m1 (SgIII) Mm00479023_m1 (PC1/3), Mm00500981_m1 (PC2), Mm04230607_s1 (BDNF) and Mm01277042_m1 (TBP, as housekeeping gene). The 20 µl PCR included 0.01 µl RT product, 1× PerfeCTa® qPCR FastMix® II with ROX (Quanta BioSciences, Inc.) and 1 µL TaqMan probe. The reactions were incubated in a 384-well plate at 95ºC for 5 min, followed by 42 cycles of 95ºC for 15 s, 58ºC for 15 s and 72ºC for 30 s. All reactions were run in triplicate. The threshold cycle (C_T) is defined as the fractional cycle number at which the fluorescence passes the fixed threshold and fold change was determined using the equation $2^{-\Delta\Delta CT}$.

Statistical analysis

Data are shown as the mean ± Standard Error of the Mean (SEM) corresponding to at least 5 animals. Non-parametric one-way ANOVA were calculated to determine significant effects of treatments, and, when appropriate, changes were calculated in relation to the average of controls using non-paired Student t-test or Mann-Whitney U-test. Significance was set at *p<0.05, **<0.01 and ***<0.001.

4 RESULTS

Levels of DCV protein levels are increased in cerebral cortex and decreased in CSF of aged mice

Peptide processing enzymes as proprotein convertase 1/3 (PC1/3), proprotein convertase 2 (PC2) and carboxypeptidase E (CPE), and granin family members, as secretogranin III (SgIII) are common cargo of DCVs, being considered hallmarks of RSP. To study peptidergic secretory components in the cerebral cortex of wildtype mice we analyzed three groups of differently aged animals, in which we determined changes in RSP proteins with aging. First, we analyzed mRNA levels obtained from the brain of young and mature animals (n=5) was retrotranscribed and quantitative PCR (q-PCR) was performed for PC1/3, PC2, CPE and SgIII (Fig 1A). Gene

expression analysis shown consistent changes for PC1/3 in aged mice, with more than 2-fold increase of its production (230% vs control). Other gene transcription remained unchanged for CPE, SgIII and PC2 proteins, indicating that mRNA expression of most of the peptidergic vesicle proteins remains relatively stable during aging.

Subsequently, to determine possible changes in the DCV proteins contend along with age, a study was performed on young, mature and old wildtype mice (Fig 1B, C). Brains from these animals (n=5) were extracted and equal amounts of post-nuclear frontal cortex and hippocampus fractions (5 μg protein/lane) were assessed by western blot to analyze the levels of secretory proteins in the tissue (Fig 1B). Immunodetection showed that, while there is no apparent change in the levels of PC1/3, a significant and progressive increase of PC2, CPE and SgIII (proform and mature) was found in frontal cortex both in mature and old mice (152.8 and 195.1% for PC2, 171.1 and 226.9% for CPE, 184.2 and 222.9% for pSgIII and 151.2 and 212.0% for mSgIII vs control) (Fig 1C). Also, a noteworthy rise in the levels of CPE and pSgIII in older animals was found in hippocampus compared with young controls. An opposite profile was found for proprotein convertases protein levels (153.9 and 197.6% for CPE and 162.0 and 231.9% for pSgIII vs control), with the only exception being the increase of PC1/3 in the oldest group (149.8% vs control). No changes were observed for hippocampal levels of mSgIII in neither of the analyzed ages. Those changes in the tissue secretory proteins contend indicate a consistent increase of CPE and pSgIII in cortical tissues, and an area specific changes for PC1/3, PC2 and mSgIII. Observed general increase could suggest the occurrence of an underlying modulation of the pathway with aging.

As constituents are exchanged freely between interstitial fluid, in direct contact with neurons and glial cells, and CSF, changes in the last could reflect extracellular environment alterations occurring in the brain. For that reason, we studied the forms of the vesicle markers in the mouse CNS and in the extracellular media by western blot of total brain homogenates and CSF collected from the cisterna magna of wildtype adult animals (Fig 1D, E). PC1/3 is produced as a proprotein of 87 kDa (pPC1/3) that is subsequently processed to an intermediate 74 kDa-form (iPC1/3) and, finally, the mature active form of 66 kDa (mPC1/3). Careful analysis of samples showed that differential forms were detectable in CSF and mouse brain tissue. In the mouse brain homogenates, the main form of PC2 is the proform (71 kDa, pPC2). Although non-processed and mature PC2 (68 kDa, mPC2) were found in the CSF, the presence of the heavy chain of immunoglobulins (HC) in this biological fluid (band at 50 kDa) precludes the analysis of the mPC2. Also, since non-neuronal cells did not express either PC1/3 or PC2 proteins (Plá et al, chapter 2), the protein production could be restricted to neurons, allowing the separate evaluation of the secretory activity of this cells. For CPE, a robust band at 55 kDa was detected in mouse brain, while much lower relative levels of the protein were present in mice CSF, finding no apparent electrophoretical mobility differences between their forms. The proform and mature SgIII, of ~80-75 kDa (double band, pSgIII) and 53

kDa (mSgIII) respectively, were found abundantly both in brain tissue and CSF. Previous reports for SgIII (Paco et al., 2010) have shown that astrocytes *in vitro* only produce and release pSgIII, suggesting an exclusive neuronal origin for the secreted mSgIII. In the CSF, where apparently predominant form was pSgIII, striking levels of the protein were detected, being measurable even in minimal quantities of sample. These results indicate that the DCV proteins present in brain tissue and CSF undergo differential processing that could depend on their cellular origin.

Finally, we performed CSF western blot analysis to measure the presence of DCV proteins and determine their possible changes with aging in young, mature and old wildtype mice. Since the western blot sensitivity and the quantity of sample was limiting, only the most abundant proteins (PC1/3 and SgIII) were determined. A precise analysis of the biological fluid exhibited a dramatic increase PC1/3 in mature and old animals. Oppositely, SgIII displayed a striking decrease for both pSgIII and mSgIII forms in aged animals. The absence of changes in the mRNA expression, together with a rise in the tissue content and the reduction of CSF levels, suggest a reduction of the release of some of the RSP proteins, that are accumulated in the brain tissue with aging.

Increased levels of RSP components in frontal cortex and hippocampal tissue induced by Aβ start before the appearance of senile plaques

To further investigate these RSP alterations *in vivo* in response to β-amyloid production, the AD animal model APPswe/PS1ΔE9 was studied. Due to the over expression of the amyloidogenic form of APP and the overactive form of PS1 present in this transgenic, we started by determining the plaque production on differently aged animals (Fig 2, left). Immunohistochemistry analysis showed no apparent presence of pathological hallmarks in young animals, whereas senile plaques were found in hippocampus and cerebral cortex around 5-6 months of age, accordingly with previous results (Ruan et al., 2009). To determine the existence of neuroinflammation, the glial reactivity was evaluated by immunodetection with GFAP and Iba1 markers (Fig 2, center and right). Astroglial reactivity was not noticeable at 3 months, while a dramatical increase of activated hypertrophic cells was found along with the Aβ-deposits occurrence. Similar results were found for microglia, where the ramified cells present in young transgenic mice changed to activated amoeboid-shaped glia in matured animals. Based on this results we considered the pre-plaque state, young, and the post-plaque state, mature and old animals, in which the pathological alterations are totally developed.

Next, we performed qPCR to compare expression of regulated secretory proteins to analyze the effects of Aβ overproduction on this pathway (Fig 3). In young animals, we found an increase on the PC1/3 production (176.6% vs control), while gene expression remained unchanged for PC2, CPE and SgIII genes. Strikingly, expression changes in pre-plaque mice outline changes found for wildtype animals with aging, suggesting that aberrant Aβ levels could accelerate the natural fate of

the DCV molecular machinery. The analysis of 12-month-old mice exhibit a general decrease in the expression of the vesicle-related protein, with a reduction for PC1/3, PC2 and SgIII (59.7%, 62.0% and 66.2% vs control, respectively). Interestingly, CPE mRNA expression exhibit an increase, which could be related with the recently described function as a trophic factor (Cheng et al., 2014). As a control, the mRNA expression for the extensively studied neurotrophic factor BDNF was analyzed, finding a significative rise in young animals and no changes in mature animals, accordingly with previous results (Peng et al., 2009; Rantamäki et al., 2013; Szapacs et al., 2004).

Taken together, these results point to a transcriptional alteration of the RSP proteins in response to Aβ, which could take place before the appearance of the first neuropathological hallmarks.

To assess the effects of the amyloid-β on the brain homeostasis *in vivo*, peptidergic protein levels were analyzed by western blot in frontal cortex and hippocampal homogenates. No differences were found in the proteins forms present in transgenic compared to age-paired control animals (n=5) (Figure 4). Protein quantification showed an overall increment on the DCV proteins at pre- and post- plaque stages on APP/PS1 animals compared to age-paired controls, that in was extended until old mice for CPE and SgIII (proform and mature). However, PC2 protein levels at the frontal cortex samples did not follow the general trend. Because of being the most affected area in the Alzheimer's disease, we next evaluated the changes in total protein in the hippocampus of transgenic mice. Results exhibit a consistent accumulation of all the studied proteins in the tissue from mature animals compared to controls. For PC2 and CPE, those increases were also present at young samples. CysC, an extensively-studied Alzheimer's related protein, was analyzed as a positive control, finding an aberrant presence in tissue agreeing with previous results (Hasanbasic et al., 2016; Kaur and Levy, 2012). Peptidergic vesicle proteins raise in tissue is could be a consequence of the aberrant accumulation in cortical plaques in mature and old animals, but changes in pre-plaque stage animals may suggest protein retention in the cerebral cortex.

The increase of PC1/3, PC2, CPE and SgIII tissue content points to a global affectation of the RSP as an AD target. Also, the presence of alterations in the levels of DCV proteins in the pre-plaque stage suggest that aberrant accumulation of peptidergic transmitters in the tissue could be an early consequence of the Aβ overexpression.

To further evaluate histological changes of DCV markers, we analyzed the distribution and subcellular localization of CPE and SgIII and the proprotein convertases PC1/3 and PC2 by immunohistological methods in wildtype mice (Fig 5A). Also, the immunostaining for the protease inhibitor Cystatin C (CysC) was evaluated as a non-RSP protein.

CPE and SgIII were found abundantly in neurons and astrocytes from different areas of the cerebral cortex across the brain (data not shown). Especially high CPE levels were found in dendritic shafts along all cortical layers (Fig 5A, left), while SgIII was mainly associated with perikarya and diffuse puncta resembling axon terminals (data not shown). In astrocytes, both proteins were present in the somata and filling the fine processes. The proprotein convertases were mainly located in in the cell body of neurons in the superficial layers of the neocortex (Fig 5A, center). In the hippocampus, PC1/3 and PC2 were decorating pyramidal neurons in the *cornus ammonis* and in scattered interneurons (Fig 5A right). PC1/3 and PC2 were detected in discrete spots in the neuronal soma, coherently with secretory organelles location. Oppositely to CPE and SgIII, astrocytes were depleted of immunoreactivity for PC1/3 nor PC2 (data not shown), which may suggest a differential protein processing within this cells. CysC was present abundantly as discrete puncta in neurons and inside astroglial cells.

In young transgenic mice, no differences were found for any of the proteins analyzed (Fig 5B and data not shown). Also, no changes in cellular morphology were appreciable. Instead, dramatical changes of DCV labelling were found for PC1/3, PC2, CPE and SgIII (Fig 5C and data not shown). An aberrant accumulation of RSP proteins were found associated with the senile plaques present in the tissue (Fig 5C, up to the right and data not shown). Also, intense immunostaining was found for astrocyte-expressed DCV proteins -CPE and SgIII- in glial cells surrounding amyloid depositions (Fig 5C, bottom). CysC was also associated with cortical plaques and a strikingly increase of protein was found upfilling neurons, accordingly with previous results (Hasanbasic et al., 2016; Kaur and Levy, 2012).

We conclude that the DCV proteins PC1/3, PC2, CPE and SgIII are aberrantly accumulated in amyloid plaques and CPE and SgIII are accumulated in activated glia, in agreement with previous results for AD patients (Plá et al., 2013).

Peptidergic transmitters levels are specifically reduced in CSF of transgenic animals

Finally, to determine the changes in extracellular levels of DCV proteins, the CSF of APP/PS1 and non-transgenic animals was examined by immunoblotting (Fig 6). A consistent decrease was found for mature form of SgIII in young and mature transgenic mice (52.84% and 40.47% respectively, vs age-paired controls) (Fig 6A). PC1/3 displayed analogous results in either of the ages analyzed, with a clear reduction in response to Aβ progressive accumulation (39.11% for young, 46.77% for mature and 53.54% for old, versus age-paired controls) (Fig 6B). Taken together, both results could suggest a decrease in the neuronal DCV proteins released to the media. The non-processed form of SgIII, showed, conversely, an outstanding increase in mature and old APP/PS1 mice. Given the fact that the glial reactivity is completely stablished at that point and that an overexpression of this granin has been described in response to astrocytic activation (Paco et al.,

2010), this raise on pSgIII could be consequence of glial response to the Aβ deposition. The analysis of CysC displayed no changes in the CSF levels of this proteins, which support a specific effect of the Aβ on the DCV pathway proteins.

5 DISCUSSION

In the present study, we report for the first time undergoing changes of the DCV pathway with aging and new evidences supporting a possible impairment of the peptidergic secretion in response to the Aβ neurotoxicity. Also, we provide new information about the aberrant accumulation of PC1/3 and PC2 in senile plaques of APP/PS1 transgenic mice. Furthermore, a cerebral cortex and CSF DCV profile is performed, demonstrating unknown Aβ-related disturbances that gradually developed along with the progression of the pathology and could have a possible role as AD biomarkers.

Changes in cerebral cortex DCV cargo with aging

Previous results have shown disturbances in vesicular trafficking and release in age-related cognitive impairment (Deák, 2014; Poon et al., 2011), as well as vesicle fusion disturbances (Zanin et al., 2011) that could affect RSP function. In agree with them, our results showed a progressive increase in tissue levels of typical DCV cargos, as previously described (Dicson et al., 1999), compatible with an accumulation due to transport and/or release breakdown. Supporting this hypothesis, the detected decrease in the SgIII CSF content could reflect a minor peptidergic input from producing cells, not being related to changes in gene expression, which remained stable. Although CSF content abnormalities could be associated with disorders in clearance mechanisms of the brain or a decline in the number or fire rate of neurons, both of which have also been described in the elderly (Dickstein et al., 2007; Kress et al., 2014; Wang et al., 2011), the opposite effect found for the PC1/3 argue for specify of the SgIII drop-off.

CPE, SgIII, PC 1/3 and PC2 have been widely described as peptidergic vesicle markers, since they participate in the molecular sorting of cargos and/or their processing to generate the active form of several neuropeptides. So, changes in the levels of these proteins should be reflected in their associated vesicular content. Even when the direct mechanism remains to be determined, changes in the DCV secretion could have a crucial effect on the modulation of neuronal networks and brain activity, which could justify the age-related cognitive impairment found in elderly.

Peptidergic secretory pathway in AD

Gene expression results reflect profound changes in the RSP in response to Aβ overproduction, resulting in a downregulation of DCV related genes in post-plaque stages. Contrastingly, a high rise in the levels of CPE mRNA was found compared to age-paired non-

transgenic animals. Considering recent evidences, which suggest a role for CPE as a neuroprotective trophic factor (Cheng et al., 2014), this upturn in the production could respond to a biological function that remains to be elucidated.

Here, we show that DCV markers are aberrantly located in senile plaques of APP/PS1 mice, as was previously reported for CPE and SgIII (Plá et al., 2013), which could reflect a tissue retention of peptidergic vesicles in this aberrant structures. Tissue content analysis for PC1/3, PC2, CPE and SgIII showed an general increase of DCV protein levels in frontal cortex and hippocampus. Taken together both results, a release breakdown could be suggested, since the protein production was stable.

As protein content changes were detectable before the apparition of the first neuropathological amyloid deposits, they may be consequence of an interaction with the Aβ soluble species occurring at the early stages of the disease. Previous results have shown a probably impairment of the regulated secretion in *in vitro* neuronal and glial cell cultures and *in situ* acute brain slices after short-time treatment with Aβ peptide (Plá et al, in revision). Taken together, our recent *in vivo* results support and impairment of the RSP and reinforce that the DCV secretion could be a new target for Aβ neurotoxicity. Due to the great implications of peptidergic transmitters in regulation of cognitive and behavioural functions, a dysbalance of this release could be related with the progression of AD symptomatology.

Also, in agreement with previous results, CPE and SgIII were found in secretory organelles-compatible locations in neurons and astrocytes (Plá et al., 2013), but labelling for PC1/3 or PC2 was absent in astrocytes, suggesting that even when it is possible that glial cells could have DCV secretion in vivo, the vesicle cargo should go through a differential processing.

RSP proteins as stage biomarkers of AD progression

Even when transgenic mice models only reproduce familiar AD (fAD), it has been suggested that the pathophysiology of the sporadic AD could follow the same guiding principles, being the neuropathology and clinical phenotype generally indistinguishable (Hardy and Selkoe, 2002). The huge number of factors possibly affecting the ongoing disease and the lack of consistent stage biomarkers to characterize the AD patients in clinical trials, make difficult to determine the concrete sequence of events occurring in the brain (Fjell et al., 2014). For that reason it is necessary to determine biomarkers that allow to follow up the neuropathological process ongoing in AD patients brain and help to determine the sequence of events that take part in the disease progression. Present results suggest the possible use of DCV markers as a potential biomarkers for AD, since the present a characteristic CSF signature. Recent findings in human CSF analysis also supports a decrease of the RSP proteins in early stages of AD and, importantly, correlate them with cognitive impairment (not published results). Altogether, those results implicate that DCV cargo changes could allow the

tracking of pathology progression in AD, which could be crucial in the development of new clinical approaches.

In conclusion, this study supports that the DCV secretion undergoes age-related modulation and could be a possible target of Aβ toxicity, being RSP impairment an early event of the physiopathology of the disease. Moreover, a possible role of DCV proteins as biomarkers of the AD progression has been suggested.

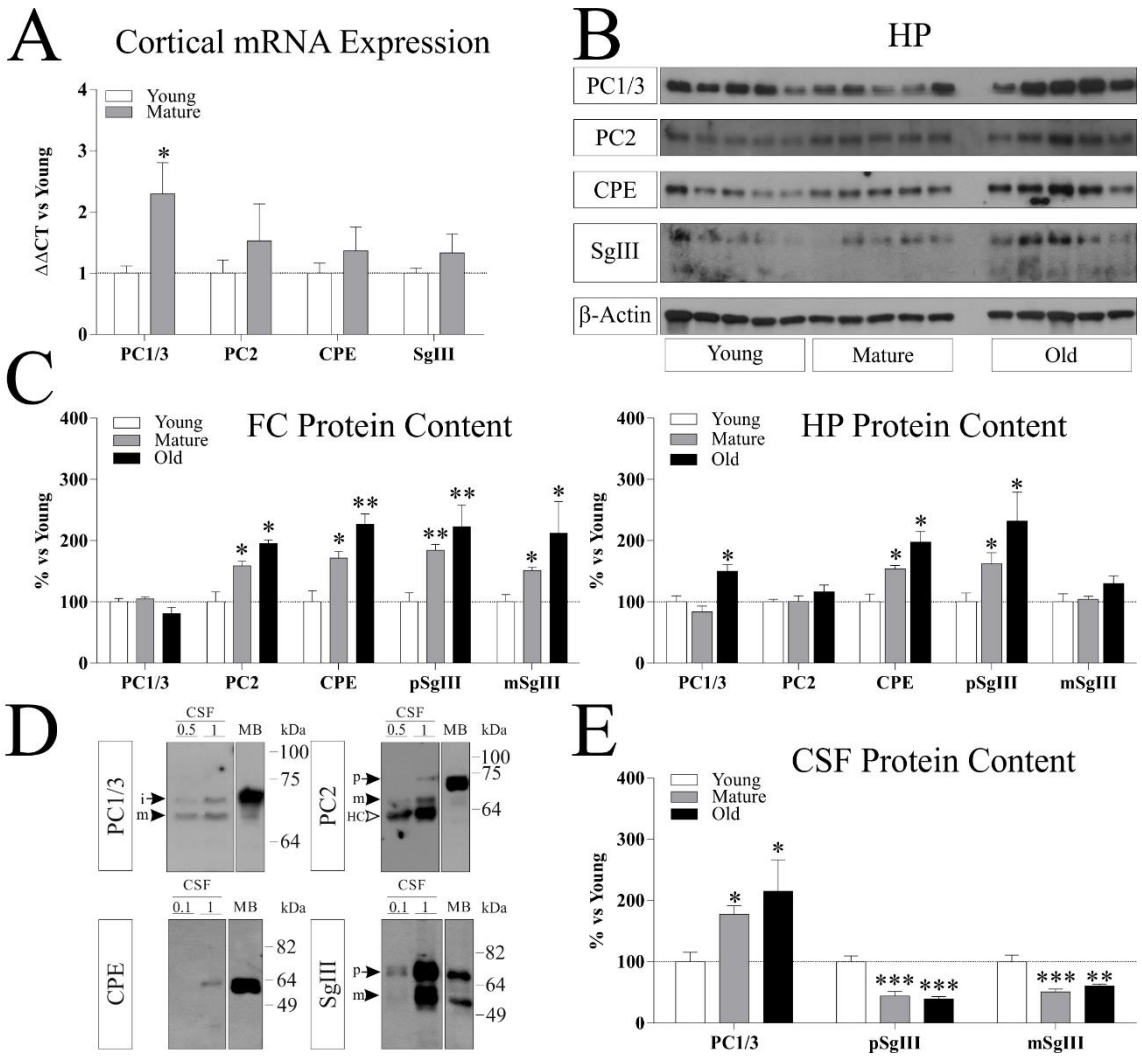

Figure 1. Changes in DCV cargo with aging. A. Graphical representation of mRNA expression of PC1/3, PC2, CPE and SgIII genes in cerebral cortex of young and mature wildtype mice. Values represent percent variation compared with controls and are presented as the mean ± SEM. B. Post-nuclear hippocampus homogenates (5µg/lane) were analyzed by western blot, to asses DCV proteins levels. β-Actin was used as load control. C. Graphs summarizing the obtained results of frontal cortex (FC) and hippocampus (HP) analysis in young, mature and old mice. All β-actin-normalized values were represented normalized versus young controls. D. Western blot for PC1/3, PC2, CPE and SgIII showed that differential protein forms were present in CSF and brain mouse tissue. Numbers indicate charged CSF volume in µL. MB, 10 µg of total protein, p, proform, i, intermedia, and m, mature. E. Young, mature and old CSF protein content was determined by western blot and mean ±SEM is represented, normalized by young controls. *p < 0.05; **p< 0.01; ***p < 0.001

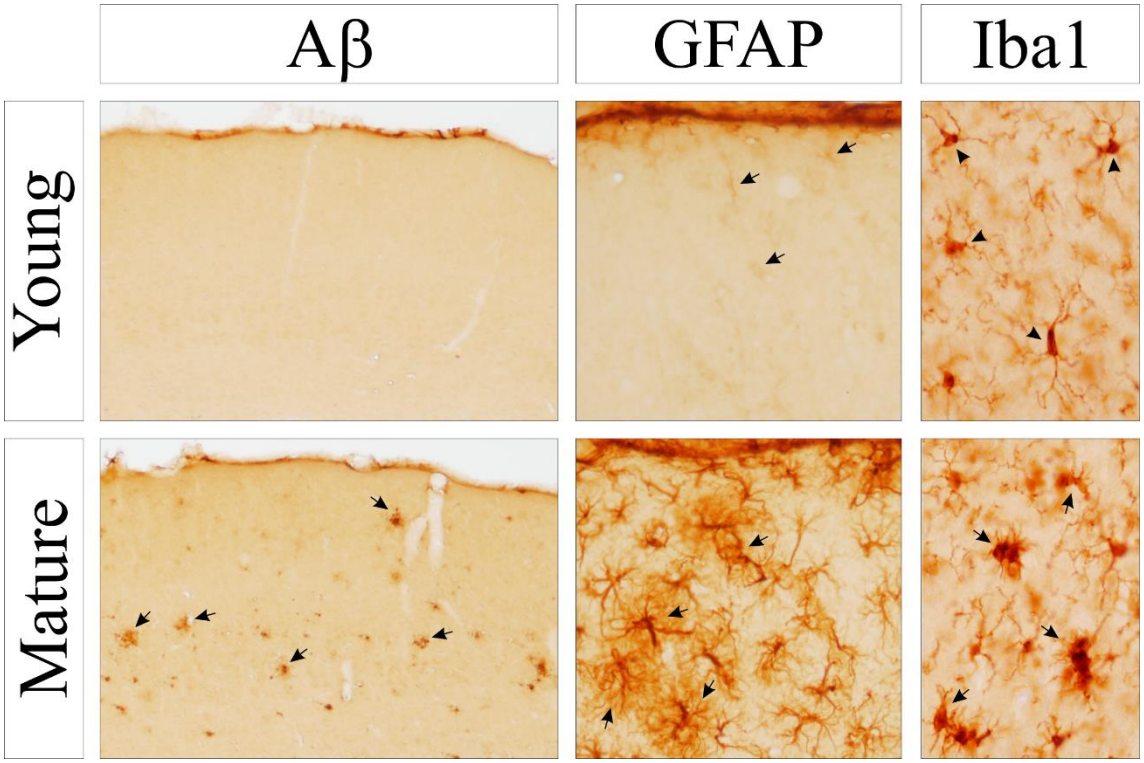

Figure 2. Pathological alterations in the brain of APP/PS1 mice. Immunohistochemistry analysis were performed in order to detect the existence of morphologic changes in cerebral cortex of young and mature APP/PS1. Antibodies against Aβ showed no apparent presence of senile plaques in young animals, while occurrence was abundant in aged animals (arrows). In mature transgenic animals, hypertrophic glial cells were found expressing abundantly GFAP (arrows), used as a marker of astrocyte reactivity. Unlikely, very low levels of GFAP were found in young mice cortex. Iba1 immunolabelling was used to determine cellular state of microglia. Resting, ramified microglia (arrowheads) was found in young mice, while amoeboid activated microglia were detected in mature brain tissue (arrows).

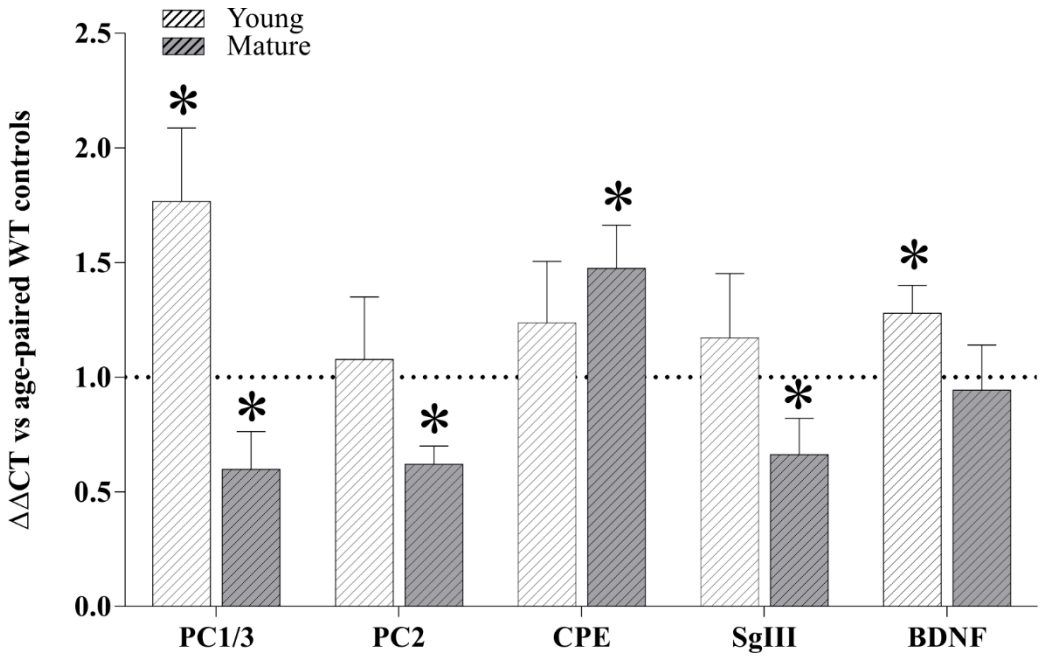

Figure 3. Changes in mRNA expression in APP/PS1 animals versus their age-paired controls. To analyze changes in gene expression, RT-PCR of differently aged control and transgenic mice were performed. Fold change is represented as a mean ± SEM. *p < 0.05; **p< 0.01; ***p < 0.001

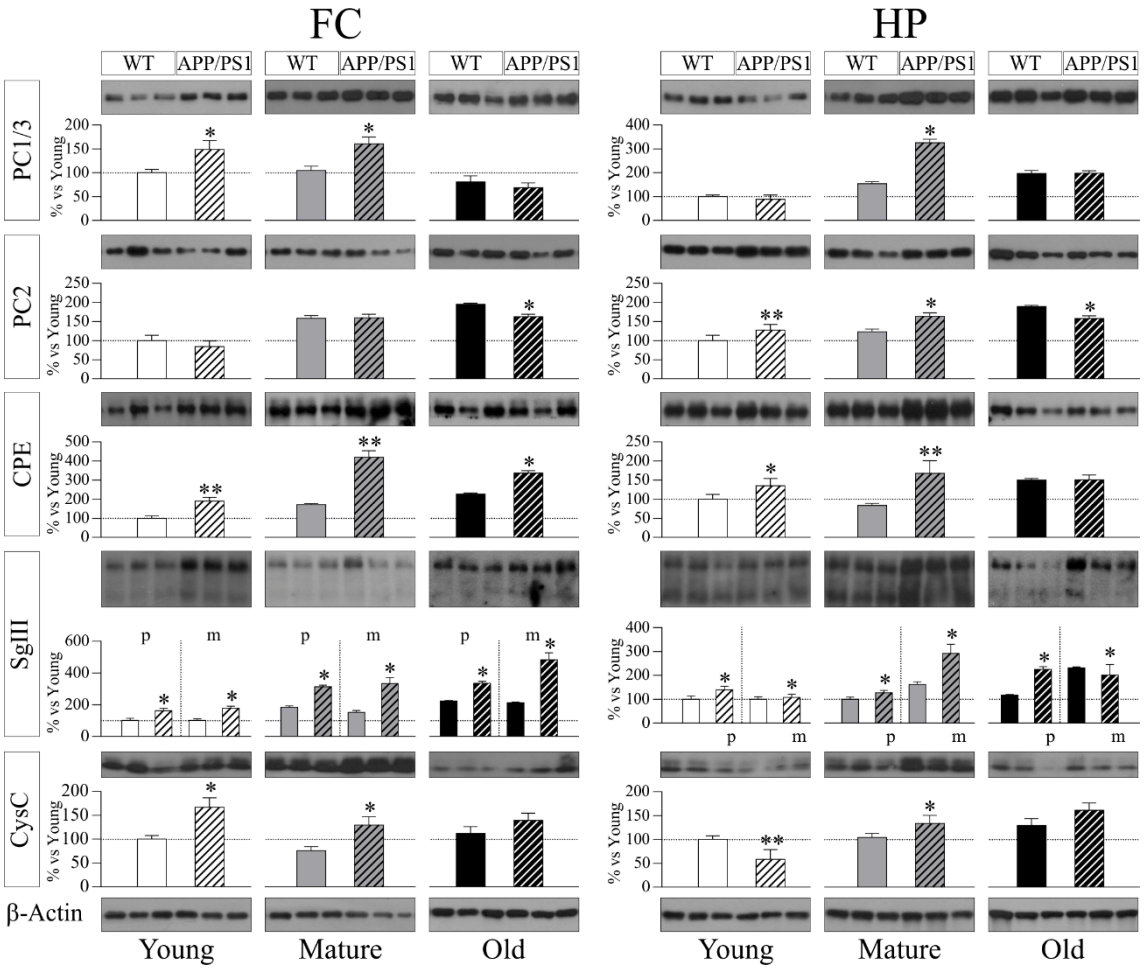

Figure 4. Levels of DCV proteins in frontal cortex and hippocampus of differently-aged APP/PS1 mice and wildtype littermates. Western blot results are displayed in upper boxes, comparing 5 μg of total protein per lane for frontal cortex and hippocampus. Values are represented as mean±SEM normalized by young control animals, separated by age. β-actin levels were used to normalize the protein content. *p < 0.05; **p< 0.01; ***p < 0.001

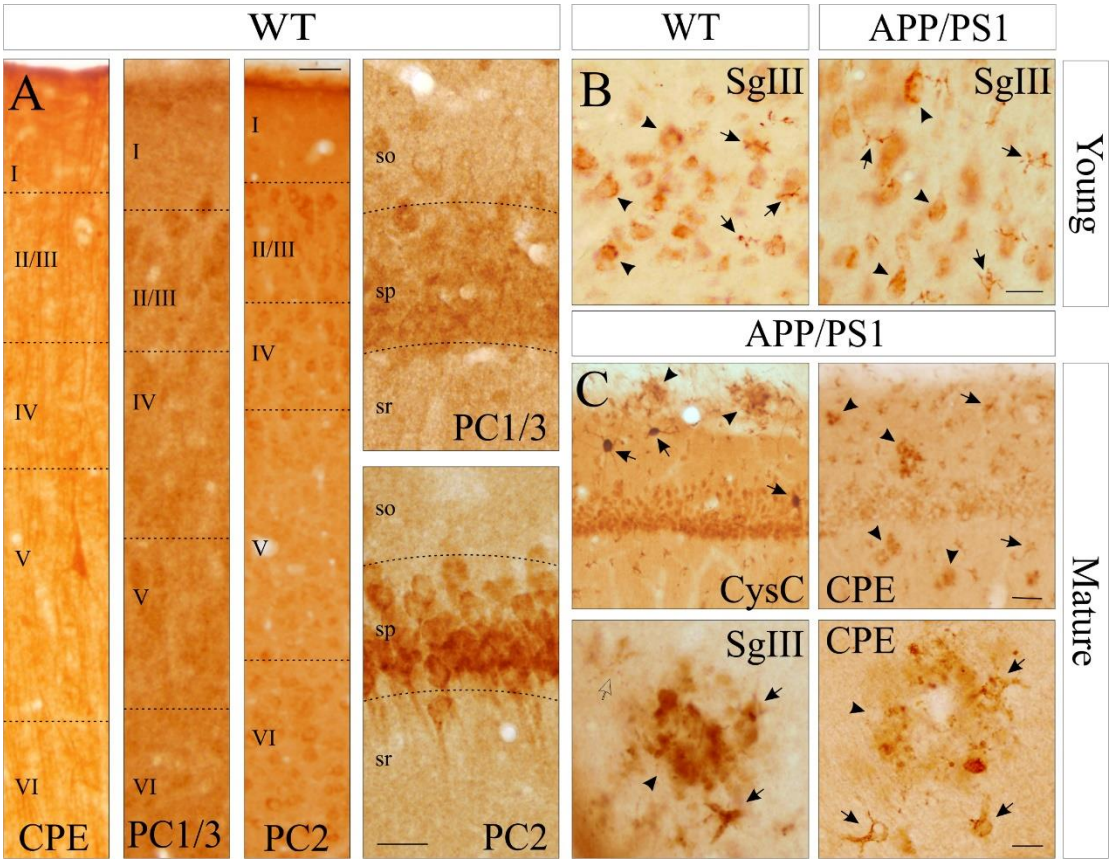

Figure 5. Histologic characterization of DCV cargos in normal and APP/PS1 brain. A. In the neocortex, CPE was found in dendrites and neuronal perikarya through all the cortical layers and, less abundantly, in astrocytes. PC1/3 and PC2 were mainly found in cell body of neurons in the superficial layers of the neocortex and virtually all astrocytes were deployed of the convertases. In the hippocampus, both proteins showed intense signal in the *cornu ammonis*, as is showed for PC1/3 and PC2 in right upper and bottom right image, respectively. B. Young APP/PS1 animals did not show appreciable alterations in the neocortex (arrows, glial cells, arrowheads, neurons) C. Cortical immunolabelling in mature transgenic animals displayed a high number of senile plaques (arrowheads) surrounded by activated astrocytes as is showed for CysC, CPE and SgIII. Scale bars (in μ): A, 100 B, 15; C, 50 (upper) and 20 (bottom).

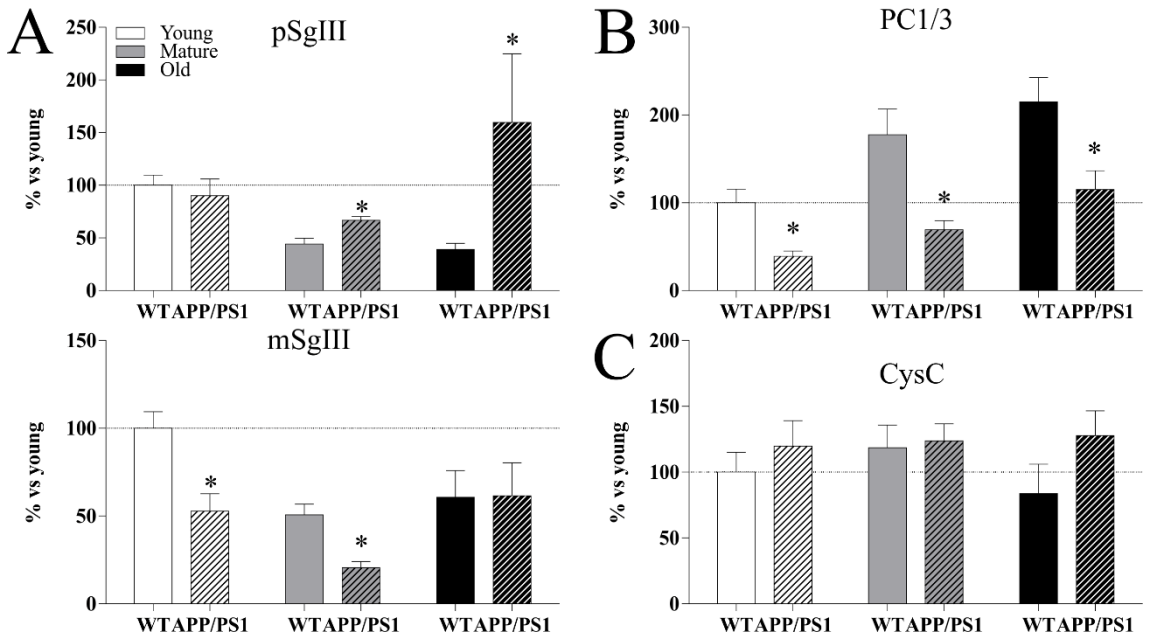

Figure 6. Graphical representations of western quantifications showing CSF content of differently aged transgenic and control mice. A. Levels of the mature form of SgIII are decreased in CSF, while non-processed form levels raised progressively. B. PC1/3 showed a tendency to increase with aging, but in all cases, APP/PS1 mice CSF levels were always lower than the non-mutated controls. C. Cystatin levels showed no changes in neither of the analyzed conditions. *p < 0.05; **p< 0.01; ***p < 0.001

Barage, S. H., and Sonawane, K. D. (2015). Amyloid cascade hypothesis: Pathogenesis and therapeutic strategies in Alzheimer's disease. *Neuropeptides* 52, 1–18. doi:10.1016/j.npep.2015.06.008.

Borchelt, D. R., Thinakaran, G., Eckman, C. B., Lee, M. K., Davenport, F., Ratovitsky, T., Prada, C. M., Kim, G., Seekins, S., Yager, D., Slunt, H. H., Wang, R., Seeger, M., Levey, A. I., Gandy, S. E., Copeland, N. G., Jenkins, N. A., Price, D. L., Younkin, S. G., et al. (1996). Familial Alzheimer's disease-linked presenilin 1 variants elevate Abeta1-42/1-40 ratio in vitro and in vivo. *Neuron* 17, 1005–13. Available at: http://www.ncbi.nlm.nih.gov/pubmed/8938131 [Accessed June 2, 2017].

Cheng, Y., Cawley, N. X., and Loh, Y. P. (2014). Carboxypeptidase E (NF-α1): a new trophic factor in neuroprotection. *Neurosci. Bull.* 30, 692–6. doi:10.1007/s12264-013-1430-z.

Davies, P., Katzman, R., and Terry, R. D. (1980). Reduced somatostatin-like immunoreactivity in cerebral cortex from cases of Alzheimer disease and Alzheimer senile dementa. *Nature* 288, 279–80. Available at: http://www.ncbi.nlm.nih.gov/pubmed/6107862 [Accessed June 1, 2017].

Deák, F. (2014). Neuronal vesicular trafficking and release in age-related cognitive impairment. *J. Gerontol. A. Biol. Sci. Med. Sci.* 69, 1325–30. doi:10.1093/gerona/glu061.

Dickstein, D. L., Kabaso, D., Rocher, A. B., Luebke, J. I., Wearne, S. L., and Hof, P. R. (2007). Changes in the structural complexity of the aged brain. *Aging Cell* 6, 275–84. doi:10.1111/j.1474-9726.2007.00289.x.

Fjell, A. M., McEvoy, L., Holland, D., Dale, A. M., Walhovd, K. B., and Alzheimer's Disease Neuroimaging Initiative (2014). What is normal in normal aging? Effects of aging, amyloid and Alzheimer's disease on the cerebral cortex and the hippocampus. *Prog Neurobiol* 117, 20–40. doi:10.1016/j.pneurobio.2014.02.004.

Goedert, M., and Spillantini, M. G. (2006). A century of Alzheimer's disease. *Science* 314, 777–81. doi:10.1126/science.1132814.

Hardy, J., and Selkoe, D. J. (2002). The amyloid hypothesis of Alzheimer's disease: progress and problems on the road to therapeutics. *Science* 297, 353–6. doi:10.1126/science.1072994.

Hasanbasic, S., Jahic, A., Karahmet, E., Sejranic, A., and Prnjavorac, B. (2016). THE ROLE OF CYSTEINE PROTEASE IN ALZHEIMER DISEASE. *Mater. Sociomed.* 28, 235–8. doi:10.5455/msm.2016.28.235-238.

Kaur, G., and Levy, E. (2012). Cystatin C in Alzheimer's disease. *Front. Mol. Neurosci.* 5, 79. doi:10.3389/fnmol.2012.00079.

Kress, B. T., Iliff, J. J., Xia, M., Wang, M., Wei, H. S., Zeppenfeld, D., Xie, L., Kang, H., Xu, Q., Liew, J. A., Plog, B. A., Ding, F., Deane, R., and Nedergaard, M. (2014). Impairment of paravascular clearance pathways in the aging brain. *Ann. Neurol.* 76, 845–861. doi:10.1002/ana.24271.

Liu, L., and Duff, K. (2008). A Technique for Serial Collection of Cerebrospinal Fluid from the Cisterna Magna in Mouse. *J. Vis. Exp.*, e960–e960. doi:10.3791/960.

Paco, S., Pozas, E., and Aguado, F. (2010). Secretogranin III is an astrocyte granin that is overexpressed in reactive glia. *Cereb. Cortex* 20, 1386–97. doi:10.1093/cercor/bhp202.

Palop, J. J., Chin, J., Roberson, E. D., Wang, J., Thwin, M. T., Bien-Ly, N., Yoo, J., Ho, K. O., Yu, G.-Q., Kreitzer, A., Finkbeiner, S., Noebels, J. L., and Mucke, L. (2007). Aberrant excitatory neuronal activity and compensatory remodeling of inhibitory hippocampal circuits in mouse models of Alzheimer's disease. *Neuron* 55, 697–711. doi:10.1016/j.neuron.2007.07.025.

Palop, J. J., and Mucke, L. (2016). Network abnormalities and interneuron dysfunction in Alzheimer disease. *Nat. Rev. Neurosci.* 17, 777–792. doi:10.1038/nrn.2016.141.

Peng, S., Garzon, D. J., Marchese, M., Klein, W., Ginsberg, S. D., Francis, B. M., Mount, H. T. J., Mufson, E. J., Salehi, A., and Fahnestock, M. (2009). Decreased Brain-Derived Neurotrophic Factor Depends on Amyloid Aggregation State in Transgenic Mouse Models of Alzheimer's Disease. *J. Neurosci.* 29, 9321–9329. doi:10.1523/JNEUROSCI.4736-08.2009.

Plá, V., Paco, S., Ghezali, G., Ciria, V., Pozas, E., Ferrer, I., and Aguado, F. (2013). Secretory sorting receptors carboxypeptidase E and secretogranin III in amyloid β-associated neural degeneration in Alzheimer's disease. *Brain Pathol.* 23, 274–84. doi:10.1111/j.1750-3639.2012.00644.x.

Poon, W. W., Blurton-Jones, M., Tu, C. H., Feinberg, L. M., Chabrier, M. A., Harris, J. W., Jeon, N. L., and Cotman, C. W. (2011). β-Amyloid impairs axonal BDNF retrograde trafficking. *Neurobiol. Aging* 32, 821–833. doi:10.1016/j.neurobiolaging.2009.05.012.

Querfurth, H. W., and LaFerla, F. M. (2010). Alzheimer's disease. *N. Engl. J. Med.* 362, 329–44. doi:10.1056/NEJMra0909142.

Rantamäki, T., Kemppainen, S., Autio, H., Stavén, S., Koivisto, H., Kojima, M., Antila, H., Miettinen, P. O., Kärkkäinen, E., Karpova, N., Vesa, L., Lindemann, L., Hoener, M. C., Tanila, H., and Castrén, E. (2013). The impact of Bdnf gene deficiency to the memory impairment and brain pathology of APPswe/PS1dE9 mouse model of Alzheimer's disease.

PLoS One 8, e68722. doi:10.1371/journal.pone.0068722.

Ruan, L., Kang, Z., Pei, G., and Le, Y. (2009). Amyloid deposition and inflammation in APPswe/PS1dE9 mouse model of Alzheimer's disease. *Curr. Alzheimer Res.* 6, 531–40. Available at: http://www.ncbi.nlm.nih.gov/pubmed/19747158 [Accessed June 5, 2017].

Sala Frigerio, C., and De Strooper, B. (2016). Alzheimer's Disease Mechanisms and Emerging Roads to Novel Therapeutics. *Annu. Rev. Neurosci.* 39, 57–79. doi:10.1146/annurev-neuro-070815-014015.

Szapacs, M. E., Numis, A. L., and Andrews, A. M. (2004). Late onset loss of hippocampal 5 - HT and NE is accompanied by increases in BDNF protein expression in mice co - expressing mutant APP and PS1. doi:10.1016/j.nbd.2004.04.010.

van den Pol, A. N. (2012). Neuropeptide Transmission in Brain Circuits. *Neuron* 76, 98–115. doi:10.1016/j.neuron.2012.09.014.

Wang, M., Gamo, N. J., Yang, Y., Jin, L. E., Wang, X.-J., Laubach, M., Mazer, J. A., Lee, D., and Arnsten, A. F. T. (2011). Neuronal basis of age-related working memory decline. *Nature* 476, 210–3. doi:10.1038/nature10243.

Zanin, M. P., Phillips, L., Mackenzie, K. D., and Keating, D. J. (2011). Aging differentially affects multiple aspects of vesicle fusion kinetics. *PLoS One* 6, e27820. doi:10.1371/journal.pone.0027820.

5 RESUME AND GLOBAL DISCUSSION OF THE OBTAINED RESULTS

5.1 REGULATED SECRETORY PATHWAY IN NEURONS AND ASTROCYTES

The obtained results showed that neurons and astrocytes abundantly produce and release proteins of the RSP both *in vitro* and *in vivo*. Immunolabeling performed in mouse and human brain tissue samples have revealed high levels of the proteins in differential cellular locations, compatible with secretory organelles within the cells. Previous studies have reported the presence of CPE and SgIII in rodents (Lynch et al., 1990; Ottiger et al., 1990), but these DCV proteins have been poorly characterized in the human brain. In endocrine secretory granules, a direct interaction has been described for CPE and SgIII, collaborating in cargo selection (Hosaka et al., 2005). However, our results showed a mostly non-overlapping pattern of intracellular location of both proteins in neurons and glial cells, which may suggest the existence of distinctive RSP characteristics in endocrine and neural cells, pointing to the existence of differential routing inside the cells. Also, the performed immunocytochemistry analysis of astrocytes and neuronal primary cell cultures showed that DCV proteins are produced independently by these two cellular types, accordingly with previous results (Calegari *et al.*, 1999; Hur *et al.*, 2010; Paco *et al.*, 2010).

On the other hand, the DCV proteins production in astrocytes could implicate the existence of a RSP in these cells. Since currently available results shown inconsistent results regarding the existence of regulated secretion in astrocytes, the existence of this mechanism in astrocytes is still controversial. Even when the DCV occurrence has been described in cultured astrocytes (Verkhratsky et al., 2016), the described characteristics of these organelles did not fulfil those classically described, such as size, synaptobrevin 2 immunolabelling, core density and retention time in the cytoplasm (Crippa *et al.*, 2006; Potokar *et al.*, 2008; Paco *et al.*, 2009). Moreover, astrocyte release was only partially dependent of calcium entrance, since the treatment with the ionophore ionomycin was not capable to elicit a robust response, although a secretagogue-elicited release of SgIII has been described (Calegari *et al.*, 1999). Also, the absence of proprotein convertases in astrocytes might implicate a different processing of DCV cargos. Taken together, these results support the existence of a RSP in astrocytes, but with a non-classical secretory profile that would need further analysis of release dynamics to settle the question.

5.2 CHANGES IN THE CEREBRAL CORTEX DCV CARGO WITH AGING

Recent results have shown age-related disturbances in vesicular trafficking and vesicle fusion (Zanin *et al.*, 2011; Deák, 2014),. Taking this into account, added to the progressive accumulation of peptidergic vesicle markers with aging found here, an impairment of the RSP with aging could be suggested. In addition to the increase cerebral in cortex protein content in differently aged mice showed

by western blot analysis, the progressive decrease in the CSF levels of DCV proteins present along with aging points to a reduction of the release of secretory vesicle proteins. Accordingly with this hypothesis, similar results have shown chromogranin A decline in CSF (Blennow *et al.*, 1995) and some protein screen results have report non-confirmed changes in others DCV-components (Perrin *et al.*, 2011; Fagan & Perrin, 2012). Even when this changes may be physiological, a clinical continuum between elderly and AD has been suggested, considering the pathology an inevitable consequence of aging (Serrano-Pozo *et al.*, 2013).

5.3 PEPTIDERGIC SECRETION AS Aβ TARGET: PATHOPHYSIOLOGIC IMPLICATIONS OF PEPTIDERGIC TRANSMISSION IMPAIRMENT IN AD

The obtained results demonstrate a direct effect of Aβ on DCV secretion of *in vitro*, *in situ* and *in vivo* neural cells. Since peptidergic transmission controls circuitry function and neural homeostasis, its impairment could lead to synaptic dysfunction and network disorganization, events that have been widely described in early stages of AD.

Firstly, the acute exposition of cultured astrocytes to amyloid neurotoxic species decreased dramatically the release of CPE and SgIII, increasing the intracellular content of the proteins. As CPE and SgIII usually undergo rapid release on this cells, this effect could suggest an impairment of the regulated secretion. In neuronal cultures, short time Aβ incubation provoked a specifically reduction of the basal and stimulated secretion, since no changes were found for the classical neurotransmitter glutamate. Importantly, those results were reproduced by *in situ* acute brain slices, reinforcing the possible role of RSP as a direct target of AD. The increasing number of evidences showing Aβ-driven abnormalities on vesicular trafficking (Decker *et al.*, 2010; Gan & Silverman, 2015), could suggest that vesicle transport disturbance could be sustaining the described release impairment. Furthermore, this could be supported by the dramatically accumulation of DCV cargos in dystrophic neurites found both in AD as in APP/PS1 mice brains ((Willis *et al.*, 2011; Plá *et al.*, 2013).

Secondly, the important alterations of proteins of the RSP machinery found in animal models of the disease, additionally indicate that the DCV pathway could act as an early event in the pathophysiology the disease. The fact that the CSF decrease and tissue accumulation occurrence started before the apparition of the first histological hallmarks of the disease, could suggest the existence of an underlying effect of Aβ on the secretory pathway. According to this possibility, previous results have described neuropeptides alterations in early stages of AD (Davis *et al.*, 1999; Dam *et al.*, 2013; Barage & Sonawane, 2015), although, the mechanism of these events needs to be determined.

5.4 CHANGES OF DCV PROTEINS IN CSF OF AD PATIENTS

The aberrant accumulation of DCV components in dystrophic neurites, indicates an intracellular retention that could be consequence of failures in vesicular biogenesis due to ER stress or Golgi fragmentation (Alberdi *et al.*, 2013; Joshi *et al.*, 2014), vesicle trafficking malfunction or disrupted exocytosis through SNARE (Russell *et al.*, 2012; Yang *et al.*, 2015), resulting in impaired release of vesicular cargo. Even when clearance mechanism disorders or CSF production abnormalities could be affecting the linearity of the correspondence, the CSF levels decline should reflect and impairment of DCV markers release, allowing to get a glimpse of its function in the SNC. The shrinkage on the RSP protein levels in early stages AD patients supported by recently proteomic results (Abdi et al., 2006; Perrin et al., 2011; Fagan and Perrin, 2012), demonstrate that an alteration of DCV secretion might be an initial event in the pathology progression. Furthermore, the correlate of these disturbances with cognitive impairment, have remarked the potential role of these proteins as a biomarker for AD, which possible clinical value remains to be evaluated.

The main goal of this thesis is to have contributed to the advance in the knowledge of the regulated secretory pathway, a critical process in the maintenance of the neuronal function, even when their mechanisms are not fully understood. The evidence of an impairment of DCV secretion in early stages of AD, highlights the necessity of a better understanding of this complex process.

6 FINAL CONCLUSIONS

The main objective of this PhD thesis was to study the cortical alterations of peptidergic secretion in Alzheimer's disease. During its elaboration, the following conclusions have been obtained:

1. **Cargos of the regulated secretory pathway produced by neurons and astrocytes show differential processing and release dynamics**

2. **Dense core vesicle secretory pathway undergoes age-related changes resulting in a progressive cortical accumulation of vesicle markers**

3. **Amyloid-β impairs the regulated peptidergic secretion in neuronal and astroglial populations *in vitro* and *in situ***

4. **Dense core vesicle components are aberrantly accumulated in dystrophic neurites, granulovacuolar degeneration bodies and reactive astrocytes in Alzheimer's disease patients and transgenic animal models**

5. **Correlating with cognitive decline, levels of peptidergic secretory components are decreased in cerebrospinal fluid of early stages Alzheimer's disease patients**

6. **The Alzheimer's disease-related impairment of dense core vesicle secretory pathway supports a potential use of regulated secreted peptides as biomarkers of disease network dysfunction**

7 BIBLIOGRAPHY

Alberdi, E., Wyssenbach, A., Alberdi, M., Sánchez-Gómez, M. V., Cavaliere, F., Rodríguez, J.J., Verkhratsky, A., & Matute, C. (2013) Ca2+-dependent endoplasmic reticulum stress correlates with astrogliosis in oligomeric amyloid β-treated astrocytes and in a model of Alzheimer's disease. *Aging Cell*, **12**, 292–302.

Albert, M.S., DeKosky, S.T., Dickson, D., Dubois, B., Feldman, H.H., Fox, N.C., Gamst, A., Holtzman, D.M., Jagust, W.J., Petersen, R.C., Snyder, P.J., Carrillo, M.C., Thies, B., & Phelps, C.H. (2011) The diagnosis of mild cognitive impairment due to Alzheimer's disease: recommendations from the National Institute on Aging-Alzheimer's Association workgroups on diagnostic guidelines for Alzheimer's disease. *Alzheimers. Dement.*, **7**, 270–279.

Alcolea, D., Carmona-Iragui, M., Suárez-Calvet, M., Sánchez-Saudinós, M.B., Sala, I., Antón-Aguirre, S., Blesa, R., Clarimón, J., Fortea, J., & Lleó, A. (2014) Relationship Between β-Secretase, Inflammation and Core Cerebrospinal Fluid Biomarkers for Alzheimer's Disease. *J. Alzheimer's Dis.*, **42**, 157–167.

American Psychiatric Association (2013) *Diagnostic and Statistical Manual of Mental Disorders Fifth Edition*. American Psychiatric Association.

Araque, A., Parpura, V., Sanzgiri, R.P., & Haydon, P.G. (1999) Tripartite synapses: glia, the unacknowledged partner. *Trends Neurosci.*, **22**, 208–215.

Arendt, T., Bigl, V., Arendt, A., & Tennstedt, A. (1983) Loss of neurons in the nucleus basalis of Meynert in Alzheimer's disease, paralysis agitans and Korsakoff's Disease. *Acta Neuropathol.*, **61**, 101–108.

Ashe, K.H. & Zahs, K.R. (2010) Probing the Biology of Alzheimer's Disease in Mice. *Neuron*, **66**, 631–645.

Bakkour, A., Morris, J.C., Wolk, D.A., & Dickerson, B.C. (2013) The effects of aging and Alzheimer's disease on cerebral cortical anatomy: Specificity and differential relationships with cognition. *Neuroimage*, **76**, 332–344.

Barage, S.H. & Sonawane, K.D. (2015) Amyloid cascade hypothesis: Pathogenesis and therapeutic strategies in Alzheimer's disease. *Neuropeptides*, **52**, 1–18.

Bareggi, S.R., Franceschi, M., Bonini, L., Zecca, L., & Smirne, S. (1982) Decreased CSF concentrations of homovanillic acid and gamma-aminobutyric acid in Alzheimer's disease. Age- or disease-related modifications? *Arch. Neurol.*, **39**, 709–712.

Bartkowska, K., Turlejski, K., & Djavadian, R.L. (2010) Neurotrophins and their receptors in early development of the mammalian nervous system. *Acta Neurobiol. Exp. (Wars).*, **70**, 454–467.

Bartus, R.T. (2000) On neurodegenerative diseases, models, and treatment strategies: lessons learned and lessons forgotten a generation following the cholinergic hypothesis. *Exp. Neurol.*, **163**, 495–529.

Bayer, T.A. & Wirths, O. (2010) Intracellular accumulation of amyloid-beta – a predictor for synaptic dysfunction and neuron loss in Alzheimer's disease. *Front. Aging Neurosci.*, **2**, 8.

Beal, M.F., Mazurek, M.F., Chattha, G.K., Svendsen, C.N., Bird, E.D., & Martin, J.B. (1986) Neuropeptide Y immunoreactivity is reduced in cerebral cortex in Alzheimer's disease. *Ann. Neurol.*, **20**, 282–288.

Berridge, M.J. (2014) Calcium regulation of neural rhythms, memory and Alzheimer's disease. *J. Physiol.*, **592**, 281–293.

Bialas, A.R. & Stevens, B. (2013) TGF-β signaling regulates neuronal C1q expression and developmental synaptic refinement. *Nat. Neurosci.*, **16**, 1773–1782.

Bird, T.D. (1993) *Early-Onset Familial Alzheimer Disease*, GeneReviews(®). University of Washington, Seattle.

Blennow, K. (2005) CSF biomarkers for Alzheimer's disease: use in early diagnosis and evaluation of drug treatment. *Expert Rev. Mol. Diagn.*, **5**, 661–672.

Blennow, K., Davidsson, P., Wallin, A., & Ekman, R. (1995) Chromogranin A in cerebrospinal fluid: a biochemical marker for synaptic degeneration in Alzheimer's disease? *Dementia*, **6**, 306–311.

Blennow, K., Dubois, B., Fagan, A.M., Lewczuk, P., de Leon, M.J., & Hampel, H. (2015) Clinical utility of cerebrospinal fluid biomarkers in the diagnosis of early Alzheimer's disease. *Alzheimer's Dement.*, **11**, 58–69.

Blennow, K., Hampel, H., Drzezga, A., al., et, Drzezga, A., Kurz, A., & Hernanz, A. (2003) CSF markers for incipient Alzheimer's disease. *Lancet. Neurol.*, **2**, 605–613.

Bloom, G.S. (2014) Amyloid-β and Tau: the trigger and bullet in Alzheimer disease pathogenesis. *JAMA Neurol.*, **71**, 505.

Bothwell, M. (2016) Recent advances in understanding neurotrophin signaling. *F1000Research*, **5**.

Buckner, R.L. (2004) Memory and executive function in aging and AD: multiple factors that cause decline and reserve factors that compensate. *Neuron*, **44**, 195–208.

Budni, J., Bellettini-Santos, T., Mina, F., Garcez, M.L., Zugno, A.I., Lima Garcez, M., & Ioppi Zugno, A. (2015) The involvement of BDNF, NGF and GDNF in aging and Alzheimer's disease. *Aging Dis.*, **6**, 331.

Burns, A. & Iliffe, S. (2009) Alzheimer's disease. *BMJ*, **158**, 1–13.

Calegari, F., Coco, S., Taverna, E., Bassetti, M., Verderio, C., Corradi, N., Matteoli, M., & Rosa, P. (1999) A Regulated Secretory Pathway in Cultured Hippocampal Astrocytes. *J. Biol. Chem.*, **274**, 22539–22547.

Callahan, C.M., Hendrie, H.C., & Tierney, W.M. (1995) Documentation and evaluation of cognitive impairment in elderly primary care patients. *Ann. Intern. Med.*, **122**, 422–429.

Chevalier-Larsen, E. & Holzbaur, E.L.F. (2006) Axonal transport and neurodegenerative disease. *Biochim. Biophys. Acta*, **1762**, 1094–1108.

Chung, W.-S., Allen, N.J., & Eroglu, C. (2015) Astrocytes Control Synapse Formation, Function, and Elimination. *Cold Spring Harb. Perspect. Biol.*, **7**, a020370.

Chung, W.-S., Clarke, L.E., Wang, G.X., Stafford, B.K., Sher, A., Chakraborty, C., Joung, J., Foo, L.C., Thompson, A., Chen, C., Smith, S.J., & Barres, B.A. (2013) Astrocytes mediate synapse elimination through MEGF10 and MERTK pathways. *Nature*, **504**, 394–400.

Chung, W.-S., Verghese, P.B., Chakraborty, C., Joung, J., Hyman, B.T., Ulrich, J.D., Holtzman, D.M., & Barres, B.A. (2016) Novel allele-dependent role for APOE in controlling the rate of synapse pruning by astrocytes. *Proc Natl Acad Sci U S A*, **113**, 10186–10191.

Chung, W.-S., Welsh, C. a, Barres, B. a, & Stevens, B. (2015) Do glia drive synaptic and cognitive impairment in disease? *Nat. Publ. Gr.*, **18**, 1539–1545.

Clarys, D., Bugaiska, A., Tapia, G., & Alexia Baudouin, and (2009) Ageing, remembering, and executive function. *Memory*, **17**, 158–168.

Connor, B. & Dragunow, M. (1998) The role of neuronal growth factors in neurodegenerative disorders of the human brain. *Brain Res. Brain Res. Rev.*, **27**, 1–39.

Crippa, D., Schenk, U., Francolini, M., Rosa, P., Verderio, C., Zonta, M., Pozzan, T., Matteoli, M., & Carmignoto, G. (2006) Synaptobrevin2-expressing vesicles in rat astrocytes: insights into molecular characterization, dynamics and exocytosis. *J. Physiol.*, **570**, 567–582.

Crystal, H.A. & Davies, P. (1982) Cortical substance P-like immunoreactivity in cases of Alzheimer's disease and senile dementia of the Alzheimer type. *J. Neurochem.*, **38**, 1781–1784.

Cummings, J.L. (2008) The Black Book of Alzheimer's Disease, Part 1. *Prim psychiatry*, **15**, 66–76.

Cummings, J.L. & Cole, G. (2002) Alzheimer Disease. *Jama*, **287**, 2335.

Dam, D. Van, Dijck, A. Van, Janssen, L., & Deyn, P.P. De (2013) Neuropeptides in Alzheimer`s Disease: From Pathophysiological Mechanisms to Therapeutic Opportunities. *Curr. Alzheimer Res.*, **10**, 449–468.

Danysz, W. & Parsons, C.G. (2012) Alzheimer's disease, β-amyloid, glutamate, NMDA receptors and memantine-searching for the connections. *Br. J. Pharmacol.*, **167**, 324–352.

Davies, P., Katzman, R., & Terry, R.D. (1980) Reduced somatostatin-like immunoreactivity in cerebral cortex from cases of Alzheimer disease and Alzheimer senile dementa. *Nature*, **288**, 279–280.

Davis, K.L., Mohs, R.C., Marin, D.B., Purohit, D.P., Perl, D.P., Lantz, M., Austin, G., Haroutunian, V., P, K., & KL, D. (1999) Neuropeptide Abnormalities in Patients With Early Alzheimer Disease.

Arch. Gen. Psychiatry, **56**, 981.
Deák, F. (2014) Neuronal vesicular trafficking and release in age-related cognitive impairment. *J. Gerontol. A. Biol. Sci. Med. Sci.*, **69**, 1325–1330.
De Strooper, B. & Karran, E. (2016) The Cellular Phase of Alzheimer's Disease. *Cell*, **164**, 603–615.
Decker, H., Lo, K.Y., Unger, S.M., Ferreira, S.T., & Silverman, M.A. (2010) Amyloid-β peptide oligomers disrupt axonal transport through an NMDA receptor-dependent mechanism that is mediated by glycogen synthase kinase 3beta in primary cultured hippocampal neurons. *J. Neurosci.*, **30**, 9166–9171.
DeKosky, S.T. & Scheff, S.W. (1990) Synapse loss in frontal cortex biopsies in Alzheimer's disease: correlation with cognitive severity. *Ann. Neurol.*, **27**, 457–464.
Etcheberrigaray, R., Hirashima, N., Nee, L., Prince, J., Govoni, S., Racchi, M., Tanzi, R.E., & Alkon, D.L. (1998) Calcium Responses in Fibroblasts from Asymptomatic Members of Alzheimer's Disease Families. *Neurobiol. Dis.*, **5**, 37–45.
Ewers, M., Sperling, R.A., Klunk, W.E., Weiner, M.W., & Hampel, H. (2011) Neuroimaging markers for the prediction and early diagnosis of Alzheimer's disease dementia. *Trends Neurosci.*, **34**, 430–442.
Fagan, A.M. & Perrin, R.J. (2012) Upcoming candidate cerebrospinal fluid biomarkers of Alzheimer's disease. *Biomark. Med.*, **6**, 455–476.
Fjell, A.M., McEvoy, L., Holland, D., Dale, A.M., Walhovd, K.B., & Alzheimer's Disease Neuroimaging Initiative (2014) What is normal in normal aging? Effects of aging, amyloid and Alzheimer's disease on the cerebral cortex and the hippocampus. *Prog Neurobiol*, **117**, 20–40.
Fujiyoshi, K., Suga, H., Okamoto, K., Nakamura, S., & Kameyama, M. (1987) Reduction of arginine-vasopressin in the cerebral cortex in Alzheimer type senile dementia. *J. Neurol. Neurosurg. Psychiatry*, **50**, 929–932.
Gan, K.J. & Silverman, M.A. (2015) Dendritic and axonal mechanisms of Ca2+ elevation impair BDNF transport in Aβ oligomer-treated hippocampal neurons. *Mol. Biol. Cell*, **26**, 1058–1071.
Goedert, M. & Spillantini, M.G. (2006) A century of Alzheimer's disease. *Science*, **314**, 777–781.
Gottfries, C.G., Gottfries, I., & Roos, B.E. (1969) Homovanillic acid and 5-hydroxyindoleacetic acid in the cerebrospinal fluid of patients with senile dementia, presenile dementia and parkinsonism. *J. Neurochem.*, **16**, 1341–1345.
Götz, J., Chen, F., van Dorpe, J., & Nitsch, R.M. (2001) Formation of Neurofibrillary Tangles in P301L Tau Transgenic Mice Induced by Aβ42 Fibrils. *Science (80-.).*, **293**.
Götz, J., Deters, N., Doldissen, A., Bokhari, L., Ke, Y., Wiesner, A., Schonrock, N., & Ittner, L.M. (2007) A Decade of Tau Transgenic Animal Models and Beyond. *Brain Pathol.*, **17**, 91–103.
Green, M.S., Kaye, J.A., & Ball, M.J. (2000) The Oregon brain aging study: neuropathology accompanying healthy aging in the oldest old. *Neurology*, **54**, 105–113.
Gueli, M.C. & Taibi, G. (2013) Alzheimer's disease: amino acid levels and brain metabolic status. *Neurol. Sci.*, **34**, 1575–1579.
Haass, C. & Selkoe, D.J. (2007) Soluble protein oligomers in neurodegeneration: lessons from the Alzheimer's amyloid β-peptide. *Nat. Rev. Mol. Cell Biol.*, **8**, 101–112.
Halassa, M.M., Fellin, T., & Haydon, P.G. (2007) The tripartite synapse: roles for gliotransmission in health and disease. *Trends Mol. Med.*, **13**, 54–63.
Hampel, H. & Lista, S. (2016) Dementia: The rising global tide of cognitive impairment. *Nat. Rev. Neurol.*, **12**, 131–132.
Harada, K., Kamiya, T., & Tsuboi, T. (2016) Gliotransmitter release from astrocytes: Functional, developmental, and pathological implications in the brain. *Front. Neurosci.*, **9**, 1–9.
Hardy, J.A. & Higgins, G.A. (1992) Alzheimer's disease: The amyloid cascade hypothesis.
Hardy, J. & Selkoe, D.J. (2002) The amyloid hypothesis of Alzheimer's disease: progress and problems on the road to therapeutics. *Science*, **297**, 353–356.
Head, D., Snyder, A.Z., Girton, L.E., Morris, J.C., & Buckner, R.L. (2005) Frontal-hippocampal double dissociation between normal aging and Alzheimer's disease. *Cereb. Cortex*, **15**, 732–739.
Henneberger, C., Papouin, T., Oliet, S.H.R., & Rusakov, D.A. (2010) Long-term potentiation depends

on release of d-serine from astrocytes. *Nature*, **463**, 232–236.
Herrup, K. (2015) The case for rejecting the amyloid cascade hypothesis. *Nat. Neurosci.*, **18**, 794–799.
Hong, S., Beja-Glasser, V.F., Nfonoyim, B.M., Frouin, A., Li, S., Ramakrishnan, S., Merry, K.M., Shi, Q., Rosenthal, A., Barres, B.A., Lemere, C.A., Selkoe, D.J., Stevens, B., Lemere, C.A., Selkoe, D.J., & Stevens, B. (2016) Complement and microglia mediate early synapse loss in Alzheimer mouse models. *Science (80-.).*, **352**, 712–716.
Hosaka, M., Watanabe, T., Sakai, Y., Kato, T., & Takeuchi, T. (2005) Interaction between secretogranin III and carboxypeptidase E facilitates prohormone sorting within secretory granules. *J. Cell Sci.*, **118**, 4785–4795.
Hur, Y.S., Kim, K.D., Paek, S.H., & Yoo, S.H. (2010) Evidence for the existence of secretory granule (dense-core vesicle)-based inositol 1,4,5-trisphosphate-dependent Ca2+ signaling system in astrocytes. *PLoS One*, **5**, e11973.
Hyman, B.T., Phelps, C.H., Beach, T.G., Bigio, E.H., Cairns, N.J., Carrillo, M.C., Dickson, D.W., Duyckaerts, C., Frosch, M.P., Masliah, E., Mirra, S.S., Nelson, P.T., Schneider, J.A., Thal, D.R., Thies, B., Trojanowski, J.Q., Vinters, H. V., & Montine, T.J. (2012) National Insitute on Aging-Alzheimer's Association guidelines for the neuropathologic assessment of Alzheimer's disease. *Alzheimer's Dement.*, **8**, 1–13.
Iqbal, K., Liu, F., Gong, C.-X., Alonso, A. del C., & Grundke-Iqbal, I. (2009) Mechanisms of tau-induced neurodegeneration. *Acta Neuropathol.*, **118**, 53–69.
Ito, E., Oka, K., Etcheberrigaray, R., Nelson, T.J., McPhie, D.L., Tofel-Grehl, B., Gibson, G.E., & Alkon, D.L. (1994) Internal Ca2+ mobilization is altered in fibroblasts from patients with Alzheimer disease. *Proc. Natl. Acad. Sci. U. S. A.*, **91**, 534–538.
Jack, C.R. (2012) Alzheimer disease: new concepts on its neurobiology and the clinical role imaging will play. *Radiology*, **263**, 344–361.
Ji, Y., Gong, Y., Gan, W., Beach, T., Holtzman, D.., & Wisniewski, T. (2003) Apolipoprotein E isoform-specific regulation of dendritic spine morphology in apolipoprotein E transgenic mice and Alzheimer's disease patients. *Neuroscience*, **122**, 305–315.
Jiménez-Corral, C., Morán-Sánchez, J.C., & Alonso-Navarro, H. (2006) [Neuropeptides in Alzheimer's disease]. *Rev. Neurol.*, **42**, 354–359.
Joshi, G., Chi, Y., Huang, Z., & Wang, Y. (2014) Aβ-induced Golgi fragmentation in Alzheimer's disease enhances Aβ production. *Proc. Natl. Acad. Sci. U. S. A.*, **111**, E1230-9.
Keverne, J. & Ray, M. (2008) Neurochemistry of Alzheimer's disease. *Psychiatry*, **7**, 6–8.
Khachaturian, Z.S. (1989) Calcium, membranes, aging, and Alzheimer's disease. Introduction and overview. *Ann. N. Y. Acad. Sci.*, **568**, 1–4.
Khakh, B.S. & McCarthy, K.D. (2015) Astrocyte Calcium Signaling: From Observations to Functions and the Challenges Therein. *Cold Spring Harb. Perspect. Biol.*, **7**, a020404.
Kim, T., Gondré-Lewis, M.C., Arnaoutova, I., & Loh, Y.P. (2006) Dense-Core Secretory Granule Biogenesis. *Physiology*, **21**.
Kuchibhotla, K. V., Goldman, S.T., Lattarulo, C.R., Wu, H.-Y., Hyman, B.T., & Bacskai, B.J. (2008) Aβ Plaques Lead to Aberrant Regulation of Calcium Homeostasis In Vivo Resulting in Structural and Functional Disruption of Neuronal Networks. *Neuron*, **59**, 214–225.
Kuchibhotla, K. V., Lattarulo, C.R., Hyman, B.T., & Bacskai, B.J. (2009) Synchronous Hyperactivity and Intercellular Calcium Waves in Astrocytes in Alzheimer Mice. *Science (80-.).*, **323**.
Lang, U.E., Jockers-Scherübl, M.C., & Hellweg, R. (2004) State of the art of the neurotrophin hypothesis in psychiatric disorders: implications and limitations. *J. Neural Transm.*, **111**, 387–411.
Lee, C.Y.D. & Landreth, G.E. (2010) The role of microglia in amyloid clearance from the AD brain. *J. Neural Transm.*, **117**, 949–960.
Lessmann, V., Gottmann, K., & Malcangio, M. (2003) Neurotrophin secretion: current facts and future prospects. *Prog. Neurobiol.*, **69**, 341–374.
Levi-Montalcini, R. (1987) The nerve growth factor: thirty-five years later. *EMBO J.*, **6**, 1145–1154.
Lin, W.-J. & Salton, S.R. (2013) The regulated secretory pathway and human disease: insights from gene

variants and single nucleotide polymorphisms. *Front. Endocrinol. (Lausanne).*, **4**, 96.
Lista, S., O'Bryant, S.E., Blennow, K., Dubois, B., Hugon, J., Zetterberg, H., & Hampel, H. (2015) Biomarkers in Sporadic and Familial Alzheimer's Disease. *J. Alzheimer's Dis.*, **47**, 291–317.
Lleó, A., Cavedo, E., Parnetti, L., Vanderstichele, H., Herukka, S.K., Andreasen, N., Ghidoni, R., Lewczuk, P., Jeromin, A., Winblad, B., Tsolaki, M., Mroczko, B., Visser, P.J., Santana, I., Svenningsson, P., Blennow, K., Aarsland, D., Molinuevo, J.L., Zetterberg, H., & Mollenhauer, B. (2015) Cerebrospinal fluid biomarkers in trials for Alzheimer and Parkinson diseases. *Nat. Rev. Neurol.*, **11**, 41–55.
Lleó, A., Greenberg, S.M., & Growdon, J.H. (2006) Current pharmacotherapy for Alzheimer's disease. *Annu. Rev. Med.*, **57**, 513–533.
Lopez, J.R., Lyckman, A., Oddo, S., LaFerla, F.M., Querfurth, H.W., & Shtifman, A. (2008) Increased intraneuronal resting [Ca^{2+}] in adult Alzheimer's disease mice. *J. Neurochem.*, **105**, 262–271.
Lynch, D.R., Braas, K.M., Hutton, J.C., & Snyder, S.H. (1990) Carboxypeptidase E (CPE): immunocytochemical localization in the rat central nervous system and pituitary gland. *J. Neurosci.*, **10**, 1592–1599.
Magi, S., Castaldo, P., Macrì, M.L., Maiolino, M., Matteucci, A., Bastioli, G., Gratteri, S., Amoroso, S., & Lariccia, V. (2016) Intracellular Calcium Dysregulation: Implications for Alzheimer's Disease. *Biomed Res. Int.*, **2016**, 6701324.
Masters, C.L., Bateman, R., Blennow, K., Rowe, C.C., Sperling, R.A., & Cummings, J.L. (2015) Alzheimer's disease. *Nat. Rev. Dis. Prim.*, **3**, 15056.
Masters, C.L., Simms, G., Weinman, N.A., Multhaup, G., McDonald, B.L., & Beyreuther, K. (1985) Amyloid plaque core protein in Alzheimer disease and Down syndrome. *Proc. Natl. Acad. Sci. U. S. A.*, **82**, 4245–4249.
McKhann, G., Drachman, D., Folstein, M., Katzman, R., Price, D., & Stadlan, E.M. (1984) Clinical diagnosis of Alzheimer's disease: report of the NINCDS-ADRDA Work Group under the auspices of Department of Health and Human Services Task Force on Alzheimer's Disease. *Neurology*, **34**, 939–944.
McKhann, G.M., Knopman, D.S., Chertkow, H., Hyman, B.T., Jack, C.R., Kawas, C.H., Klunk, W.E., Koroshetz, W.J., Manly, J.J., Mayeux, R., Mohs, R.C., Morris, J.C., Rossor, M.N., Scheltens, P., Carrillo, M.C., Thies, B., Weintraub, S., Phelps, C.H., & Phelps, C.H. (2011) The diagnosis of dementia due to Alzheimer's disease: recommendations from the National Institute on Aging-Alzheimer's Association workgroups on diagnostic guidelines for Alzheimer's disease. *Alzheimers. Dement.*, **7**, 263–269.
Michaelson, D.M. (2014) APOE ε4: The most prevalent yet understudied risk factor for Alzheimer's disease. *Alzheimer's Dement.*, **10**, 861–868.
Moreira, P.I., Honda, K., Liu, Q., Santos, M.S., Oliveira, C.R., Aliev, G., Nunomura, A., Zhu, X., Smith, M.A., & Perry, G. (2005) Oxidative stress: the old enemy in Alzheimer's disease pathophysiology. *Curr. Alzheimer Res.*, **2**, 403–408.
Mucke, L. & Selkoe, D.J. (2012) Neurotoxicity of Amyloid-β Protein: Synaptic and Network Dysfunction. *Cold Spring Harb. Perspect. Med.*, **2**, a006338–a006338.
Navarrete, M., Perea, G., de Sevilla, D.F., Gómez-Gonzalo, M., Núñez, A., Martín, E.D., & Araque, A. (2012) Astrocytes Mediate In Vivo Cholinergic-Induced Synaptic Plasticity. *PLoS Biol.*, **10**, e1001259.
Nedergaard, M., Rodríguez, J.J., & Verkhratsky, A. (2010) Glial calcium and diseases of the nervous system. *Cell Calcium*, **47**, 140–149.
Nedergaard, M. & Verkhratsky, A. (2012) Artifact versus reality-How astrocytes contribute to synaptic events. *Glia*, **60**, 1013–1023.
Nelson, P.T., Alafuzoff, I., Bigio, E.H., Bouras, C., Braak, H., Cairns, N.J., Castellani, R.J., Crain, B.J., Davies, P., Del Tredici, K., Duyckaerts, C., Frosch, M.P., Haroutunian, V., Hof, P.R., Hulette, C.M., Hyman, B.T., Iwatsubo, T., Jellinger, K.A., Jicha, G.A., Kövari, E., Kukull, W.A., Leverenz, J.B., Love, S., Mackenzie, I.R., Mann, D.M., Masliah, E., McKee, A.C., Montine, T.J., Morris, J.C.,

Schneider, J.A., Sonnen, J.A., Thal, D.R., Trojanowski, J.Q., Troncoso, J.C., Wisniewski, T., Woltjer, R.L., & Beach, T.G. (2012) Correlation of Alzheimer disease neuropathologic changes with cognitive status: a review of the literature. *J. Neuropathol. Exp. Neurol.*, **71**, 362–381.

Nilsson, L., Nordberg, A., Hardy, J., Wester, P., & Winblad, B. (1986) Physostigmine restores 3H-acetylcholine efflux from Alzheimer brain slices to normal level. *J. Neural Transm.*, **67**, 275–285.

Norton, S., Matthews, F.E., Barnes, D.E., Yaffe, K., & Brayne, C. (2014) Potential for primary prevention of Alzheimer's disease: an analysis of population-based data. *Lancet. Neurol.*, **13**, 788–794.

Olsson, B., Lautner, R., Andreasson, U., Öhrfelt, A., Portelius, E., Bjerke, M., Hölttä, M., Rosén, C., Olsson, C., Strobel, G., Wu, E., Dakin, K., Petzold, M., Blennow, K., & Zetterberg, H. (2016) CSF and blood biomarkers for the diagnosis of Alzheimer's disease: a systematic review and meta-analysis. *Lancet Neurol.*, **15**, 673–684.

Ottiger, H.P., Battenberg, E.F., Tsou, A.P., Bloom, F.E., & Sutcliffe, J.G. (1990) 1B1075: a brain- and pituitary-specific mRNA that encodes a novel chromogranin/secretogranin-like component of intracellular vesicles. *J. Neurosci.*, **10**, 3135–3147.

Paco, S., Margelí, M.A., Olkkonen, V.M., Imai, A., Blasi, J., Fischer-Colbrie, R., & Aguado, F. (2009) Regulation of exocytotic protein expression and Ca2+-dependent peptide secretion in astrocytes. *J. Neurochem.*, **110**, 143–156.

Paco, S., Pozas, E., & Aguado, F. (2010) Secretogranin III is an astrocyte granin that is overexpressed in reactive glia. *Cereb. Cortex*, **20**, 1386–1397.

Palop, J.J., Chin, J., Roberson, E.D., Wang, J., Thwin, M.T., Bien-Ly, N., Yoo, J., Ho, K.O., Yu, G.-Q., Kreitzer, A., Finkbeiner, S., Noebels, J.L., & Mucke, L. (2007) Aberrant excitatory neuronal activity and compensatory remodeling of inhibitory hippocampal circuits in mouse models of Alzheimer's disease. *Neuron*, **55**, 697–711.

Palop, J.J. & Mucke, L. (2010) Amyloid-β-induced neuronal dysfunction in Alzheimer's disease: from synapses toward neural networks. *Nat. Neurosci.*, **13**, 812–818.

Patapoutian, A. & Reichardt, L.F. (2001) Trk receptors: mediators of neurotrophin action. *Curr. Opin. Neurobiol.*, **11**, 272–280.

Perrin, R.J., Craig-Schapiro, R., Malone, J.P., Shah, A.R., Gilmore, P., Davis, A.E., Roe, C.M., Peskind, E.R., Li, G., Galasko, D.R., Clark, C.M., Quinn, J.F., Kaye, J.A., Morris, J.C., Holtzman, D.M., Townsend, R.R., & Fagan, A.M. (2011) Identification and Validation of Novel Cerebrospinal Fluid Biomarkers for Staging Early Alzheimer's Disease. *PLoS One*, **6**, e16032.

Petersen, R.C., Caracciolo, B., Brayne, C., Gauthier, S., Jelic, V., & Fratiglioni, L. (2014) Mild cognitive impairment: a concept in evolution. *J Intern Med*, **275**, 214–228.

Pihlaja, R., Koistinaho, J., Malm, T., Sikkilä, H., Vainio, S., & Koistinaho, M. (2008) Transplanted astrocytes internalize deposited β-amyloid peptides in a transgenic mouse model of Alzheimer's disease. *Glia*, **56**, 154–163.

Plá, V., Paco, S., Ghezali, G., Ciria, V., Pozas, E., Ferrer, I., & Aguado, F. (2013) Secretory sorting receptors carboxypeptidase E and secretogranin III in amyloid β-associated neural degeneration in Alzheimer's disease. *Brain Pathol.*, **23**, 274–284.

Plassman, B.L., Langa, K.M., Fisher, G.G., Heeringa, S.G., Weir, D.R., Ofstedal, M.B., Burke, J.R., Hurd, M.D., Potter, G.G., Rodgers, W.L., Steffens, D.C., Willis, R.J., & Wallace, R.B. (2007) Prevalence of Dementia in the United States: The Aging, Demographics, and Memory Study. *Neuroepidemiology*, **29**, 125–132.

Potokar, M., Stenovec, M., Kreft, M., Kreft, M.E., & Zorec, R. (2008) Stimulation inhibits the mobility of recycling peptidergic vesicles in astrocytes. *Glia*, **56**, 135–144.

Qiu, C., Kivipelto, M., & von Strauss, E. (2009) Epidemiology of Alzheimer's disease: occurrence, determinants, and strategies toward intervention. *Dialogues Clin. Neurosci.*, **11**, 111–128.

Querfurth, H.W. & LaFerla, F.M. (2010) Alzheimer's disease. *N. Engl. J. Med.*, **362**, 329–344.

Rangroo Thrane, V., Thrane, A.S., Wang, F., Cotrina, M.L., Smith, N.A., Chen, M., Xu, Q., Kang, N., Fujita, T., Nagelhus, E.A., & Nedergaard, M. (2013) Ammonia triggers neuronal disinhibition and

seizures by impairing astrocyte potassium buffering. *Nat. Med.*, **19**, 1643–1648.
Raskin, J., Cummings, J., Hardy, J., Schuh, K., & Dean, R.A. (2015) Neurobiology of Alzheimer's Disease: Integrated Molecular, Physiological, Anatomical, Biomarker, and Cognitive Dimensions. *Curr. Alzheimer Res.*, **12**, 712–722.
Reisberg, B., Ferris, S.H., de Leon, M.J., Franssen, E.S.E., Kluger, A., Mir, P., Borenstein, J., George, A.E., Shulman, E., Steinberg, G., & Cohen, J. (1988) Stage-specific behavioral, cognitive, and in vivo changes in community residing subjects with age-associated memory impairment and primary degenerative dementia of the Alzheimer type. *Drug Dev. Res.*, **15**, 101–114.
Ries, M. & Sastre, M. (2016) Mechanisms of Aβ Clearance and Degradation by Glial Cells. *Front. Aging Neurosci.*, **8**, 160.
Roberson, E.D., Scearce-Levie, K., Palop, J.J., Yan, F., Cheng, I.H., Wu, T., Gerstein, H., Yu, G.-Q., & Mucke, L. (2007) Reducing Endogenous Tau Ameliorates Amyloid beta-Induced Deficits in an Alzheimer's Disease Mouse Model. *Science (80-.).*, **316**, 750–754.
Russell, C.L., Semerdjieva, S., Empson, R.M., Austen, B.M., Beesley, P.W., & Alifragis, P. (2012) Amyloid-β acts as a regulator of neurotransmitter release disrupting the interaction between synaptophysin and VAMP2. *PLoS One*, **7**, e43201.
Rylett, R.J., Ball, M.J., & Colhoun, E.H. (1983) Evidence for high affinity choline transport in synaptosomes prepared from hippocampus and neocortex of patients with Alzheimer's disease. *Brain Res.*, **289**, 169–175.
Rylett, R.J. & Williams, L.R. (1994) Role of neurotrophins in cholinergic-neurone function in the adult and aged CNS. *Trends Neurosci.*, **17**, 486–490.
Sala Frigerio, C. & De Strooper, B. (2016) Alzheimer's Disease Mechanisms and Emerging Roads to Novel Therapeutics. *Annu. Rev. Neurosci.*, **39**, 57–79.
Scheltens, P., Blennow, K., Breteler, M.M.B., de Strooper, B., Frisoni, G.B., Salloway, S., & Van der Flier, W.M. (2016) Alzheimer's disease. *Lancet*, **6736**, 1–13.
Schindowski, K., Belarbi, K., & Buée, L. (2008) Neurotrophic factors in Alzheimer's disease: role of axonal transport. *Genes, Brain Behav.*, **7**, 43–56.
Schliebs, R. & Arendt, T. (2006) The significance of the cholinergic system in the brain during aging and in Alzheimer's disease. *J. Neural Transm.*, **113**, 1625–1644.
Seidah, N.G., Benjannet, S., Pareek, S., Savaria, D., Goulet, B., Laliberte, J., Lazure, C., Chre, M., & Murphy, R.A. (1996) Cellular processing of the nerve growth factor precursor by the mammalian pro-protein convertases. *Biochem. J*, **314**, 951–960.
Selkoe, D.J. (1997) Alzheimer's disease: genotypes, phenotypes, and treatments. *Science*, **275**, 630–631.
Selkoe, D.J. (2001) Alzheimer 's Disease: Genes, Proteins, and Therapy. *Physiol. Rev.*, **81**, 741–766.
Selkoe, D.J. (2002) Alzheimer's Disease Is a Synaptic Failure. *Science (80-.).*, **298**.
Serrano-Pozo, A., Frosch, M.P., Masliah, E., & Hyman, B.T. (2011) Neuropathological alterations in Alzheimer disease. *Cold Spring Harb. Perspect. Med.*, **1**, a006189.
Serrano-Pozo, A., Qian, J., Monsell, S.E., Frosch, M.P., Betensky, R.A., & Hyman, B.T. (2013) Examination of the clinicopathologic continuum of Alzheimer disease in the autopsy cohort of the National Alzheimer Coordinating Center. *J. Neuropathol. Exp. Neurol.*, **72**, 1182–1192.
Sharma, N. & Singh, A.N. (2016) Exploring Biomarkers for Alzheimer's Disease. *J. Clin. Diagn. Res.*, **10**, KE01-6.
Sheng, M., Sabatini, B.L., & Südhof, T.C. (2012) Synapses and Alzheimer's disease. *Cold Spring Harb. Perspect. Biol.*, **4**.
Sims, N.R., Bowen, D.M., Allen, S.J., Smith, C.C., Neary, D., Thomas, D.J., & Davison, A.N. (1983) Presynaptic cholinergic dysfunction in patients with dementia. *J. Neurochem.*, **40**, 503–509.
Sivanesan, S., Tan, A., & Rajadas, J. (2013) Pathogenesis of Abeta oligomers in synaptic failure. *Curr. Alzheimer Res.*, **10**, 316–323.
Soininen, H., MacDonald, E., Rekonen, M., & Riekkinen, P.J. (1981) Homovanillic acid and 5-hydroxyindoleacetic acid levels in cerebrospinal fluid of patients with senile dementia of Alzheimer type. *Acta Neurol. Scand.*, **64**, 101–107.

Stevens, B., Allen, N.J., Vazquez, L.E., Howell, G.R., Christopherson, K.S., Nouri, N., Micheva, K.D., Mehalow, A.K., Huberman, A.D., Stafford, B., Sher, A., Litke, A.M., Lambris, J.D., Smith, S.J., John, S.W.M., & Barres, B.A. (2007) The classical complement cascade mediates CNS synapse elimination. *Cell*, **131**, 1164–1178.

Strac, D.S., Muck-Seler, D., & Pivac, N. (2015) Neurotransmitter measures in the cerebrospinal fluid of patients with Alzheimer's disease: a review. *Psychiatr. Danub.*, **27**, 14–24.

Svendsen, C.N., Cooper, J.D., & Sofroniew, M. V (1991) Trophic factor effects on septal cholinergic neurons. *Ann. N. Y. Acad. Sci.*, **640**, 91–94.

Sze, C.I., Troncoso, J.C., Kawas, C., Mouton, P., Price, D.L., & Martin, L.J. (1997) Loss of the presynaptic vesicle protein synaptophysin in hippocampus correlates with cognitive decline in Alzheimer disease. *J. Neuropathol. Exp. Neurol.*, **56**, 933–944.

Tanaka, K., Watase, K., Manabe, T., Yamada, K., Watanabe, M., Takahashi, K., Iwama, H., Nishikawa, T., Ichihara, N., Kikuchi, T., Okuyama, S., Kawashima, N., Hori, S., Takimoto, M., & Wada, K. (1997) Epilepsy and exacerbation of brain injury in mice lacking the glutamate transporter GLT-1. *Science*, **276**, 1699–1702.

Tang, Y.-P. & Gershon, E.S. (2003) Genetic studies in Alzheimer's disease. *Dialogues Clin. Neurosci.*, **5**, 17–26.

Teter, B. (2004) ApoE-Dependent Plasticity in Alzheimer's Disease. *J. Mol. Neurosci.*, **23**, 167–180.

Thal, D.R., Griffin, W.S.T., de Vos, R.A.I., & Ghebremedhin, E. (2008) Cerebral amyloid angiopathy and its relationship to Alzheimer's disease. *Acta Neuropathol.*, **115**, 599–609.

Turner, G.R. & Spreng, R.N. (2012) Executive functions and neurocognitive aging: dissociable patterns of brain activity. *Neurobiol. Aging*, **33**, 826.e1-826.e13.

Turner, P.R., O'Connor, K., Tate, W.P., & Abraham, W.C. (2003) Roles of amyloid precursor protein and its fragments in regulating neural activity, plasticity and memory. *Prog. Neurobiol.*, **70**, 1–32.

Van Dam, D., Van Dijck, A., Janssen, L., & De Deyn, P.P. (2013) Neuropeptides in Alzheimer's disease: from pathophysiological mechanisms to therapeutic opportunities. *Curr. Alzheimer Res.*, **10**, 449–468.

Verkhratsky, A., Matteoli, M., Parpura, V., Mothet, J.-P., & Zorec, R. (2016) Astrocytes as secretory cells of the central nervous system: idiosyncrasies of vesicular secretion. *EMBO J.*, **35**, e201592705.

Walker, L.C. & Jucker, M. (2015) Neurodegenerative Diseases: Expanding the Prion Concept. *Annu. Rev. Neurosci.*, **38**, 87–103.

Walsh, D.M. & Selkoe, D.J. (2007) Aβ Oligomers: a decade of discovery. *J. Neurochem.*, **101**, 1172–1184.

Wang, H.Y., Lee, D.H., D'Andrea, M.R., Peterson, P.A., Shank, R.P., & Reitz, A.B. (2000) beta-Amyloid(1-42) binds to alpha7 nicotinic acetylcholine receptor with high affinity. Implications for Alzheimer's disease pathology. *J. Biol. Chem.*, **275**, 5626–5632.

Wegiel, J., Wang, K.C., Tarnawski, M., & Lach, B. (2000) Microglia cells are the driving force in fibrillar plaque formation, whereas astrocytes are a leading factor in plague degradation. *Acta Neuropathol.*, **100**, 356–364.

Wilcock, G.K., Esiri, M.M., Bowen, D.M., & Smith, C.C. (1982) Alzheimer's disease. Correlation of cortical choline acetyltransferase activity with the severity of dementia and histological abnormalities. *J. Neurol. Sci.*, **57**, 407–417.

Williams, R. (2011) Biomarkers: Warning signs. *Nature*, **475**, S5–S7.

Willis, M., Leitner, I., Jellinger, K.A., & Marksteiner, J. (2011) Chromogranin peptides in brain diseases. *J. Neural Transm.*, **118**, 727–735.

Wilson, R.S., Leurgans, S.E., Boyle, P.A., & Bennett, D.A. (2011) Cognitive decline in prodromal Alzheimer disease and mild cognitive impairment. *Arch. Neurol.*, **68**, 351–356.

Winblad, B., Amouyel, P., Andrieu, S., Ballard, C., Brayne, C., Brodaty, H., Cedazo-Minguez, A., Dubois, B., Edvardsson, D., Feldman, H., Fratiglioni, L., Frisoni, G.B., Gauthier, S., Georges, J., Graff, C., Iqbal, K., Jessen, F., Johansson, G., Jönsson, L., Kivipelto, M., Knapp, M., Mangialasche, F., Melis, R., Nordberg, A., Rikkert, M.O., Qiu, C., Sakmar, T.P., Scheltens, P., Schneider, L.S., Sperling, R., Tjernberg, L.O., Waldemar, G., Wimo, A., & Zetterberg, H. (2016) Defeating Alzheimer's disease

and other dementias: a priority for European science and society. *Lancet Neurol.*, **15**, 455–532.
Xiao, M. & Hu, G. (2014) Involvement of Aquaporin 4 in Astrocyte Function and Neuropsychiatric Disorders. *CNS Neurosci. Ther.*, **20**, 385–390.
Yang, G., Pan, F., & Gan, W.-B. (2009) Stably maintained dendritic spines are associated with lifelong memories. *Nature*, **462**, 920–924.
Yang, Y., Kim, J., Kim, H.Y., Ryoo, N., Lee, S., Kim, Y., Rhim, H., & Shin, Y.-K. (2015) Amyloid-β Oligomers May Impair SNARE-Mediated Exocytosis by Direct Binding to Syntaxin 1a. *Cell Rep.*, **12**, 1244–1251.
Ye, X., Tai, W., & Zhang, D. (2012) The early events of Alzheimer's disease pathology: from mitochondrial dysfunction to BDNF axonal transport deficits. *Neurobiol. Aging*, **33**, 1122.e1-1122.e10.
Yoon, S.-S. & Jo, S.A. (2012) Mechanisms of Amyloid-β Peptide Clearance: Potential Therapeutic Targets for Alzheimer's Disease. *Biomol. Ther. (Seoul).*, **20**, 245–255.
Zanin, M.P., Phillips, L., Mackenzie, K.D., & Keating, D.J. (2011) Aging differentially affects multiple aspects of vesicle fusion kinetics. *PLoS One*, **6**, e27820.
Zetterberg, H. & Blennow, K. (2008) Biological CSF Markers of Alzheimer's Disease. In *Handbook of Clinical Neurology*. pp. 261–268.
Zetterberg, H., Blennow, K., & Hanse, E. (2010) Amyloid β and APP as biomarkers for Alzheimer's disease. *Exp. Gerontol.*, **45**, 23–29.
Zhao, Y. & Zhao, B. (2013) Oxidative stress and the pathogenesis of Alzheimer's disease. *Oxid. Med. Cell. Longev.*, **2013**, 316523.
Zheng, W.-H., Bastianetto, S., Mennicken, F., Ma, W., & Kar, S. (2002) Amyloid β peptide induces tau phosphorylation and loss of cholinergic neurons in rat primary septal cultures. *Neuroscience*, **115**, 201–211.